THE IDENTIFICATION OF THE MICROORGANISMS AND THE FUNCTIONAL GENES RESPONSIBLE FOR THE BIODEGRADATION OF VINYL CHLORIDE AND RDX USING SAMPLES FROM CONTAMINATED SITES

By

Fernanda Paes Wilson

A DISSERTATION

Submitted to
Michigan State University
in partial fulfillment of the requirements
for the degree of

Environmental Engineering – Doctor of Philosophy

2016

ABSTRACT

THE IDENTIFICATION OF THE MICROORGANISMS AND THE FUNCTIONAL GENES RESPONSIBLE FOR THE BIODEGRADATION OF VINYL CHLORIDE AND RDX USING SAMPLES FROM CONTAMINATED SITES

By

Fernanda Paes Wilson

Environmental contamination by organic pollutants threatens both human and environmental health. The use of microorganisms to remediate pollution is a viable option for site remediation. However, limited knowledge exists concerning the key microorganisms involved in the degradation of many pollutants. In this study, specific aspects of the biodegradation of vinyl chloride (VC) and hexahydro- 1,3,5-trinitro-1,3,5-triazine (RDX) were investigated. The overall objectives were to 1) identify the key microorganisms responsible for the degradation of VC and RDX in samples derived from a number of contaminated sites and 2) design specific primers towards the key phylotypes involved in VC degradation and 3) design specific primers towards the functional genes associated with RDX degradation and quantify these RDX degrading genes in contaminated samples and experimental microcosms. The first study examined the microorganisms involved in the degradation of VC in a mixed culture derived from a VC contaminated site. This culture degraded VC slowly (120 μmol in ~45 days). Using stable isotope probing (SIP) and high throughput sequencing (Illumina MiSeq), VC degraders were putatively identified as belonging to the genera *Nocardioides* (previously linked to VC degradation), *Gp4, Brevundimonas, Tissierella, Sediminibacterium* and *Rhodoferax* (novel genera). The results suggest that previous work involving isolations may not accurately represent active VC assimilators in mixed communities. In a second study, another mixed culture derived from contaminated groundwater was able to degrade VC rapidly (~120 μmol in 7 days). Stable

isotope probing and high throughput sequencing identified the dominant VC degraders in this culture. Specific primers were then designed towards the novel VC degrading phylotypes (*Sediminibacterium, Aquabacterium* and *Variovorax*) and tested in quantitative PCR (qPCR) to confirm label uptake by these phylotypes. Both studies indicated that microorganisms previously linked to vinyl chloride degradation as well as novel genera could have significant roles in carbon uptake from this pollutant.

The third study investigated the microorganisms and functional genes (*xenA, xenB* and *xplA*) linked to RDX biodegradation in microcosms composed of sediments or groundwater from two RDX-contaminated Navy sites. Sediment samples from five depths (5 ft to 30 ft) at two wells were studied from one Navy site. Also, groundwater samples both upstream and downstream of an emulsified biobarrier were studied from another Navy site. The study found that phylotypes from *Firmicutes, Actinobacteria, Proteobacteria, Acidobacteria* and *Bacteroidetes* benefited from RDX degradation. A notable trend was the increase in *xplA* and *xenB* gene copies in the majority of sediment microcosms derived from one Navy site compared to the controls. Gene copies of *xenA* increased in a smaller number of the treatments. Interestingly, *Pseudomonas* (previously associated with *xenA* and *xenB*) and *Rhodococcus (*associated with *xplA)* also illustrated a high level of enrichment in many of these RDX microcosms. The data provide insight into the microorganisms linked to *in situ* RDX degradation. Further, the functional gene primers designed in this study could be used to facilitate the prediction of RDX biodegradation rates at contaminated sites.

Dedicated to all the people who never stop working toward a healthier environment.

ACKNOWLEDGEMENTS

The years dedicated to this work were the most transforming years of my life and the accomplishment of these milestones were only possible due to the great people that surrounded me. While the space here might not allow me to list them all, I will do my best to list most. First of all, I am very grateful to my advisor and mentor, Dr. Alison M. Cupples. She gave me the opportunity to conduct my doctoral research in her laboratory while offering me valuable support, encouragement and advise. Through many of our weekly meetings, she patiently helped me to develop my knowledge in the field, while genuinely hearing my thoughts and trusting my work. Dr. Timothy Mattes, from the University of Iowa, for the enthusiastic collaboration on the Vinyl Chlorine project. Thank you for the constructive inputs and motivation during the development of this research project. I also would like to thank my dissertation committee members Dr. Syed Hashsham, Dr. Irene Xagoraraki and Dr. Dawn Reinhold, whose guidance, support and comments make this work complete. I am grateful to Yanlyang Pan for his assistance with the analytical instruments. I would also like to extend my thanks to my colleagues from Dr. Cupples group, Dr. Weimin Sun, Dr. Indumathy Jayamani, Dr. Fang Ting, Yang Song, Liang Ding, Jean Rene Thelusmond and Yogendra Kanitkar. Special thanks to my friend and colleague Dr. Indumathy Jayamani for the numerous scientific discussions and experiment brainstorming sections of each other research work and for her constant support through my academic years. I am indebted to her for teaching me the needed skills for HPLC use and RDX research work developed on Chapter 4. I am also thankful to Kathleen Haynes, Alyse Way and Jordyn Davis who allowed me to mentor them as part of their undergraduate research work. Thanks to Lori Larner, Margaret Connor, Mary Morz and Laura Taylor for their support during my studies. The research work presented here was funded by two different research grants

funded to Dr. Cupples and I am grateful for that (National Science Foundation grant number 1233154 and Strategic Environmental Research and Development Program, Project ER1606). My sincere thanks to the members of Dr. Patrick Schloss laboratory, at the University of Michigan, for their assistance during the Mothur analysis. Also thanks to Dr. Mark E. Fuller and Dr. Paul Hatzinger (CB&I Federal Services) for providing samples from the Navy Base Sites for the work presented in Chapter 4. Also, thanks to all my amazing friends, especially those who crossed my life on these many years in Michigan. Special thanks to Dr. Vania Melo and Dr. James Tiedje who first brought me to Michigan State University as a visiting scholar in 2007. Warming thanks to my two loving families: The Paes family (in Brazil) and The Wilson family (in Michigan). All of you are an important piece of the life support that allows me to happily continuing my life journey daily. Last but not least, I am grateful to my loving husband John Edward Wilson III for his love and unconditional support through my endeavors.

TABLE OF CONTENTS

LIST OF TABLES ..... **ix**

LIST OF FIGURES ..... **x**

KEY TO ABBREVIATIONS ..... **xiii**

CHAPTER 1 ..... **1**
INTRODUCTION **1**
Environmental pollution by vinyl chloride and RDX **1**
Biodegradation of vinyl chloride and RDX **2**
Stable isotope probing and high throughput sequencing **3**
Primer development for monitoring field bioremediation **4**
Objectives **4**
REFERENCES **6**

CHAPTER 2 ..... **11**
ELUCIDATING CARBON UPTAKE FROM VINYL CHLORIDE USING STABLE ISOTOPE PROBING AND ILLUMINA SEQUENCING **11**
Abstract **11**
Introduction **12**
Materials and methods **14**
Site information and groundwater collection ***14***
Development of VC degrading enrichment cultures ***14***
Analytical methods ***15***
SIP experimental design, DNA extraction, ultracentrifugation and fractionation ***15***
MiSeq Illumina sequencing and SIP fraction analysis ***17***
Functional gene (etnE) qPCR and clone libraries ***18***
Genbank accession numbers ***20***
Results **21**
VC degradation and total microbial community characterization ***21***
Identification of VC assimilators ***23***
Functional gene (etnE) abundance in SIP fractions ***25***
Phylogenetic analysis of etnE in SIP fractions ***25***
Discussion **27**
Acknowledgments **29**
APPENDIX **30**
REFERENCES **36**

CHAPTER 3 ..... **41**
NOVEL GENERA IDENTIFIED AS VINYL CHLORIDE ASSIMILATING MICROORGANISMS USING STABLE ISOTOPE PROBING **41**
Abstract **41**

Introduction **42**
Methods **43**
Experimental design *43*
Analytical methods *44*
DNA extraction, ultracentrifugation and fractionation *44*
MiSeq Illumina sequencing and SIP fraction analysis *45*
Primer design, 16S rRNA gene clone libraries and qPCR *46*
Isolations *48*
Microbial community analysis during VC degradation *48*
Results **49**
VC degradation, fraction generation, DNA quantification and sequencing data *49*
Identification of VC assimilators in heavy fractions *52*
Primer design, specificity test and abundance in SIP fractions *54*
Isolations *57*
Microbial community during VC degradation *57*
Discussion **60**
REFERENCES **64**

CHAPTER 4 ..... **69**
MICROBIAL COMMUNITY CHARACTERIZATION AND FUNCTIONAL GENE QUANTIFICATION IN RDX DEGRADING COMMUNITIES DERIVED FROM TWO NAVAL SITES **69**
Abstract **69**
Introduction **70**
Methods **73**
Chemicals *73*
Experimental design *74*
Analytical methods *75*
DNA extraction *75*
Quantitative PCR (qPCR) *76*
MiSeq Illumina sequencing and data analysis *77*
Results **78**
RDX degradation and quantitative PCR (qPCR) *78*
MiSeq Illumina sequencing and data analysis *88*
Discussion **98**
APPENDIX **105**
REFERENCES **108**

CHAPTER 5 ..... **115**
CONCLUSIONS **115**
Future work *117*

LIST OF TABLES

Table S2.1. *etnE* qPCR data on fractions from the ^{13}C-VC and ^{12}C-VC amended enrichment cultures. 34

Table S2.2. Percent identity matrix of *etnE* from clones of heavy fraction L4 and light fraction L9. 35

Table 4.1. T-test results (*p* values) comparing *xenA, xenB* and *xplA* gene copies between RDX amended samples and the No-RDX controls from sediment and groundwater inoculated microcosms. 86

Table 4.2. Most dominant phylotypes in DNA extracted from RDX- amended microcosms containing sediments from MW 58 at depths 5, 10 and 25 ft depth at day 90 and 130 and analyzed by MiSeq Illumina. 94

Table 4.3. Most dominant phylotypes in DNA extracted from RDX- amended microcosms containing sediments from MW 61 at depths 5, 10 and 20 ft depth at day 45 and 90 and analyzed by MiSeq Illumina. 95

Table 4.4. Most dominant phylotypes in DNA extracted from RDX- amended microcosms (both with and without glucose) containing groundwater from downstream and upstream of an installed buffered emulsified oil biobarrier and analyzed by MiSeq Illumina. 97

Table S4.1. Sequence, target and amplicon length of the primers designed to amplify the three RDX-degrading functional genes**.** 106

Table S4.2. Characteristics of the standard curves used to enumerate *xplA, xenA* and *xenB* in sediment (MW 58 and 61) and groundwater (GW) microcosms..... 107

LIST OF FIGURES

Figure 2.1. Microbial composition at the genus level (unless unclassified) of the four VC enrichment cultures. Only those with a relative abundance of 1% or more in at least one of the cultures are included. The data were obtained from total DNA extracts (before ultracentrifugation). 22

Figure 2.2. Normalized abundance of dominant phylotypes in ultracentrifugation fractions from the labeled (13C) VC-amended culture compared to their abundance in the unlabeled (12C) VC-amended culture from day 32 (first column) and day 45 (second column). The axis represents the relative abundance of each phylotype (determined by Illumina sequencing) normalized by the amount of DNA in that fraction (determined by Qubit). Error bars represent the standard deviations from triplicate values of Illumina data. 24

Figure 2.3. *etnE* copies after fractionation from 13C-VC amended (triangles, labeled) and 12C-VC amended (diamonds, unlabeled) cultures at day 15 (A), day 32 (B), and day 45 (C). The etnE abundance represents the average of duplicate samples and the error bars depict the standard deviation. 26

Figure S2.1. Vinyl chloride concentrations in ^{13}C vinyl chloride amended (□), ^{12}C vinyl chloride amended (◆) microcosms and abiotic controls (●). Arrows indicate when DNA was extracted (day 15, 32 and 45). 31

Figure S2.2. Phylogenetic tree based on 16S rRNA gene sequences showing the relationships of the *Nocardioides* sequences identified in this study to the most similar sequences in RDP Seqmatch (Cole et al 2014). Illumina sequences were the most abundant *Nocardioides* sequences at day 32 and 45. Ten sequences were aligned and trimmed to 254 bp and visualized in MEGA (Tamura et al 2011). The evolutionary history was inferred using the maximum likelihood method with the bootstrap test (5,000 replicates) (Felsenstein 1985). The evolutionary distances were computed using the Jukes-Cantor method (Jukes and Cantor 1969) with the scale bar representing 1.0% sequence difference. The tree was rooted with 16S rRNA gene from *Mycobacterium rhodesiae* strain JS60, a VC- and ethene-assimilating bacterium. 32

Figure S2.3. Phylogenetic relationships of selected *etnE* fragments recovered from fractions L4 and L9 of Carver MA composite groundwater ^{13}C-labeled VC enrichment culture, with sequences from previous Carver site enrichments and Genbank. All the sequences were aligned using ClustalW (Thompson et al 2002) and trimmed to 733 bp (with gaps). A maximum likelihood tree was constructed based on this 733 bp nucleotide alignment and visualized by MEGA5 (Tamura et al 2011),with the scale bar representing 5% sequence differences. Bootstrap values between 80-95% were indicated by open circles and above 95% were indicated by solid circles. The tree was rooted with the 2-hydroxypropyl-CoM lyase gene from the propene-oxidizing *Xanthobacter autotrophicus* Py2. Sequences from SIP fractions are denoted with solid squares. 33

Figure 3.1. VC degradation over time in cultures amended with 13C vinyl chloride (□), 12C vinyl chloride (■) and abiotic controls (□). Arrows indicate when DNA was extracted. 50

Figure 3.2. DNA concentration (ng/µL) at day 3 (A) and day 7 (B) in fractions obtained from the labeled VC and unlabeled VC amended cultures. The complete and dashed lines represent DNA concentrations from the unlabeled and labeled cultures, respectively. Replicate DNA measurements are shown. Arrows indicate samples selected for sequencing. 51

Figure 3.3. Relative abundance of phylotypes in the four heavy fractions from 13C VC amended cultures. The error bars represent standard deviations from six samples that were submitted for sequencing..... 53

Figure 3.4. *Sediminibacterium, Aquabacterium and Variovorax* 16S rRNA gene copies over the buoyant density range in DNA extracted from labeled and unlabeled VC amended cultures at days 3 and 7. Error bars represent standard deviation from three qPCR measurements. 56

Figure 3.5. Vinyl chloride remaining over time in triplicate live culturesand an abiotic control. The arrows indicate when DNA was extracted from these samples for Illumina sequencing..... 58

Figure 3.6. The relative abundance *Pseudomonas* (A), *Sediminibacterium* (B), *Aquabacterium* (C) and *Nocardioides* (D) in a vinyl chloride degrading culture. The y-axis has different scales. The relative abundance of *Variovorax* was <0.0017% in these cultures. 59

Figure 4.1. RDX concentrations (mg/L) in RDX-amended microcosms and abiotic controls containing sediment from well 58 at 5 ft (A), 10 ft (B), 20 ft (C), 25 ft (D) and 30 ft depth (E). The samples subjected to DNA extraction and community analysis are circled (days 90 and 130). .. 79

Figure 4.2. RDX concentrations (mg/L) in RDX amended microcosms and abiotic controls containing sediment from well 61 at 5 ft deep (A), 10 ft deep (B) and 20 ft depth (C). The samples subject to DNA extraction and community analysis are circled (days 45 and 90). 80

Figure 4.3. RDX concentrations (mg/L) in RDX-amended microcosms and abiotic controls containing groundwater from downstream (A, B) and upstream (C, D) of a buffered emulsified oil biobarrier. The samples subjected to DNA extraction and community analysis are circled (days 67 and 100 for downstream and upstream respectively). 81

Figure 4.4. Average (±SD, and n= 3) gene copies of *xplA* (A)*, xenA* (B) and *xenB* (C) in the initial samples, RDX- and No-RDX- amended microcosms containing sediment from well 58 at 5 ft, 10 ft and 25 ft depth on day 90 and 130 (a, b and c indicate the three replicates of each treatment).82

Figure 4.5. Average (±SD, and n= 3) gene copies of *xplA* (A)*, xenA* (B) and *xenB* (C) in the initial samples, RDX- and No-RDX- amended microcosms containing sediment from well 61 at 5 ft, 10 ft and 20 ft depth on day 45 and 90 (a, b and c indicate the three replicates of each treatment).. 84

Figure 4.6. Average (±SD, and n= 3) gene copies of *xplA* (A, B)*, xenA* (C, D) and *xenB* (E, F) in the initial samples, RDX- and No-RDX- amended microcosms with and without glucose) containing groundwater from downstream (day 67) and upstream (day 100) of an installed buffered emulsified oil biobarrier (a, b and c indicate the three replicates of each treatment). 85

Figure 4.7. Relative abundance (RA, %) of phylotypes in DNA extracted from initial samples, RDX- and No-RDX- amended microcosms containing sediments from MW 58 at depths 5 (A, B), 10 (C, D) and 25 ft (E, F) at day 90 and 130 in triplicates. 89

Figure 4.8. Relative abundance (RA, %) of phylotypes in DNA extracted from initial samples, RDX- and No-RDX- amended microcosms containing sediments from MW 61 at depths 5 (A, B), 10 (C, D) and 20 ft (E, F) at day 45 and 90 in triplicates. 90

Figure 4.9. Relative abundance (RA, %) of phylotypes in DNA extracted from initial samples, RDX- and No-RDX- amended microcosms (both with and without glucose) containing groundwater from downstream (A and B, day 67) and upstream (C and D, day 100) of an installed buffered emulsified oil biobarrier in triplicates. 91

KEY TO ABBREVIATIONS

DGGE – Denaturing gradient gel electrophoresis

DNA - Deoxyribonucleic acid

OTU - Operational taxonomic unit

PCR - Polymerase chain reaction

RDX – Royal demolition explosive (hexahydro-1,3,5-trintro-1,3,5-triazine)

rRNA - Ribosomal RNA

SIP – Stable isotope probing

TRFLP - Terminal restriction fragment length polymorphism

VC – Vinyl chloride

CHAPTER 1

INTRODUCTION

Environmental pollution by vinyl chloride and RDX

Vinyl chloride (VC) is a common contaminant in surface water and groundwater. This chemical is classified as a human carcinogen, with a Maximum Contamination Level of 0.002 mg L^{-1} and Public Health Goal of zero mg L^{-1} [1]. VC is the most carcinogenic of the chloroethenes and has the lowest regulatory limit in drinking water [2]. VC in groundwater originates primarily from the transformation of tetrachloroethene (PCE) and trichloroethene (TCE). These chlorinated ethenes are common contaminants due to their widespread use and previous careless disposal. In groundwater, natural biotic and abiotic processes degrade these solvents, leading to the accumulation of their more problematic metabolites, *cis*-dichloroethene and VC [3, 4].

Military sites are commonly contaminated by the nitroamine explosive hexahydro-1,3,5-trinitro-1,3,5- triazine, also known as royal demolition explosive (RDX), due to the explosive's manufacturing and handling, notoriously after World War II. RDX has replaced trinitrotoluene (TNT) over the past few decades as the primary nitroaromatic compound used in explosives [5]. RDX is mobile from sediments to groundwater due to its moderate solubility, low sorption and vapor pressure [6]. Thus, the RDX contamination problem also extends to groundwater within the surroundings of these military sites. Groundwater contamination by such organic pollutants threatens drinking water sources and human health due to their neurotoxic effects and potential

carcinogenic nature. The lifetime Federal Health Advisory for RDX established by the U.S. Environmental Protect Agency (EPA) in drinking water is 2 μg L^{-1}.

Bioremediation is a viable option to address both VC and RDX contamination. The research presented in this thesis relates to identifying the microorganisms involved in the biodegradation of the organic contaminants VC and RDX.

Biodegradation of vinyl chloride and RDX

The biodegradation of pollutants by microorganisms, whether aerobically or anaerobically, allows scientists to further develop ways to utilize the enzymatic pathways of microorganisms to remediate environmental contamination. This concept is called bioremediation and it has been extensively studied over the last decades. Bioremediation is a viable option for cleaning and reclaiming sites contaminated with pollutants amenable to microbial transformation. The use of microorganisms in bioremediation occurs either through monitored natural attenuation, biostimulation or bioaugmentation. To apply any bioremediation approach, extensive data is needed concerning the presence and abundance of the key microorganisms at the contaminated site.

The biodegradation of VC can occur by either anaerobic or aerobic pathways and by co-metabolism or direct VC assimilation [2]. Anaerobic transformation of VC by *Dehalococcoides spp.* can occur either by co-metabolism or direct VC reduction [4, 7, 8]. For the aerobic metabolism of VC, several bacteria belonging to the phyla *Actinobacteria* and *Proteobacteria* have been isolated from various environments or have been obtained in the laboratory [9-19].

For RDX, both aerobic and anaerobic biodegradation have also been reported. As sites contaminated with RDX are usually oxygen depleted, it is more suitable to consider RDX

biodegradation under these conditions. A number of RDX degrading bacteria have been isolated from environmental samples to date [20]. Known RDX degrading isolates classify within the phyla *Firmicutes, Actinobacteria, Proteobacteria* and *Fusobacteria*.

While information gained from isolates has greatly contributed to our understanding of VC and RDX metabolism, limitations associated with culture-based methods have likely resulted in an incomplete understanding of VC- and RDX-assimilating microorganisms at field sites. To address this unknown, several molecular biology methods, including SIP, high throughput sequencing and qPCR, were used in this research.

Stable isotope probing and high throughput sequencing

To address the limitations associated with culture-based methods, molecular biology tools have been applied in many environmental studies. For example, SIP has the advantage of linking function (e.g. carbon uptake) to microorganism identity in mixed microbial communities. The SIP method involves amending a stable isotope labeled (e.g. ^{13}C, ^{15}N) compound to a mixed microbial community, such as a soil, groundwater sample or a mixed culture. The ultracentrifugation of the extracted DNA from these samples in cesium chloride gradients allows the DNA to separate based on its buoyant density. By this approach, the SIP technique allows the separation of DNA by weight. DNA that has incorporated the labeled chemical C and/or N (heavy DNA) will appear in the heavy fractions. To avoid false positives, an unlabeled control accounting for the background community DNA within these heavy fractions (DNA with high CG contents) is used.

SIP studies have identified microorganisms involved in biogeochemical cycles [23] and environmental pollutant remediation [24-26]. Following SIP, these studies applied fingerprinting

techniques such as denaturing gradient gel electrophoresis (DGGE), terminal restriction fragment length polymorphism (TRFLP) and cloning libraries and Sanger sequencing. Recently, a combination of the SIP technique with high throughput sequencing, such as pyrosequencing and Illumina, have been proposed as it allows the recovery of a much higher number of sequences for the studied samples[27-30]. In the current work, SIP was combined with high throughput amplicon sequencing (Illumina MiSeq) to identify the microorganisms in mixed communities involved in VC biodegradation. Illumina sequencing was also applied to identify microorganisms benefiting from RDX degradation. The generated data is crucial for the development of biomarkers to be used on monitoring field studies.

Primer development for monitoring field bioremediation

In the past decade, it has become common to use qPCR targeted to either 16S rRNA genes or functional genes to determine the potential for bioremediation at a given site. In the present work, primers were designed toward phylotypes (16S rRNA genes) identified as VC degraders. Also, the aerobic VC degradation functional gene *etnE* was measured in SIP samples. In addition, primers were designed towards the functional genes *xenA, xenB* and *xplA* involved in RDX biodegradation. All primers developed in this research have the potential for use at sites where VC or RDX bioremediation is being applied.

Objectives

The overall objectives were,

1) To identify the key microorganisms responsible for the degradation of VC and RDX in samples derived from a number of contaminated sites (Chapters 2, 3 and 4).

2) To design specific primers to quantify the key phylotypes involved in VC degradation (Chapter 3).

3) To design specific primers towards the functional genes associated with RDX degradation and quantify these RDX degrading genes in contaminated samples and experimental microcosms (Chapter 4).

The research in Chapters 2 and 3 was funded by a collaborative NSF grant awarded to Dr. Mattes (University of Iowa) and Dr. Cupples entitled "Collaborative research: stable isotope-based differentiation of vinyl chloride assimilators from cometabolizers in contaminated groundwater" (Grant Number 1233154). The research performed in Chapter 4 was funded by a grant awarded to Dr. Cupples from Strategic Environmental Research and Development Program (SERDP) entitled "Development of biomarkers for assessing in situ RDX biodegradation potential" (Grant number ER1606).

Chapter 2 was published in Applied Microbiology and Biotechnology [36].

A version of Chapter 3 was awarded "Best Student Paper" and was published in the Proceedings of the Third International Symposium on Bioremediation and Sustainable Environmental Technologies (Miami, FL 18-21 May 2015).

Chapter 4 is in preparation for submission to a peer-reviewed journal.

REFERENCES

REFERENCES

[1] US Environmental Protect Agency, Basic information about vinyl chloride in drinking water, in, 2012.

[2] T.E. Mattes, A.K. Alexander, N.V. Coleman, Aerobic biodegradation of the chloroethenes: pathways, enzymes, ecology, and evolution, Fems Microbiology Reviews, 34 (2010) 445-475.

[3] P.M. Bradley, History and ecology of chloroethene biodegradation: A review, Bioremediation Journal, 7 (2003) 81-109.

[4] J. He, Kirsti M. Ritalahti, Kun-Lin Yang, Stephen S. Koenigsberg, F.E. Löffler, Detoxification of vinyl chloride to ethene coupled to growth of an anaerobic bacterium, Nature, 424 (2003) 62-65.

[5] K.-S. Ju, R.E. Parales, Nitroaromatic Compounds, from Synthesis to Biodegradation, Microbiology and Molecular Biology Reviews, 74 (2010) 250-+.

[6] E.L. Rylott, N.C. Bruce, Plants disarm soil: engineering plants for the phytoremediation of explosives, Trends in Biotechnology, 27 (2009) 73-81.

[7] A.M. Cupples, A.M. Spormann, P.L. McCarty, Growth of a *Dehalococcoides*-like microorganism on vinyl chloride and cis-dichloroethene as electron acceptors as determined by competitive PCR, Applied and Environmental Microbiology, 69 (2003) 953-959.

[8] F.E. Loffler, J. Yan, K.M. Ritalahti, L. Adrian, E.A. Edwards, K.T. Konstantinidis, J.A. Muller, H. Fullerton, S.H. Zinder, A.M. Spormann, *Dehalococcoides mccartyi* gen. nov., sp nov., obligately organohalide-respiring anaerobic bacteria relevant to halogen cycling and bioremediation, belong to a novel bacterial class, *Dehalococcoidia classis* nov., order *Dehalococcoidales* ord. nov and family *Dehalococcoidaceae* fam. nov., within the phylum *Chloroflexi*, International Journal of Systematic and Evolutionary Microbiology, 63 (2013) 625-635.

[9] S. Hartmans, J.A.M. Debont, J. Tramper, K. Luyben, Bacterial degradation of vinyl chloride, Biotechnol. Lett., 7 (1985) 383-388.

[10] S. Hartmans, J.A.M. Debont, Aerobic vinyl chloride metabolism in *Mycobacterium aurum* L1, Applied and Environmental Microbiology, 58 (1992) 1220-1226.

[11] M.F. Verce, R.L. Ulrich, D.L. Freedman, Characterization of an isolate that uses vinyl chloride as a growth substrate under aerobic conditions, Applied and Environmental Microbiology, 66 (2000) 3535-3542.

[12] N.V. Coleman, T.E. Mattes, J.M. Gossett, J.C. Spain, Phylogenetic and kinetic diversity of aerobic vinyl chloride-assimilating bacteria from contaminated sites, Applied and Environmental Microbiology, 68 (2002) 6162-6171.

[13] A.S. Danko, M.Z. Luo, C.E. Bagwell, R.L. Brigmon, D.L. Freedman, Involvement of linear plasmids in aerobic biodegradation of vinyl chloride, Applied and Environmental Microbiology, 70 (2004) 6092-6097.

[14] B.Z. Fathepure, V.K. Elango, H. Singh, M.A. Bruner, Bioaugmentation potential of a vinyl chloride-assimilating *Mycobacterium* sp., isolated from a chloroethene-contaminated aquifer, Fems Microbiology Letters, 248 (2005) 227-234.

[15] V.K. Elango, A.S. Liggenstoffer, B.Z. Fathepure, Biodegradation of vinyl chloride and *cis*-dichloroethene by a *Ralstonia* sp strain TRW-1, Applied Microbiology and Biotechnology, 72 (2006) 1270-1275.

[16] A.E. Taylor, M.E. Dolan, P.J. Bottomley, L. Semprini, Utilization of fluoroethene as a surrogate for aerobic vinyl chloride transformation, Environmental Science & Technology, 41 (2007) 6378-6383.

[17] Y.O. Jin, T.E. Mattes, Adaptation of aerobic, ethene-assimilating *Mycobacterium* strains to vinyl chloride as a growth substrate, Environmental Science & Technology, 42 (2008) 4784-4789.

[18] Y.O. Jin, S. Cheung, N.V. Coleman, T.E. Mattes, Association of missense mutations in epoxyalkane coenzyme M transferase with adaptation of *Mycobacterium* sp strain JS623 to growth on vinyl chloride, Applied and Environmental Microbiology, 76 (2010) 3413-3419.

[19] H. Fullerton, R. Rogers, D. Freedman, S. Zinder, Isolation of an aerobic vinyl chloride oxidizer from anaerobic groundwater, Biodegradation, 25 (2014) 893-901.

[20] M.I. Khan, J. Lee, J. Park, Microbial degradation and toxicity of hexahydro-1,3,5-trinitro-1,3,5-triazine, Journal of Microbiology and Biotechnology, 22 (2012) 1311-1323.

[21] R.W. Li, J.G. Giarrizzo, S.T. Wu, W.Z. Li, J.M. Duringer, A.M. Craig, Metagenomic Insights into the RDX-Degrading Potential of the Ovine Rumen Microbiome, Plos One, 9 (2014) 11.

[22] A.M. Cupples, RDX degrading microbial communities and the prediction of microorganisms responsible for RDX bioremediation, Int Biodeter Biodegr, 85 (2013) 260-270.

[23] S. Radajewski, P. Ineson, N.R. Parekh, J.C. Murrell, Stable-isotope probing as a tool in microbial ecology, Nature, 403 (2000) 646-649.

[24] D.R. Singleton, S.N. Powell, R. Sangaiah, A. Gold, L.M. Ball, M.D. Aitken, Stable-isotope probing of bacteria capable of degrading salicylate, naphthalene, or phenanthrene in a bioreactor treating contaminated soil, Applied and Environmental Microbiology, 71 (2005) 1202-1209.

[25] C. Luo, S. Xie, W. Sun, X. Li, A.M. Cupples, Identification of a novel toluene-degrading bacterium from the candidate phylum TM7, as determined by DNA stable isotope probing, Applied and Environmental Microbiology, 75 (2009) 4644-4647.

[26] W.M. Sun, A.M. Cupples, Diversity of five anaerobic toluene-degrading microbial communities investigated using stable isotope probing, Applied and Environmental Microbiology, 78 (2012) 972-980.

[27] Y. Xia, L. Cai, T. Zhang, H.H.P. Fang, Effects of substrate loading and co-substrates on thermophilic anaerobic conversion of microcrystalline cellulose and microbial communities revealed using high-throughput sequencing, International Journal of Hydrogen Energy, 37 (2012) 13652-13659.

[28] T.H. Bell, E. Yergeau, C. Martineau, D. Juck, L.G. Whyte, C.W. Greer, Identification of nitrogen-incorporating Bacteria in petroleum-contaminated Arctic soils by using [N-15] DNA-based stable isotope probing and pyrosequencing, Applied and Environmental Microbiology, 77 (2011) 4163-4171.

[29] G. Pilloni, F. von Netzer, M. Engel, T. Lueders, Electron acceptor-dependent identification of key anaerobic toluene degraders at a tar-oil-contaminated aquifer by Pyro-SIP, FEMS Microbiology Ecology, 78 (2011) 165-175.

[30] I. Jayamani, A.M. Cupples, Stable isotope probing reveals the importance of *Comamonas* and *Pseudomonadaceae* in RDX degradation in samples from a Navy Detonation Site, Environmental Science and Pollution Research, 22 (2015) 10340-10350.

[31] K. Nagarajan, K.-C. Loh, Molecular biology-based methods for quantification of bacteria in mixed culture: perspectives and limitations, Applied Microbiology and Biotechnology, 98 (2014) 6907-6919.

[32] Y.O. Jin, T.E. Mattes, A Quantitative PCR Assay for Aerobic, Vinyl Chloride- and Ethene-Assimilating Microorganisms in Groundwater, Environmental Science & Technology, 44 (2010) 9036-9041.

[33] Y.O. Jin, T.E. Mattes, Assessment and modification of degenerate qPCR primers that amplify functional genes from etheneotrophs and vinyl chloride-assimilators, Letters in Applied Microbiology, 53 (2011) 576-580.

[34] B.M. Patterson, R. Aravena, G.B. Davis, A.J. Furness, T.P. Bastow, D. Bouchard, Multiple lines of evidence to demonstrate vinyl chloride aerobic biodegradation in the vadose zone, and factors controlling rates, Journal of Contaminant Hydrology, 153 (2013) 69-77.

[35] S. Atashgahi, F. Maphosa, E. Dogan, H. Smidt, D. Springael, W. Dejonghe, Small-scale oxygen distribution determines the vinyl chloride biodegradation pathway in surficial sediments of riverbed hyporheic zones, FEMS Microbiol Ecol, 84 (2013) 133-142.

[36] F. Paes, X. Liu, T.E. Mattes, A.M. Cupples, Elucidating carbon uptake from vinyl chloride using stable isotope probing and Illumina sequencing, Applied Microbiology and Biotechnology, 99 (2015) 7735-7743.

CHAPTER 2

ELUCIDATING CARBON UPTAKE FROM VINYL CHLORIDE USING STABLE ISOTOPE PROBING AND ILLUMINA SEQUENCING

Abstract

Vinyl chloride (VC), a known human carcinogen, is a common and persistent groundwater pollutant at many chlorinated solvent contaminated sites. The remediation of such sites is challenging because of the lack of knowledge on the microorganisms responsible for *in situ* VC degradation. To address this, the microorganisms involved in carbon assimilation from VC were investigated in a culture enriched from contaminated site groundwater using stable isotope probing (SIP) and high throughput sequencing. The mixed culture was added to aerobic media and these were amended with labeled (^{13}C-VC) or unlabeled VC (^{12}C-VC). The cultures were sacrificed on days 15, 32 and 45 for DNA extraction. DNA extracts and SIP ultracentrifugation fractions were subject to sequencing as well as qPCR for a functional gene linked to VC-assimilation (*etnE*). The gene *etnE* encodes for epoxyalkane coenzyme M transferase, a critical enzyme in the pathway for VC degradation. The relative abundance of phylotypes were compared across ultracentrifugation fractions obtained from the ^{13}C-VC and ^{12}C-VC amended cultures. Four phylotypes were more abundant in the heavy fractions (those of greater buoyant density) from the ^{13}C-VC amended cultures compared to from the ^{12}C-VC amended cultures, including *Nocardioides, Brevundimonas, Tissierella* and *Rhodoferax.* Therefore, both a previously identified VC-assimilating genus (*Nocardioides*) as well as novel microorganisms

were responsible for carbon uptake. Enrichment of *etnE* with time was observed in the heavy fractions, and *etnE* sequences illustrated VC-assimilators harbor similar *Nocardioides*-like *etnE*. This research provides novel data on the microorganisms able to assimilate carbon from VC.

Introduction

Groundwater contamination by vinyl chloride (VC) remains an important environmental problem and human health concern worldwide. VC is a known human carcinogen [1] and has been found at many US Environmental Protection Agency National Priority List sites in soils, surface water and groundwater. VC pollution in groundwater originates primarily from the higher-chlorinated ethenes including tetrachloroethene (PCE) and trichloroethene (TCE) [2]. Leakage of these chemicals to aquifers, followed by their reduction by certain anaerobic bacteria (e.g. *Dehalococcoides* spp.) yields the lesser chlorinated ethenes, *cis*-1,2-dichloroethene and VC. These secondary pollutants are often more problematic than the parent compounds because they tend to accumulate.

Biological degradation is becoming an increasingly common remediation method for groundwater contaminants, either through natural attenuation or enhanced bioremediation. Microbial VC degradation can occur under both anaerobic and aerobic conditions and by co-metabolism or direct VC assimilation [3]. However, linking specific microorganisms and enzymes to *in situ* activities remains a major challenge. Several bacteria belonging to the phyla *Actinobacteria* and *Proteobacteria* are capable of direct aerobic VC consumption and have been isolated from various environments or have been obtained in the laboratory [4-13]. While these organisms have greatly contributed to our understanding of VC metabolism, the limitations

associated with culture-based methods has likely resulted in an incomplete understanding of VC-assimilating microorganisms at field sites.

To overcome the limitations associated with culture-based methods, molecular testing during groundwater monitoring has become popular. For example, a quantitative PCR (qPCR) assay has been developed [14, 15] and applied [6, 16, 17] to detect VC-oxidizing bacteria at contaminated sites. This qPCR method targets the functional genes *etnC* and *etnE*, which encode the alkene monooxygenase (AkMO) alpha subunit and the epoxyalkane coenzyme M transferase (EaCoMT), respectively. In VC-assimilators, AkMO is responsible for the initial attack on VC to convert it to VC epoxide. The epoxide is then conjugated to CoM by EaCoMT, which is a critical step to the central metabolic pathway. Therefore, presence of *etnE* gene indicates the potential for VC assimilation.

To understand the diversity of mixed cultures and associated functional genes, molecular methods can often more accurately target the key active microorganisms. The stable isotope probing (SIP) method is valuable because it can identify the active microorganisms responsible for carbon or nitrogen uptake from the amended substrates [18]. The method involves sample exposure to a stable-isotope labeled compound and DNA extraction over time. The DNA is then subject to ultracentrifugation, fractionation (to separate label incorporated DNA from the unlabeled DNA) and community analysis [19-25].

The overall objective was to determine the dominant microorganisms involved in carbon uptake from VC from a mixed culture derived from contaminated site groundwater. For this, SIP fractions were subjected to high throughput sequencing. The relative abundance of phylotypes in fractions obtained from ^{13}C-VC and ^{12}C-VC amended mixed cultures were compared. The phylotypes enriched in the fractions from the ^{13}C-VC amended cultures compared to the

fractions from the ^{12}C-VC amended cultures are considered responsible for incorporating ^{13}C from VC (or VC degradation products). This is the first study to combine SIP and high throughput sequencing to examine carbon uptake from VC. Along with the information provided by qPCR and clone library analysis of *etnE*, this study contributes to our understanding of VC degradation in mixed communities and at contaminated sites.

Materials and methods

Site information and groundwater collection

Groundwater was collected in accordance with USEPA/540/S-95/504 on June 9, 2009 from several monitoring wells (RB46D, RB73, RB52I, RB60, RB64I, RB63I, and RB58I) at a site in Carver, MA. The site was contaminated by disposal of material containing PCE at a landfill in 1986, which ultimately resulted in a large, dilute VC plume. Remediation efforts for the plume have involved oxygen and ethene injections and have been described previously [15, 26-28]. The groundwater from these wells was composited, one liter was shipped to the University of Iowa, where it was stored at 4 °C in the dark.

Development of VC degrading enrichment cultures

Triplicate VC enrichment cultures were constructed in August 2009 by mixing composite groundwater with sterile minimal salts medium (MSM; prepared as described previously [12]) (1:1), placing 72 mL of the mixture into a 160 mL serum bottle (Wheaton, Millville, NJ), sealing with a butyl rubber stopper and aluminum crimp cap. Approximately 40 μmol VC (99.5% from Fluka) was added and the bottles were monitored by gas chromatography with flame ionization detection (GC-FID) as described previously [29]. VC oxidation commenced after a 63 day lag

period. Live culture samples were sent to MSU in January 2010 for the SIP experiment described below.

Analytical methods

Headspace samples of VC (100 μL) were analyzed via gas chromatography (Perkin Elmer) with flame ionization detection and a capillary column (J&W Scientific, DB-624, diameter 0.53 mm). The peak areas were compared to an external standard for VC quantification. Aqueous phase VC concentrations were calculated using a previously reported Henry's Law constant (1.069) [30].

SIP experimental design, DNA extraction, ultracentrifugation and fractionation

The SIP experimental setup consisted of sterile serum bottles (160 mL), mixed culture (5 mL), minimal salts medium (67 mL MSM) [13] and VC (~47 mg L^{-1} or 120 μmol) (the initial liquid and headspace volumes were 72 mL and 88 mL). These microcosms were prepared as previously described [31]. Based on the calculated amount of oxygen required for VC oxidation, and on previous VC studies [12], oxygen limitation was not expected under these conditions. Three abiotic microcosms (controls, obtained via autoclaving) and nine live microcosms were amended with unlabeled VC (hereafter referred to as ^{12}C-VC) (99 %, Specialty Gases of America) (to control for heavy GC microorganisms). An additional nine live microcosms were amended with labeled VC (hereafter referred to as ^{13}C-VC) ($^{13}C_2$ VC, 99 %, Cambridge Isotope Laboratories). The microcosms were sealed, protected from light, and incubated at room temperature (21-23 °C), with shaking (200-300 rpm). VC concentrations were monitored over 45 days and DNA was extracted (from ^{13}C-VC amended and ^{12}C-VC amended microcosms) at three time points during the experimental period (days 15, 32 and 45).

For DNA extraction, at each time point, the entire volume from each mixed culture bottle was centrifuged. Following this, the pellet was washed with MSM and the sample was centrifuged again. The pellet was then resuspended in Tris-EDTA (TE) buffer and DNA was extracted using the Ultra Clean Microbial DNA Isolation Kit (MO BIO Laboratories, Inc., Carlsbad, CA) according to the manufacturer's procedure. Quantified DNA extracts (~10 μg) were loaded into Quick-Seal polyallomer tubes (13 by 51 mm, 5.1 ml; Beckman Coulter (Brea, CA) along with a Tris-EDTA (10 mM Tris, 1 mM EDTA, pH 8)-CsCl solution for ultracentrifugation. Prior to sealing (cordless Quick-Seal tube topper; Beckman), the density was determined with a model AR200 digital refractometer (Leica Microsystems Inc., Buffalo Grove, IL) and adjusted by adding small volumes of CsCl solution or TE buffer with a final value of 1.730 g mL^{-1}. The tubes were ultracentrifuged at 178,000 × g (20 °C) for 48 h in a StepSaver 70 V6 vertical titanium rotor (8 by 5.1 ml capacity) within a Sorvall WX 80 Ultra Series centrifuge (Thermo Scientific, Waltham, MA). Following ultracentrifugation, the tubes were placed onto a fraction recovery system (Beckman Coulter), and fractions (~20, 150 μL) were collected. The buoyant density of each fraction was measured, and CsCl was removed by glycogen-assisted ethanol precipitation. The DNA concentration in each fraction was quantified using the Qubit assay (Quant-iT™ dsDNA High-Sensitivity Assay Kit using the Qubit® 2.0 Fluorometer). The abundance of *etnE* was determined in ultracentrifugation fractions using qPCR. For this, for each time point (days 15, 32 and 45), fractions from one ^{12}C-VC amended culture and one ^{13}C-VC amended culture were investigated. In addition, for days 32 and 45, fractions from one ^{13}C-VC amended culture and fractions from one ^{12}C-VC amended culture were subjected to Illumina sequencing.

MiSeq Illumina sequencing and SIP fraction analysis

In all, ninety-four samples were subjected to high throughput sequencing (MiSeq Illumina Sequencing at Michigan State University's Research Technology and Support Facility, RTSF). This included four DNA extracts (before ultracentrifugation) from the ^{12}C-VC and ^{13}C-VC amended cultures at day 32 and at day 45. Ninety additional samples were submitted for Illumina sequencing and these included thirty individual SIP fractions (following ultracentrifugation) sequenced in triplicate. This involved eight fractions from each of the ^{13}C-VC and ^{12}C-VC amended cultures at day 32 (8 fractions × 2 treatments × triplicates = forty-eight). Seven fractions from each of the ^{13}C-VC and ^{12}C-VC amended bottles from day 45 were also sequenced (7 fractions × 2 treatments × triplicates = forty-two).

The fractions were sequenced to determine which organisms were enriched in the heavy fractions and were therefore responsible for VC assimilation. The fractions were selected based on their buoyant density in comparison to previous SIP studies which illustrated label uptake in fractions with buoyant density values ranging from 1.74 – 1.77 g mL^{-1} [22, 32]. In the current study, the fractions selected for sequencing ranged from 1.74 to 1.785 (day 32) and 1.744 – 1.797 g mL^{-1} (day 45).

PCR and Illumina sequencing were performed at RTSF using a previously reported protocol [33]. Briefly, this involved the amplification of the V4 region of the 16S rRNA gene using a set of multiplex indexed primers. Following amplification, individual reactions were quantified (Picogreen assay), a pool of equimolar amounts of each was made and these were purified using Ampure XP beads. A final gel purification step was included to ensure non-specific products were eliminated. The combined library was loaded onto the Illumina MiSeq Platform using a standard MiSeq paired end (2×250 bp) flow cell and reagent cartridge.

Sequencing data obtained from the MiSeq platform Laboratory Information Management System were analyzed using Mothur v.1.33.2 [34] using the MiSeq standard operating procedure [35]. The sequence data in the fastq format were processed to remove the barcodes and these were then aligned to form contiguous sequences. The data were checked for sequencing errors (removing ambiguous bases) and read length (275 bp). The sequences were then aligned to the SILVA database (SILVA version 119) [36]. Additional steps included setting the maximum homopolymer length to 8, checking for chimeras using UCHIME [37], classifying with the Bayesian classifier and removing unwanted lineages. The sequences were clustered into OTU using a 0.03 cutoff level. Mothur was also used to generate information on phylotypes.

To determine which phylotypes were responsible for label uptake, the most abundant phylotypes in the heavy fractions from the ^{13}C-VC amended samples from day 32 were determined using the sort function in Excel. These values were then compared to relative abundance of these phylotypes in the fractions from the ^{12}C-VC amended samples from day 32. Additionally, the relative abundance of these phylotypes was determined in the ^{13}C-VC and ^{12}C-VC fractions from day 45. The relative abundance values were normalized to the mass of DNA in each fraction (Quant-iT™ dsDNA High-Sensitivity Assay Kit using the Qubit® 2.0 Fluorometer) by multiplying the relative abundance by the total mass of DNA in each fraction.

Functional gene (etnE) qPCR and clone libraries

Fractions from all three time points (15, 32 and 45 days) from both the ^{13}C-VC and ^{12}C-VC amended cultures were used in the *etnE* qPCR analysis. This resulted in 78 DNA fractions (buoyant density range = 0.981 - 1.799 g mL^{-1}) being analyzed by qPCR for *etnE*. An ABI 7000 Sequence Detection System (Applied Biosystems) with a 96 well plate was used for qPCR, as

described previously [6]. Reaction mixtures (25 µL) contained 12.5 µL of Power SYBR Green PCR Master Mix (Applied Biosystems), 750 nM *etnE* qPCR primers RTE_F(5'-CAGAAYGGCTGYGACATYATCCA-3') and RTE_R (5'-CSGGYGTRCCCGAGTAGTTWCC-3') [15] and 2 µL of DNA extract. Each fraction was analyzed in duplicate.

Standard curves were developed in triplicate using *etnE* from *Nocardioides* sp. strain JS614 [6] amplified using the CoMF1L (5'-AACTACCCSAAYCCSCGCTGGTACGAC-3') and CoMR2E (5'- GTCGGCAGTTTCGGTGATCGTGCTCTTGAC-3') [38]. Reactions (25 µL) contained 12.5 µL Qiagen PCR Master Mix, 0.2 µM of each primer and 2 ng of total DNA. Genes per µL of PCR product were estimated using a previously reported equation [15]. ABI 7000 System SDS software (Applied Biosystems) was used to analyze real-time PCR fluorescence data using the auto baseline function. The following information is provided in accordance with MIQE guidelines [39]: the fluorescence threshold was set manually (at 0.05505) to optimize qPCR efficiency (102.5%), and obtain a linear fit of the standard curve (>0.9976). The Y-intercept of the standard curve was 31.96.

A light fraction (denoted as L9, buoyant density=1.734 g mL^{-1}) and a heavy fraction (denoted as L4, buoyant density=1.773 g mL^{-1}) from day 45 were selected as representative fractions for the *etnE* clone libraries. The L4 and L9 fractions were purified as stated above and *etnE* was amplified using a touch-down PCR protocol. Reaction mixtures (25 µL) contained Qiagen Taq Core Kit 10X buffer (12.5 µL), 25 mM Mg^{2+} solution (0.5 µL), 10 mM dNTPs (0.5 µL), Taq polymerase (0.2 µL), the CoM-F1L/CoM-R2E primer set (0.2 µM)[38], and 1 µL DNA. The thermocycling protocol consisted of an initial denaturation step (94°C, 5 min) followed by a touch-down phase (20 cycles of 94°C for 30 s, 65°C for 45 s (0.5°C decrease of

each cycle), and 72°C for 2 min), a secondary amplification (10 cycles of 94 °C for 30 s, 55 °C for 45 s, 72 °C for 2 min) and a final extension (72 °C for 15 min). PCR products (891 bp) from L4 and L9 were purified with QIAquick PCR Purification Kit (Qiagen) and cloned with the Invitrogen TA Cloning Kit with an overnight ligation at 4°C into the pCR®2.1 vector. A 1:1 molar insert to vector ratio was used. Ligations were transformed into One Shot® TOP10 Chemically Competent *E. coli*. Transformants were analyzed according to the cloning kit instructions. Plasmids were extracted using QIAprep Spin Miniprep Kit and PCR-screened with M13F (5'-GTAAAACGACGGCCAG-3') and M13R (5'- CAGGAAACAGCTATGAC-3') primers. Those with the appropriately sized inserts were Sanger-sequenced at the University of Iowa Institute of Human Genetics Genomics Division with the M13F primer. Sequences with good quality (9 sequences from L4 and 10 sequences from L9) were used for alignment via Clustal W [40] and further phylogenetic analysis with MEGA 5 [41].

Genbank accession numbers

The *Nocardioides* sp. partial 16S rRNA gene was deposited in the NCBI Genbank Database (Accession Number: KJ509930.1). The *etnE* sequences were also placed in this database (Accession Numbers: KJ509928-KJ509936, KM245084, KM245085). Illumina sequencing data was deposited in the NCBI Sequence Read Archive under BioProject Number SAMN03202071.

Results

VC degradation and total microbial community characterization

VC degradation occurred in both of the ^{13}C-VC amended and ^{12}C-VC amended mixed cultures but not in the abiotic controls, confirming biological removal (Figure S2.1). The DNA extracted during this period (day 15, 32 and 45) was subjected to ultracentrifugation and the heavy fractions (from day 32 and 45) were submitted for Illumina sequencing. Following Mothur analysis, 9,029,943 sequences were obtained. On average, each sample generated 99,230 ± 36,815 sequences (total sequences, not unique sequences).

Illumina sequencing of the 16S rRNA gene was also performed on four total DNA extracts (before ultracentrifugation, two from day 32, and two from day 45). The most abundant phylotypes were determined (relative abundance of ≥ 1%) for each culture (Figure 2.1). Similar phylotypes were observed at both time points for the ^{13}C-VC and ^{12}C-VC amended mixed cultures. In all four cultures, the phylotype *Gp4* was present at a high relative abundance (9.9 - 30.8%). In addition, the phylotypes *Aquabacterium, Sediminibacterium, Nocardioides* and unclassified *Comamonadaceae* were all more abundant compared to the other phylotypes. The most abundant phylotypes classified within eight phyla (*Proteobacteria, Actinobacteria, Acidobacteria, Bacteroidetes, Firmicutes, Flavobacteria, Gemmatimonadetes* and *Verrucomicrobia).* The most dominant phyla included *Proteobacteria, Acidobacteria, Actinobacteria, Bacteroidetes* and *Flavobacteria*.

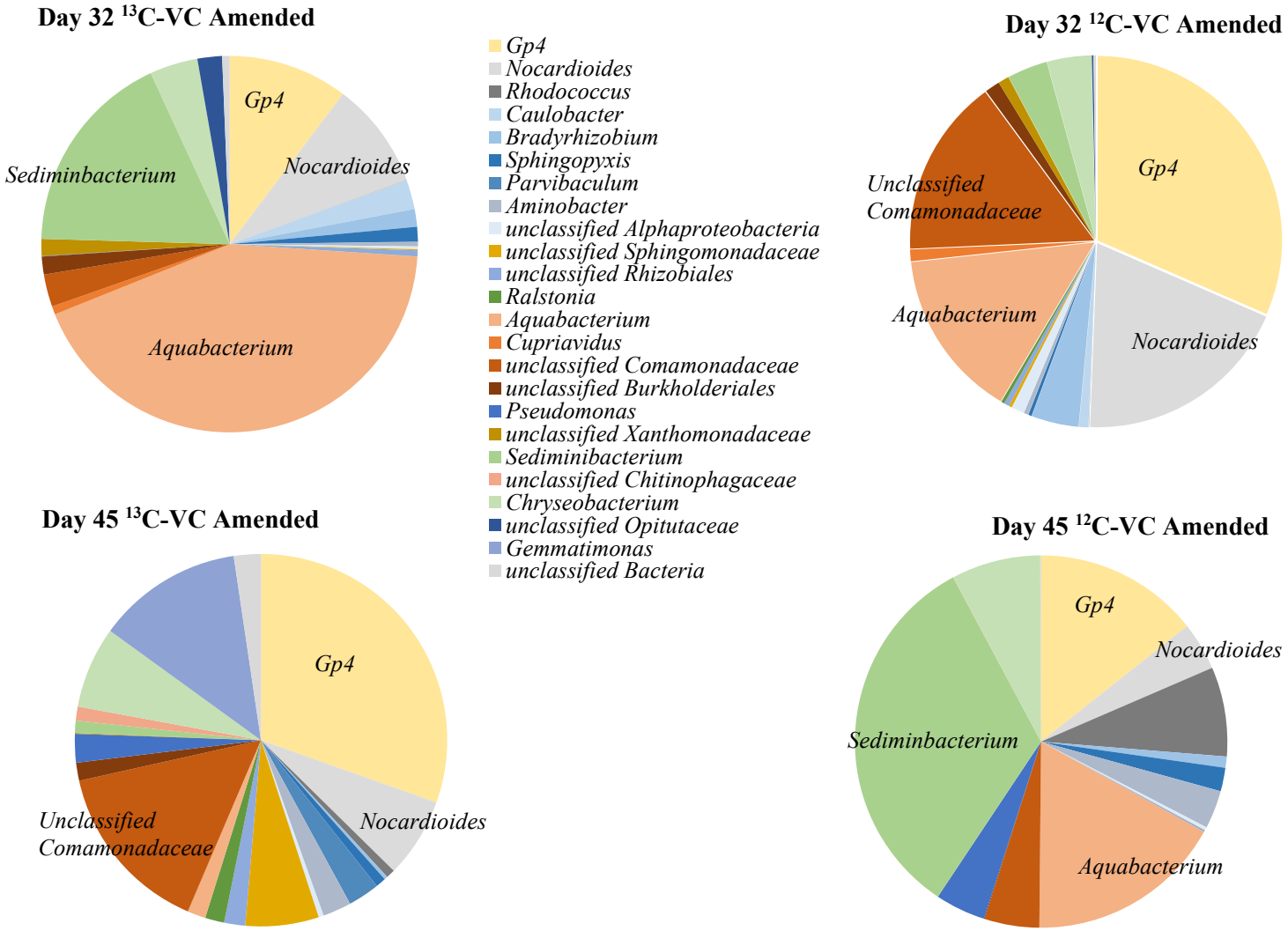

Figure 2.1. Microbial composition at the genus level (unless unclassified) of the four VC enrichment cultures. Only those with a relative abundance of 1% or more in at least one of the cultures are included. The data were obtained from total DNA extracts (before ultracentrifugation).

Identification of VC assimilators

To identify the microorganisms responsible for the uptake of ^{13}C from VC (or VC degradation products), DNA extracts from two time points (days 32 and 45) were subject to ultracentrifugation, fractioning and sequencing. For this, the most abundant phylotypes in the heavy fractions from the ^{13}C-VC amended samples were determined and compared to the relative abundance of these phylotypes in the fractions from the ^{12}C-VC amended samples (Figure 2.2). In all, four phylotypes showed dominance in the ^{13}C-VC amended cultures compared to the ^{12}C-VC amended cultures, including *Rhodoferax, Nocardioides, Tissierella* and *Brevundimonas*. As stated previously, the Illumina relative abundance data were normalized by the amount of DNA in each fraction. Only low levels of enrichment were noted from the phylotypes *Tissierella* and *Brevundimonas* at both time points. The other two phylotypes (*Nocardioides* and *Rhodoferax*) were enriched at a higher level, with *Rhodoferax* illustrating the highest level of enrichment. The *Nocardioides* sequences from these cultures were compared to those in GenBank (Figure S2.2).

The relative abundance of each of these four phylotypes was determined from the total DNA extract sequencing data. These data indicate only *Nocardioides* was a dominant community member (4.1-18.7%). The other three phylotypes illustrated only a low relative abundance in the community (<0.08%).

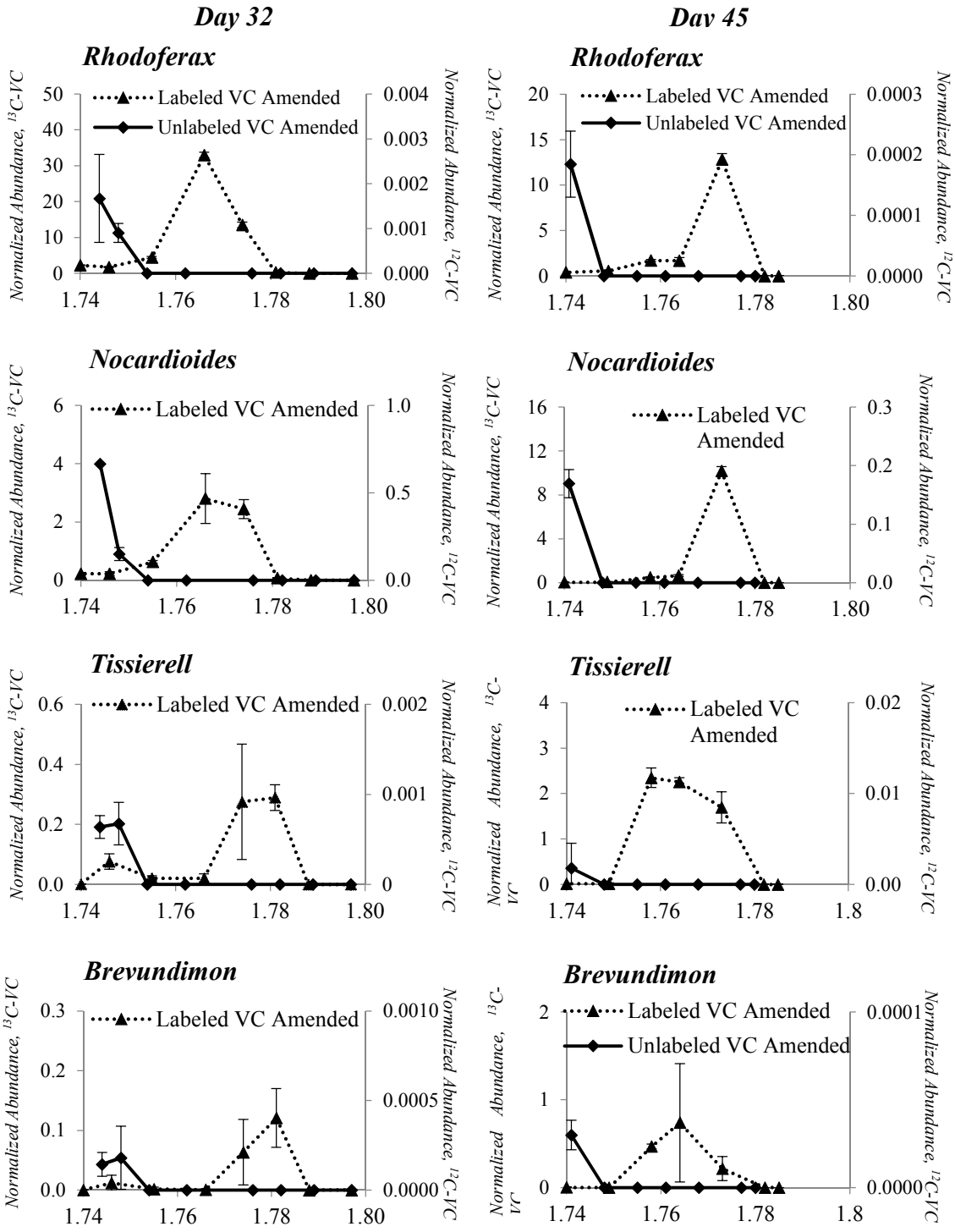

Figure 2.2. Normalized abundance of dominant phylotypes in ultracentrifugation fractions from the labeled (13C) VC-amended culture compared to their abundance in the unlabeled (12C) VC-amended culture from day 32 (first column) and day 45 (second column). The axis represents the relative abundance of each phylotype (determined by Illumina sequencing) normalized by the amount of DNA in that fraction (determined by Qubit). Error bars represent the standard deviations from triplicate values of Illumina data.

Functional gene (etnE) abundance in SIP fractions

To provide evidence that functional genes associated with VC assimilation were also enriched in the heavy fractions, we quantified *etnE* abundance by qPCR (Figure 2.3, Table S2.1). Indeed, as VC degradation proceeded, increased *etnE* abundance was observed among heavier fractions (buoyant density = 1.720 - 1.780 g mL^{-1}) from the ^{13}C-VC fed culture. Meanwhile, the majority of the *etnE* abundance in the fractions from the unlabeled VC amended cultures occurred within a lower buoyant density range (buoyant density = 1.700 - 1.740 g mL^{-1}). It is unclear why the *etnE* gene abundance values were lower at day 45 compared to days 15 and 32.

Phylogenetic analysis of etnE in SIP fractions

Clone libraries were constructed with *etnE* PCR products from one light fraction (L4) and one heavy fraction (L9) to compare the sequence diversity of ^{13}C-enriched *etnE* with the *etnE* in the unlabeled fraction. An *etnE* phylogenetic tree (Figure S2.3) revealed that the *etnE* in these two fractions were similar and that they grouped with the *etnE* from *Nocardioides* sp. JS614 (bootstrap value of 99%).

A percent identity matrix (Table S2.2) further showed that *etnE* was highly conserved among the light (L4) and heavy (L9) fractions, varying from 94.7% to 100% identical to each other. An exception is clone L4-10, which was 94.7% to 95.2% identical to the remaining sequences. Sequences from the light fraction (L4) were 97.8% to 100% identical to each other, while sequences within the heavy fraction were 99.2% to 99.9% identical to each other.

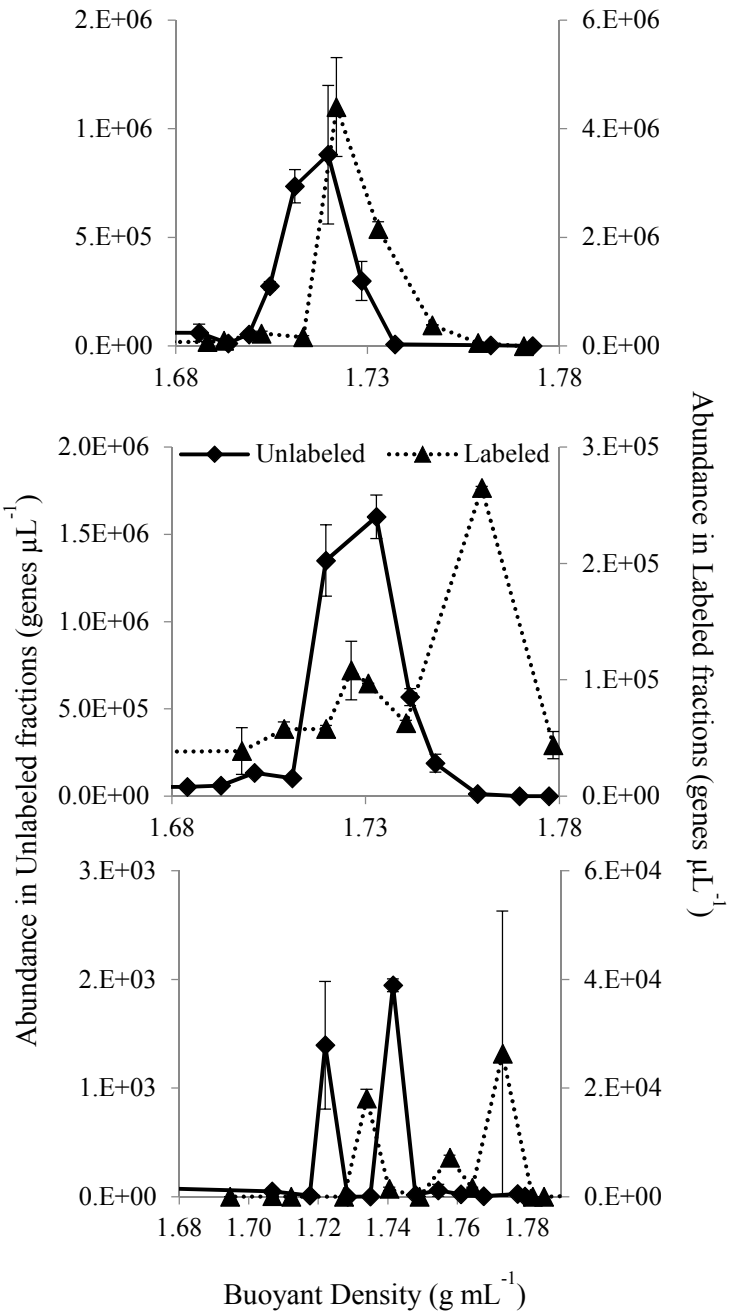

Figure 2.3. *etnE* copies after fractionation from 13C-VC amended (triangles, labeled) and 12C-VC amended (diamonds, unlabeled) cultures at day 15 (A), day 32 (B), and day 45 (C). The etnE abundance represents the average of duplicate samples and the error bars depict the standard deviation.

Discussion

In this study, VC-assimilating microorganisms were investigated in a mixed culture derived from contaminated site groundwater using SIP, high throughput sequencing and qPCR. Although others have isolated VC-assimilating microorganisms [4-13], the microorganisms responsible for VC assimilation within a mixed culture is more challenging to determine. Such research is important because there is likely a greater diversity of VC assimilators in the environment than is currently represented in pure culture.

Here, four phylotypes were responsible for ^{13}C uptake (Figure 2.2). As with many other SIP studies, it is unclear if these phylotypes were involved in label uptake directly from VC or from VC degradation products. VC-assimilators are known to use an alkene monooxygenase to attack VC [3] which forms VC epoxide (chlorooxirane). This intermediate is very unstable in aqueous systems (~1.6-minute half-life). It can spontaneously rearrange into chloroacetaldehyde [42]. It can also undergo hydrolysis to glycolaldehyde. It is possible that rearrangement or hydrolysis of VC epoxide occurred in the mixed culture and that label uptake by bacteria that are not true VC assimilators may have also occurred.

From the *Proteobacteria,* the phylotypes *Brevundimonas* (*Alphaproteobacteria*) and *Rhodoferax* (*Betaproteobacteria*) were observed in the heavy fractions from the ^{13}C-VC amended cultures at both time points. Previously identified VC-assimilators in this phylum include *Pseudomonas* (*Gammaproteobacteria*) [4, 11], *Ochrobactrum* (*Alphaproteobacteria*) [11], and *Ralstonia* (*Betaproteobacteria*) [10]. In the current study, sequences corresponding to the genera *Pseudomonas* and *Ralstonia* were present but were not enriched in the heavy fractions.

From the phylum *Firmicutes*, one phylotype (*Tissierella*) was observed in the heavy fractions from the ^{13}C VC amended cultures at both time points. This phylum (*Firmicutes*) has not yet been associated with VC assimilation, but has been previously reported in sites contaminated with chlorinated solvents [43].

Similar to previous research [12], the current study indicated the phylotype *Nocardioides* (*Actinobacteria*) was responsible for carbon assimilation from VC. This phylotype was observed in the heavy fractions from the ^{13}C-VC amended cultures at both day 32 and at day 45. Additionally, *Nocardioides* was a significant community member in all four cultures (4.1, 6.2, 8.9, 18.7 %). The other previously reported VC assimilating phylotype (*Mycobacterium*) within the *Actinobacteria* [5-9, 12, 13] was observed in the culture only at low levels (relative abundance 0.001-0.079%) and was not found in the heavy fractions, indicating it was not responsible for carbon assimilation from VC. Overall, of the four enriched phylotypes, *Nocardioides* is the only microorganism previously linked to VC assimilation.

The shift in *etnE* abundance towards the heavier fractions during VC degradation indicates the accumulation of ^{13}C in *etnE*. The strongest shift was at day 32, therefore this time likely represents the greatest label uptake from VC. The shift is less clear at day 45, possibly indicating label cross feeding. Also, the limited shift at day 15 suggests label uptake was minor early in the incubation. These observations guided the sequencing efforts to day 32 and day 45 samples. Each of the 19 unique *etnE* sequences retrieved from both light (L4) and heavy (L9) fractions formed a clade (a grouping) with the *etnE* from *Nocardioides* sp. JS614. This pattern contrasts with previous studies where VC- or ethene-degrading isolates were primarily *Mycobacterium* spp. [26]. The data suggests that potentially greater *etnE* diversity is present within the ethene- and VC-assimilating *Nocardioides* spp., or that *Nocardioides*-like *etnE*

sequences are more widely distributed in the environment than *Mycobacterium*-like *etnE*. It is interesting to note that although the VC assimilators identified by SIP are relatively diverse in comparison to known isolates, the *etnE* genes harbored by these bacteria appear to be relatively conserved.

In summary, the microorganisms responsible for assimilating ^{13}C from VC within a mixed culture derived from contaminated site groundwater were identified. SIP analysis and Illumina sequencing indicated *Nocardioides* was a dominant culture phylotype as well as a key ^{13}C assimilator. Therefore, both a previously identified VC-assimilating genus (*Nocardioides*) as well as novel microorganisms (*Rhodoferax, Tissierella* and *Brevundimonas*) were responsible for carbon uptake from VC. Interestingly, *Rhodoferax* was enriched to the highest level and could therefore represent a particularly important novel VC degrader. Despite the diversity of newly discovered VC-assimilators, the functional gene *etnE* associated with VC assimilation was relatively conserved in this mixed culture.

Acknowledgments

We thank James Begley and Bioremediation Consulting, Inc. for coordinating the sampling of Carver, MA groundwater, and Yang Oh Jin for initial development and maintenance of the VC-degrading culture used in this study. This work was funded by a collaborative NSF Grant (number 1233154) awarded to T. E. Mattes and A. M. Cupples.

The authors have no conflict of interest with the methods and data described in this manuscript.

APPENDIX

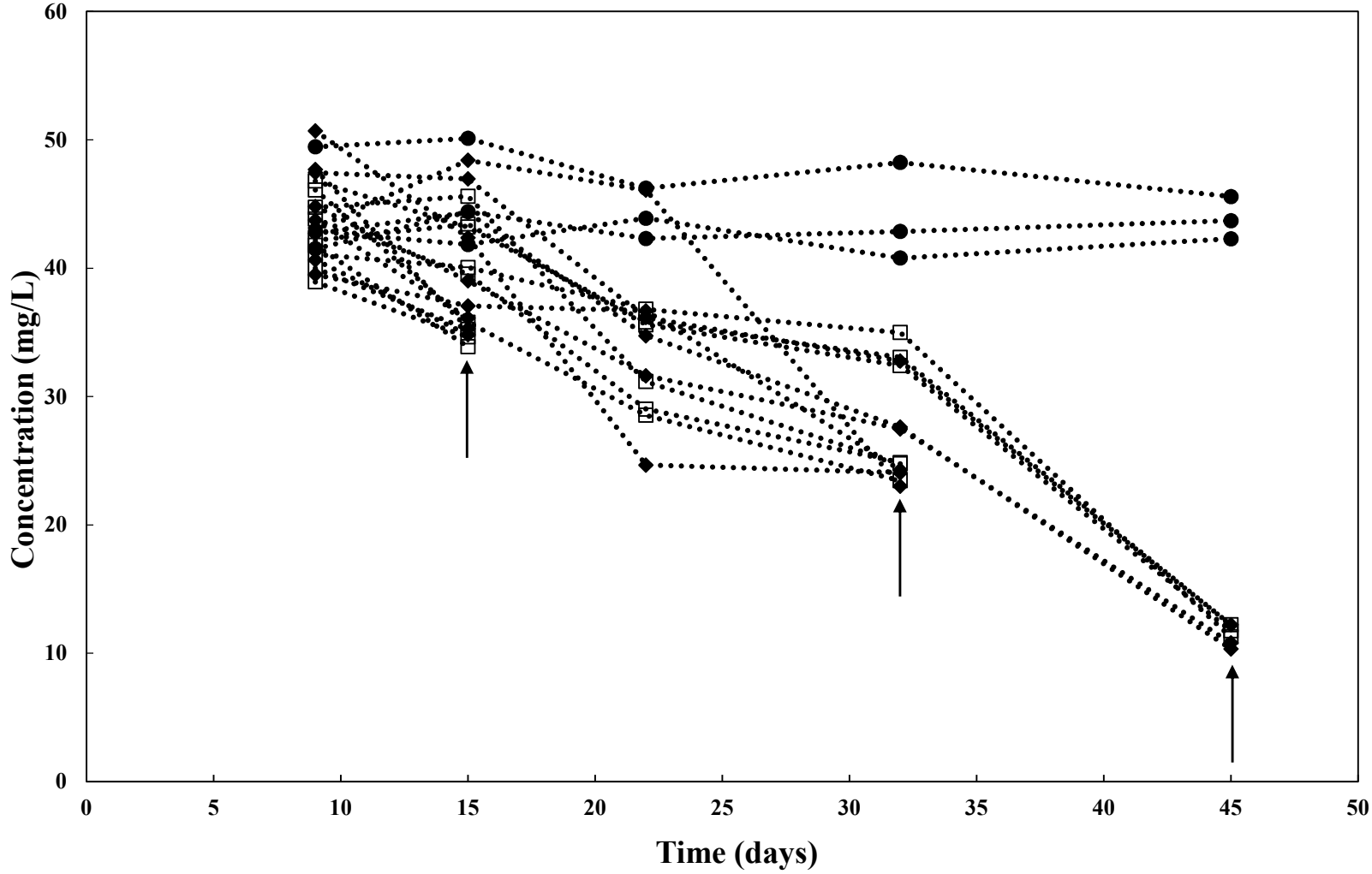

Figure S2.1. Vinyl chloride concentrations in ^{13}C vinyl chloride amended (□), ^{12}C vinyl chloride amended (◆) microcosms and abiotic controls (●). Arrows indicate when DNA was extracted (day 15, 32 and 45).

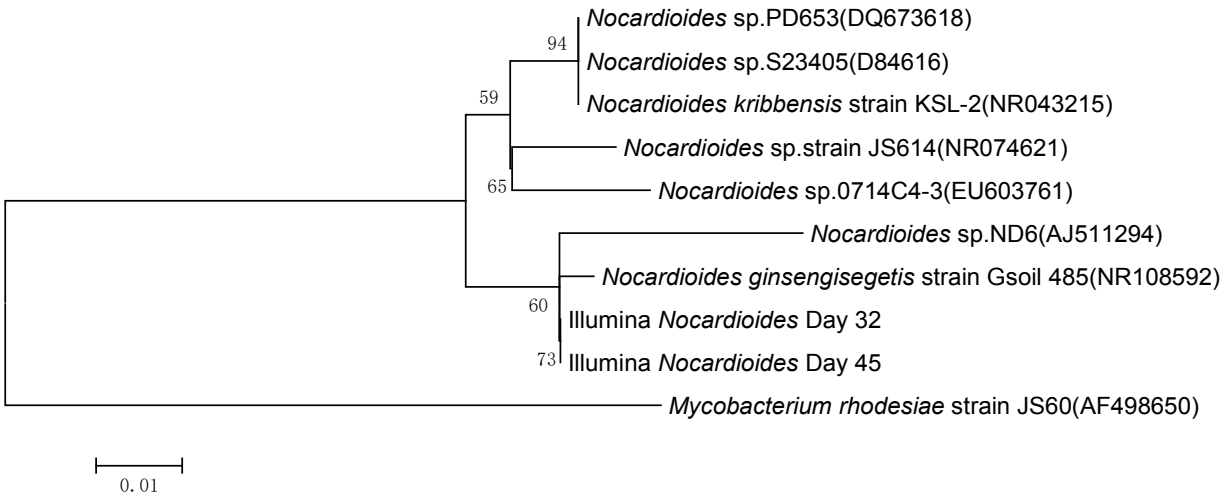

Figure S2.2. Phylogenetic tree based on 16S rRNA gene sequences showing the relationships of the *Nocardioides* sequences identified in this study to the most similar sequences in RDP Seqmatch (Cole et al 2014). Illumina sequences were the most abundant *Nocardioides* sequences at day 32 and 45. Ten sequences were aligned and trimmed to 254 bp and visualized in MEGA (Tamura et al 2011). The evolutionary history was inferred using the maximum likelihood method with the bootstrap test (5,000 replicates) (Felsenstein 1985). The evolutionary distances were computed using the Jukes-Cantor method (Jukes and Cantor 1969) with the scale bar representing 1.0% sequence difference. The tree was rooted with 16S rRNA gene from *Mycobacterium rhodesiae* strain JS60, a VC- and ethene-assimilating bacterium.

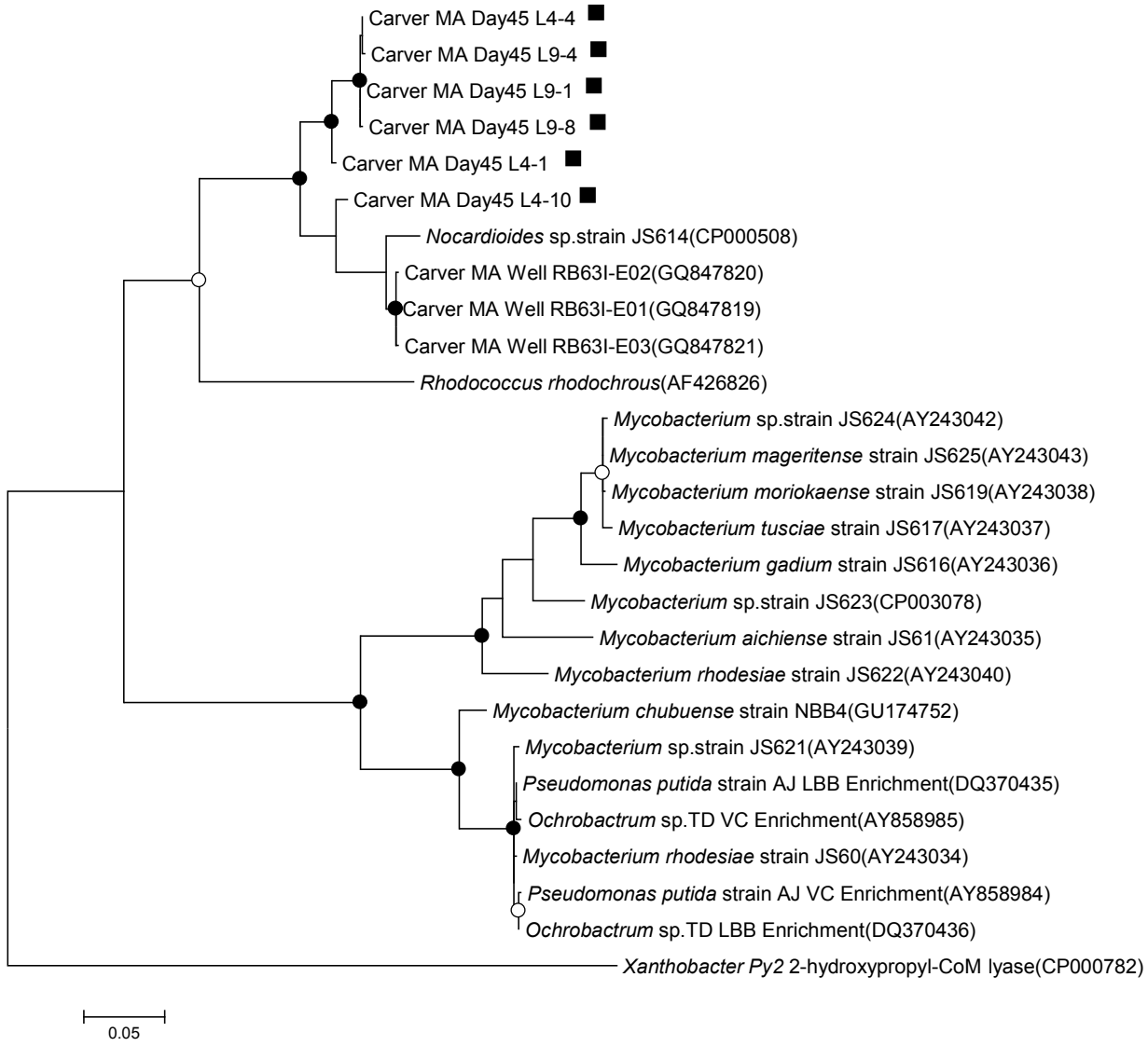

Figure S2.3. Phylogenetic relationships of selected *etnE* fragments recovered from fractions L4 and L9 of Carver MA composite groundwater ^{13}C-labeled VC enrichment culture, with sequences from previous Carver site enrichments and Genbank. All the sequences were aligned using ClustalW (Thompson et al 2002) and trimmed to 733 bp (with gaps). A maximum likelihood tree was constructed based on this 733 bp nucleotide alignment and visualized by MEGA5 (Tamura et al 2011),with the scale bar representing 5% sequence differences. Bootstrap values between 80-95% were indicated by open circles and above 95% were indicated by solid circles. The tree was rooted with the 2-hydroxypropyl-CoM lyase gene from the propene-oxidizing *Xanthobacter autotrophicus* Py2. Sequences from SIP fractions are denoted with solid squares.

Table S2.1. *etnE* qPCR data on fractions from the ^{13}C-VC and ^{12}C-VC amended enrichment cultures.

	Day 15				Day 32				Day 45			
	BD (mg/L)	Genes/ µL of fractions			BD (mg/L)	Genes/ µL of fractions			BD (mg/L)	Genes/ µL of fractions		
		Mean	SD	N		Mean	SD	N		Mean	SD	N
Labeled ^{13}C-VC	1.771	1034	291	2	1.778	43830	11686	2	1.799	359	31	2
	1.759	57467	10377	2	1.760	264703	1379	2	1.785	0	0	2
	1.747	385343	2214	2	1.740	62721	2536	2	1.782	0	0	2
	1.733	2160000	130000	2	1.731	96699	288	2	1.773	26319	26301	2
	1.722	4400000	910000	2	1.726	108039	25158	2	1.764	1624	108	2
	1.713	164845	22485	2	1.720	57907	2774	2	1.758	7171	446	2
	1.702	233083	40669	2	1.709	57634	6296	2	1.749	0	0	2
	1.693	101907	5778	2	1.698	38850	20018	2	1.740	1440	315	2
	1.688	74831	4785	2	1.621	36704	1811	2	1.734	18083	1693	2
	1.679	77290	9262	2	1.221	13671	4297	2	1.727	0	0	2
	1.478	131568	3494	2	1.020	2010	162	2	1.712	0	0	2
	1.172	68647	27598	2	0.995	17595	2574	2	1.707	79	3	2
	1.063	29750	805	2	0.981	6512	6468	2	1.694	5	1	2
Unlabeled ^{12}C-VC	1.773	506	9	2	1.777	355	98	2	1.780	3	2	2
	1.762	3311	819	2	1.770	74	14	2	1.777	26	1	2
	1.737	7035	4334	2	1.759	13135	2536	2	1.768	4	3	2
	1.728	299435	89365	2	1.748	189017	50476	2	1.761	23	4	2
	1.720	880662	318791	2	1.741	567768	48193	2	1.755	57	56	2
	1.711	735041	76711	2	1.733	1600000	125000	2	1.748	17	17	2
	1.705	276200	19972	2	1.720	1350000	205000	2	1.741	1946	58	2
	1.699	53772	13693	2	1.711	103024	469	2	1.735	1	0	2
	1.694	12694	12405	2	1.701	133876	13503	2	1.728	0	0	2
	1.686	61108	39804	2	1.693	60521	8264	2	1.722	1395	588	2
	1.537	64433	10920	2	1.684	53978	17044	2	1.718	11	2	2
	1.179	23240	4528	2	1.131	9113	295	2	1.707	48	30	2
	1.057	22013	5421	2	1.039	2071	214	2	1.625	121	121	2

Table S2.2. Percent identity matrix of *etnE* from clones of heavy fraction L4 and light fraction L9.

Sequence	L4-1	L4-2	L4-3	L4-4	L4-5	L4-6	L4-8	L4-9	L4-10	L9-1	L9-2	L9-3	L9-4	L9-5	L9-6	L9-7	L9-8	L9-9	L9-10
L4-1																			
L4-2	98.3																		
L4-3	98.3	99.8																	
L4-4	97.8	99.4	99.2																
L4-5	98.3	100	99.8	99.4															
L4-6	97.9	99.6	99.3	99.2	99.6														
L4-8	97.8	99.2	99.2	99.1	99.2	99													
L4-9	98.3	99.8	99.8	99.2	99.8	99.3	99.2												
L4-10	95.4	95	95	95	95	94.8	94.7	95											
L9-1	98.3	99.8	99.8	99.4	99.8	99.3	99.4	99.8	95										
L9-2	98.1	99.8	99.6	99.4	99.8	99.6	99.2	99.6	95	99.6									
L9-3	98.2	99.7	99.7	99.3	99.7	99.3	99.3	99.7	94.9	99.9	99.4								
L9-4	97.9	99.6	99.3	99.7	99.6	99.3	99.2	99.3	94.9	99.6	99.6	99.4							
L9-5	98.3	99.8	99.8	99.2	99.8	99.3	99.2	99.8	95	99.8	99.6	99.7	99.3						
L9-6	98.4	99.9	99.9	99.3	99.9	99.4	99.3	99.9	95.2	99.9	99.7	99.8	99.4	99.9					
L9-7	98.3	100	99.8	99.4	100	99.6	99.2	99.8	95	99.8	99.8	99.7	99.6	99.8	99.9				
L9-8	98	99.4	99.4	99.3	99.4	99.2	99.3	99.4	94.9	99.7	99.4	99.6	99.4	99.4	99.6	99.4			
L9-9	98.1	99.8	99.6	99.2	99.8	99.3	99	99.6	94.8	99.6	99.6	99.4	99.3	99.6	99.7	99.8	99.2		
L9-10	98.1	99.8	99.6	99.2	99.8	99.3	99	99.6	94.8	99.6	99.6	99.4	99.3	99.6	99.7	99.8	99.2	99.6	

<=95
95-98
99-100

Partial *etnE* sequences from cloning were aligned and trimmed down to 887bp. A percent identity matrix was generated using Clustal Omega (http://www.ebi.ac.uk/Tools/msa/clustalo/).

REFERENCES

REFERENCES

[1] J.R. Bucher, G. Cooper, J.K. Haseman, C.W. Jameson, M. Longnecker, F. Kamel, R. Maronpot, H.B. Matthews, R. Melnick, R. Newbold, Report on Carcinogens, 11th edition US Department of Health and Human Services, Public Health Service National Toxicology Program, Research Triangle Park, NC, (2005).

[2] P.M. Bradley, History and ecology of chloroethene biodegradation: A review, Bioremed J, 7 (2003) 81-109.

[3] T.E. Mattes, A.K. Alexander, N.V. Coleman, Aerobic biodegradation of the chloroethenes: pathways, enzymes, ecology, and evolution, FEMS Microbiol Rev, 34 (2010) 445-475.

[4] M.F. Verce, R.L. Ulrich, D.L. Freedman, Characterization of an isolate that uses vinyl chloride as a growth substrate under aerobic conditions, Appl Environ Microbiol, 66 (2000) 3535-3542.

[5] A.E. Taylor, M.E. Dolan, P.J. Bottomley, L. Semprini, Utilization of fluoroethene as a surrogate for aerobic vinyl chloride transformation, Environ Sci Technol, 41 (2007) 6378-6383.

[6] Y.O. Jin, S. Cheung, N.V. Coleman, T.E. Mattes, Association of missense mutations in epoxyalkane Coenzyme M transferase with adaptation of *Mycobacterium* sp strain JS623 to growth on vinyl chloride, Appl Environ Microbiol, 76 (2010) 3413-3419.

[7] Y.O. Jin, T.E. Mattes, Adaptation of aerobic, ethene-assimilating *Mycobacterium* strains to vinyl chloride as a growth substrate, Environ Sci Technol, 42 (2008) 4784-4789.

[8] S. Hartmans, J.A.M. Debont, Aerobic vinyl chloride metabolism in *Mycobacterium aurum* L1, Appl Environ Microbiol, 58 (1992) 1220-1226.

[9] B.Z. Fathepure, V.K. Elango, H. Singh, M.A. Bruner, Bioaugmentation potential of a vinyl chloride-assimilating *Mycobacterium* sp., isolated from a chloroethene-contaminated aquifer, FEMS Micro Lett, 248 (2005) 227-234.

[10] V.K. Elango, A.S. Liggenstoffer, B.Z. Fathepure, Biodegradation of vinyl chloride and *cis*-dichloroethene by a *Ralstonia* sp strain TRW-1, Appl Micro Biotec, 72 (2006) 1270-1275.

[11] A.S. Danko, M.Z. Luo, C.E. Bagwell, R.L. Brigmon, D.L. Freedman, Involvement of linear plasmids in aerobic biodegradation of vinyl chloride, Appl Environ Microbiol, 70 (2004) 6092-6097.

[12] N.V. Coleman, T.E. Mattes, J.M. Gossett, J.C. Spain, Phylogenetic and kinetic diversity of aerobic vinyl chloride-assimilating bacteria from contaminated sites, Appl Environ Microbiol, 68 (2002) 6162-6171.

[13] S. Hartmans, J.A.M. Debont, J. Tramper, K. Luyben, Bacterial degradation of vinyl chloride, Biotechnol Lett, 7 (1985) 383-388.

[14] Y.O. Jin, T.E. Mattes, Assessment and modification of degenerate qPCR primers that amplify functional genes from etheneotrophs and vinyl chloride-assimilators, Lett Appl Microbiol, 53 (2011) 576-580.

[15] Y.O. Jin, T.E. Mattes, A quantitative PCR assay for aerobic, vinyl chloride- and ethene-assimilating microorganisms in groundwater, Environ Sci Technol, 44 (2010) 9036-9041.

[16] B.M. Patterson, R. Aravena, G.B. Davis, A.J. Furness, T.P. Bastow, D. Bouchard, Multiple lines of evidence to demonstrate vinyl chloride aerobic biodegradation in the vadose zone, and factors controlling rates, J Contam Hydrol, 153 (2013) 69-77.

[17] S. Atashgahi, F. Maphosa, E. Dogan, H. Smidt, D. Springael, W. Dejonghe, Small-scale oxygen distribution determines the vinyl chloride biodegradation pathway in surficial sediments of riverbed hyporheic zones, FEMS Microbiol Ecol, 84 (2013) 133-142.

[18] S. Radajewski, P. Ineson, N.R. Parekh, J.C. Murrell, Stable-isotope probing as a tool in microbial ecology, Nature, 403 (2000) 646-649.

[19] M.G. Dumont, J.C. Murrell, Stable isotope probing - linking microbial identity to function, Nat Rev Microbiol, 3 (2005) 499-504.

[20] C. Luo, S. Xie, W. Sun, X. Li, A.M. Cupples, Identification of a novel toluene-degrading bacterium from the candidate phylum TM7, as determined by DNA stable isotope probing, Appl Environ Microbiol, 75 (2009) 4644-4647.

[21] W. Sun, S. Xie, C. Luo, A.M. Cupples, Direct link between toluene degradation in contaminated-site microcosms and a *Polaromonas* strain, Appl Environ Microbiol, 76 (2010) 956-959.

[22] W.M. Sun, A.M. Cupples, Diversity of five anaerobic toluene-degrading microbial communities investigated using stable isotope probing, Appl Environ Microbiol, 78 (2012) 972-980.

[23] T. Lueders, B. Wagner, P. Claus, M.W. Friedrich, Stable isotope probing of rRNA and DNA reveals a dynamic methylotroph community and trophic interactions with fungi and protozoa in oxic rice field soil, Environ Microbiol, 6 (2004) 60-72.

[24] D.R. Singleton, S.N. Powell, R. Sangaiah, A. Gold, L.M. Ball, M.D. Aitken, Stable-isotope probing of bacteria capable of degrading salicylate, naphthalene, or phenanthrene in a bioreactor treating contaminated soil, Appl Environ Microbiol, 71 (2005) 1202-1209.

[25] E.L. Madsen, The use of stable isotope probing techniques in bioreactor and field studies on bioremediation, Curr Opin Biotech, 17 (2006) 92-97.

[26] A.S. Chuang, Y.O. Jin, L.S. Schmidt, Y.L. Li, S. Fogel, D. Smoler, T.E. Mattes, Proteomic analysis of ethene-enriched groundwater microcosms from a vinyl chloride-contaminated site, Environ Sci Technol, 44 (2010) 1594-1601.

[27] J.F. Begley, M. Czarnecki, S. Kemen, A. Verardo, A.K. Robb, S. Fogel, G.S. Begley, Oxygen and ethene biostimulation for a persistent dilute vinyl chloride plume, Ground Water Monit R, 32 (2012) 99-105.

[28] J.F. Begley, E. Hansen, A.K. Wells, S. Fogel, G.S. Begley, Assessment and monitoring tools for aerobic bioremediation of vinyl chloride in groundwater, Remediat J, 20 (2009) 107-117.

[29] T.E. Mattes, N.V. Coleman, J.M. Gossett, J.C. Spain, Physiological and molecular genetic analyses of vinyl chloride and ethene biodegradation in *Nocardioides* sp. strain JS614, Arch Microbiol, 183 (2005) 95-106.

[30] J.M. Gossett, Measurement of Henrys Law constants for C1 and C2 chlorinated hydrocarbons, Environ Sci Technol, 21 (1987) 202-208.

[31] N.V. Coleman, T.E. Mattes, J.M. Gossett, J.C. Spain, Biodegradation of *cis*-dichloroethene as the sole carbon source by a beta-proteobacterium, Appl Environ Microbiol, 68 (2002) 2726-2730.

[32] W. Sun, X. Sun, A.M. Cupples, Anaerobic methyl tert-butyl ether-degrading microorganisms identified in wastewater treatment plant samples by stable isotope probing, Appl Environ Microbiol, 78 (2012) 2973-2980.

[33] J.G. Caporaso, C.L. Lauber, W.A. Walters, D. Berg-Lyons, C.A. Lozupone, P.J. Turnbaugh, N. Fierer, R. Knight, Global patterns of 16S rRNA diversity at a depth of millions of sequences per sample, PNAS, 108 (2011) 4516-4522.

[34] P.D. Schloss, A high-throughput DNA sequence aligner for microbial ecology studies, PLOS One, 4 (2009).

[35] J.J. Kozich, S.L. Westcott, N.T. Baxter, S.K. Highlander, P.D. Schloss, Development of a dual-index sequencing strategy and curation pipeline for analyzing amplicon sequence data on the MiSeq Illumina Sequencing Platform, Appl Environ Microbiol, 79 (2013) 5112-5120.

[36] E. Pruesse, C. Quast, K. Knittel, B.M. Fuchs, W. Ludwig, J. Peplies, F.O. Gloeckner, SILVA: a comprehensive online resource for quality checked and aligned ribosomal RNA sequence data compatible with ARB, Nucleic Acids Res, 35 (2007) 7188-7196.

[37] R.C. Edgar, B.J. Haas, J.C. Clemente, C. Quince, R. Knight, UCHIME improves sensitivity and speed of chimera detection, Bioinformatics, 27 (2011) 2194-2200.

[38] N.V. Coleman, J.C. Spain, Distribution of the coenzyme M pathway of epoxide metabolism among ethene- and vinyl chloride-degrading *Mycobacterium* strains, Appl Environ Microbiol, 69 (2003) 6041-6046.

[39] S.A. Bustin, V. Benes, J.A. Garson, J. Hellemans, J. Huggett, M. Kubista, R. Mueller, T. Nolan, M.W. Pfaffl, G.L. Shipley, J. Vandesompele, C.T. Wittwer, The MIQE guidelines: minimum information for publication of quantitative real-time PCR experiments, Clin Chem, 55 (2009) 611-622.

[40] J.D. Thompson, T.J. Gibson, D.G. Higgins, Multiple sequence alignment using ClustalW and ClustalX, in: Curr Protoc Bioinformatics, John Wiley & Sons, Inc., 2002.

[41] K. Tamura, D. Peterson, N. Peterson, G. Stecher, M. Nei, S. Kumar, MEGA5: molecular evolutionary genetics analysis using maximum likelihood, evolutionary distance, and maximum parsimony methods, Mol Biol Evol, 28 (2011) 2731-2739.

[42] A. Barbin, H. Bresil, A. Croisy, P. Jacquignon, C. Malaveille, R. Montesano, H. Bartsch, Liver-microsome-mediated formation of alkylating-agents from vinyl bromide and vinyl chloride, Biochem Biophys Res Comm, 67 (1975) 596-603.

[43] T.R. Miller, M.P. Franklin, R.U. Halden, Bacterial community analysis of shallow groundwater undergoing sequential anaerobic and aerobic chloroethene biotransformation, FEMS Microbiol Ecol, 60 (2007) 299-311.

CHAPTER 3

NOVEL GENERA IDENTIFIED AS VINYL CHLORIDE ASSIMILATING MICROORGANISMS USING STABLE ISOTOPE PROBING

Abstract

Vinyl chloride (VC) is a common contaminant in surface water and groundwater. In this study, SIP was combined with high throughput sequencing (Illumina MiSeq) and quantitative PCR (qPCR) to identify microorganisms able to uptake carbon from VC (^{13}C labeled) in a mixed culture capable of rapid VC degradation (120 μmol in 7 days). Microcosms consisted of mineral media, micronutrients, mixed culture and labeled (^{13}C) or unlabeled VC. On days 3 and 7, replicate labeled and unlabeled VC microcosms were sacrificed for DNA extraction. The extracted DNA was ultracentrifuged and fractioned. The fractions of greater buoyant density (heavy fractions) were subject to high throughput sequencing for the identification of VC assimilators. Specific primers were designed for the phylotypes identified as responsible for label uptake. The new primers were then tested for specificity using 16S rRNA gene clone libraries and Sanger sequencing. These primers were used in qPCR across the buoyant density gradient to confirm label uptake by these phylotypes. Four phylotypes were linked to VC assimilation, including *Nocardioides* (*Actinobacteria*)*, Sediminibacterium* (*Proteobacteria*)*, Aquabacterium (Proteobacteria)* and *Variovorax* (*Proteobacteria*). Therefore, both a previously identified VC-assimilating genus (*Nocardioides*) as well as novel genera were responsible for carbon uptake from VC. Identifying VC assimilators in mixed communities is important because there is likely a greater diversity of these microorganisms in the environment than is currently represented in

pure cultures. The primers designed in this study could be used to investigate the presence of these VC degraders at contaminated sites.

Introduction

Vinyl chloride (VC) is a common contaminant in surface water and groundwater, threatening both environmental and human health. This chemical is classified as a human carcinogen, with a Maximum Contamination Level of 0.002 mg L^{-1} and Public Health Goal of zero mg L^{-1} [1]. VC is the most carcinogenic of the chloroethenes and has the lowest regulatory limit in drinking water [2]. VC in groundwater originates primarily from the transformation of tetrachloroethene (PCE) and trichloroethene (TCE). These chlorinated ethenes are common contaminants due to their widespread use and previous careless disposal. In groundwater, natural biotic and abiotic processes degrade these solvents, leading to the accumulation of their more problematic metabolites, *cis*-dichloroethene and VC [3, 4].

The use of microorganisms in bioremediation occurs through monitored natural attenuation, biostimulation or bioaugmentation. To apply bioremediation, data is needed concerning the presence and abundance of the key microorganisms at the contaminated site. Frequently, this information originates from the molecular analysis of sediment or groundwater. The biodegradation of VC can occur by either anaerobic or aerobic pathways and by co-metabolism or direct VC assimilation [2]. Anaerobic transformation of VC by *Dehalococcoides spp.* can occur either by co-metabolism or direct VC reduction [4-6]. For the aerobic metabolism of VC, several bacteria belonging to the phyla *Actinobacteria* and *Proteobacteria* have been isolated from various environments or have been obtained in the laboratory [7-17]. While these organisms have greatly contributed to our understanding of VC metabolism, limitations

associated with culture-based methods have likely resulted in an incomplete understanding of VC-assimilating microorganisms at field sites.

To address the limitations associated with culture-based methods, molecular biology tools have been applied in many environmental studies. For example, SIP, has the advantage of linking function (e.g. carbon uptake) to microorganism identity in mixed microbial communities. This method was first introduced for investigating methanol-utilizing microorganisms in soil [18], but since then, has been used to identify microorganisms able to metabolize a variety of carbon and nitrogen sources. SIP involves sample exposure to a labeled compound (in this work, ^{13}C-VC) and DNA extraction over time. The DNA is then subjected to ultracentrifugation, fractionation (to separate label incorporated DNA from the unlabeled DNA) and DNA sequencing [19]. The phylotypes that are present in the heaviest fractions are considered responsible for incorporating the labeled carbon from the target chemical.

The overall objective here was to identify microorganisms associated with carbon uptake from VC in a mixed culture capable of rapid VC degradation. The present work combines SIP, high throughput sequencing and qPCR. Genus specific 16S rRNA primers were designed and tested for specificity for these VC-assimilators. These specific primers have the potential to advance our capability for monitoring VC bioremediation *in situ*.

Methods

Experimental design

Microcosms consisted of sterile serum bottles (160 mL), mixed culture (obtained from project collaborators at the University of Iowa), minimal salts medium (MSM) [7] and VC (~47

mg L^{-1}). These microcosms were prepared as previously described [20]. Two abiotic control microcosms (obtained via autoclaving) and six live microcosms were amended with unlabeled VC (99%, Specialty Gases of America, Toledo, OH) (to control for heavy GC microorganisms). In addition, six live microcosms were amended with ^{13}C-labeled VC ($^{13}C_2$ VC, 99%, Cambridge Isotope Laboratories, Xenia, OH). The microcosms were protected from light (room temperature, 21-23 °C) and were placed on a shaker (200-300 rpm). VC concentrations were monitored for 7 days and DNA was extracted (from labeled VC-amended and unlabeled VC-amended microcosms) at days 3 and 7.

Analytical methods

Headspace samples (100 μL) were analyzed via gas chromatography (Perkin Elmer, Waltham, MA) with flame ionization detection and a capillary column (DB-624, diameter 0.53 mm; J&W Scientific, Santa Clara, CA). Peak areas were compared to an external standard for VC quantification. Aqueous phase VC concentrations were calculated using previously reported Henry's Law constant [21].

DNA extraction, ultracentrifugation and fractionation

The Ultra Clean Microbial DNA Isolation Kit (MO BIO Laboratories, Inc., Carlsbad, CA) was used for total nucleic acid extraction according to the manufacturer's recommended procedure. Quantified DNA extracts (~10 μg) were loaded into Quick-Seal polyallomer tubes (13 by 51 mm, 5.1 mL; Beckman Coulter, Indianapolis, IN) along with a Tris-EDTA (pH 8.0)-CsCl solution for ultracentrifugation. Prior to sealing (cordless Quick-Seal tube topper; Beckman), the buoyant density (BD) was determined with a model AR200 digital refractometer

(Leica Microsystems Inc., Buffalo Grove, IL) and adjusted to a final BD of 1.73 g mL^{-1} by the addition of small volumes of CsCl solution or Tris-EDTA buffer. Tubes were ultracentrifuged at 178,000 × g (20 °C) for 48 h in a StepSaver 70 V6 vertical titanium rotor (8 by 5.1 mL capacity) within a Sorvall WX 80 Ultra Series centrifuge (Thermo Scientific, Waltham, MA). Following ultracentrifugation, the tubes were placed onto a fraction recovery system (Beckman), and fractions (~20, 150 µL each) were collected. The BD of each fraction was measured, and CsCl was removed by glycogen-assisted ethanol precipitation. The quantity of DNA obtained in each fraction was determined by Qubit™ (Invitrogen, Carlsbad, CA).

MiSeq Illumina sequencing and SIP fraction analysis

The four heaviest fractions from each time point (day 3 and 7) from the labeled VC-amended microcosms were analyzed to determine which microorganisms were enriched in these fractions and were therefore responsible for VC assimilation. The fractions were selected based on the DNA concentration in each fraction from the labeled VC amended microcosms compared to the unlabeled VC amended microcosms (see below). In all, 48 samples were subjected high throughput sequencing (MiSeq Illumina Sequencing) at the Research Technology Support Facility at Michigan State University (RTSF). These samples included six replicates per fraction, four fractions per time point, and two time points.

PCR and Illumina sequencing were performed at RSTF using a previously described protocol [22]. This involved the amplification of the V4 region of the 16S rRNA gene using a set of multiplex indexed primers. Following amplification, individual reactions were quantified (Picogreen assay), a pool of equimolar amounts of each was made, and these were purified using Ampure XP beads. A final gel purification step was included to ensure non-specific products

were eliminated. The combined library was loaded onto the Illumina MiSeq Platform using a standard MiSeq paired end (2x250 bp) flow cell and reagent cartridge.

The Mothur software [23] was used to analyze the data generated by MiSeq Illumina using a SOP developed by Schloss (http://www.mothur.org/wiki/MiSeq_SOP). This involved the construction of contigs, error and chimera removal followed by sequence alignment for OTU assignment based on the SILVA database [24]. Final data matrices were exported to Excel 2013 SR-1 (Microsoft Corporation, Redmond, WA). To identify which OTUs were responsible for the label uptake in each fraction at each time point, the relative abundance (%) of each OTU was calculated.

Primer design, 16S rRNA gene clone libraries and qPCR

Specific primers (*sedF* and *sedR*; *aquaF* and *aquaR*; and *varF* and *varR*) were designed to target the phylotypes responsible for the VC assimilation (identified above) using Primer-BLAST (http://www.ncbi.nlm.nih.gov/tools/primer-blast/). These new primers were tested for specificity using 16S rRNA gene clone libraries and Sanger sequencing. These primers were then used in the qPCR assays across the BD gradient to confirm label uptake.

Three 16S rRNA clone libraries were generated using total DNA extracted from the labeled microcosms from day 3. DNA was PCR-amplified using 3 primer sets: *sedF* (5'- CGG GCA GTT AAG TCA GTG GT-3') and *sedR* (5'- TGC CTT CGC AAT AGG TGT TCT-3'); *aquaF* (5'- CGT AGG GTG CGA GCG TTA AT-3') and *aquaR* (5' - CCA TCC CCC TCT ACC GTA CT-3'); and *varF* (5'-TCT GTG ACT GCA TTG CTG GA-3') and *varR* (5'-CGG TGT TCC TCC GCA TAT CT-3') (IDT, Integrated DNA Technologies, Coralville, IA). The PCR program consisted of an initial denaturation (95°C, 5 min), 29 cycles of amplification

(95°C, 30 s; 58°C, 30 s; 72°C 1:30 min), and a terminal extension step (72°C, 30 min). 3% agarose gel electrophoresis and the subsequent staining of the gels with ethidium bromide confirmed the presence of PCR products. The PCR products were purified with QIAquick PCR purification kit (Qiagen Inc., Alameda, CA) and cloned into *Escherichia coli* TOP10 vector supplied with a TOPO TA cloning kit (Invitrogen). Clones of *E. coli* were grown on Luria-Bertani (LB) medium solidified with 15 g agar L^{-1} with 50 μg ampicillin L^{-1} for 16 h at 37 ºC. Colonies with inserts were verified by PCR with primers M13F (5'-TGT AAA ACG ACG GCC AGT-3') and M13R (5'-AAC AGC TAT GA CAT G-3'), plasmids were extracted from the positive clones with a QIAprep miniprep system (Qiagen, Inc.) and the insertions were sequenced by RTSF. The clone sequences for each library were aligned against the Illumina sequences using MEGA 6 to determine the specificity of each primer set.

Amplification and qPCR measurements were conducted in a Chromo 4 real-time PCR cycler (Bio-Rad, Philadelphia, PA) using QuantiTect SYBR Green PCR Kit (Qiagen Inc.) and the primer sets *sedF-sedR*, *aquaF-aquaR* and *varF-varR*. DNA from both time points from the density gradient fractions from both the labeled VC and unlabeled VC amended microcosms were subject to qPCR in triplicate. Each 25 μL PCR mixture contained 12.5 μL QuantiTect SYBR Green PCR Master Mix solution, 1.25 μL each 10 μM primer, 9 μL DNA-free water and 1 μL DNA template. The thermal protocol consisted of an initial denaturation (95°C, 15 min), 40 cycles of amplification (95°C, 15 s; 58°C, 20 s; 72°C 20 s), and a terminal extension step (72°C, 2 min). Melting curves were constructed from 55°C to 95°C and read every 0.6°C for 2 s. Cloned plasmid DNA was used as a standard for quantification, and the numbers of gene copies were determined as previously described [25] (plasmid size was 3,931 bp, in addition to inserts of 148 bp by *sedF-sedR*, 139 bp by *aquaF-aquaR* and 86 bp by *varF-varR*).

Isolations

Aliquots from the day 7 cultures (SIP experiment, stored at 4 ºC) were diluted to 10^{-5} times the original solution. Dilutions of 0, 0.1, 0.001 and 0.00001 were spread plated on R2 agar. These plates were incubated for 48 h at 30 ºC under aerobic conditions, and the resulting visually distinct colonies were selected. Selected isolated colonies were re-inoculated into new R2 agar plates, until colonies were visually pure (between 5-10 rounds). Isolate identity was investigated using MiSeq Illumina sequencing and Mothur software (as described above).

Microbial community analysis during VC degradation

The VC experiment described above did not include a community analysis over the time course of VC degradation. Therefore, a new experiment was initiated to obtain these data. For this, frozen culture aliquots (5 mL) were incubated for 30 days in a sterile serum bottle (160 mL) containing minimal salts medium (MSM) and VC (~20 mg L^{-1}). Following VC degradation, 5 mL of fresh culture was added to sterile serum bottles (160 mL) containing minimal salts medium (MSM) [7] and VC (~47 mg L^{-1}). These microcosms were prepared as previously described [20], and included one abiotic control microcosm (obtained via autoclaving) and three live microcosms. The microcosms were protected from light (room temperature, 21-23 °C) and were placed on a shaker (200-300 rpm). VC concentrations were monitored for 18 days. DNA was extracted (as described above) from 6 time points and was analyzed using MiSeq Illumina and Mothur (as described above).

Results

VC degradation, fraction generation, DNA quantification and sequencing data

VC degradation occurred in both the labeled and unlabeled VC amended microcosms but not in the abiotic controls, confirming biological removal of VC by the mixed culture over a period of 7 days (Figure 3.1). The DNA samples extracted on days 3 and 7 were subjected to ultracentrifugation. On day 3, the DNA concentrations in each of these fractions varied from ~2-15 ng μL^{-1} for the labeled VC amended samples and from ~0.5 - 65 ng μL^{-1} for the unlabeled VC amended samples. On day 7, DNA concentrations varied from ~0.6-14 ng μL^{-1} and ~4 -55 ng μL^{-1}, for the labeled and unlabeled VC amended samples, respectively. DNA concentrations were plotted against BD values (Figure 3.2). The presence DNA in the lighter BD fractions from the unlabeled VC amended samples and DNA in the heavier fractions from the labeled VC amended samples confirms the uptake of labeled carbon by the microorganisms in the mixed community.

The DNA from the four heaviest fractions from the labeled microcosms on day 3 (BD values of 1.780, 1.772, 1.757 and 1.749 g mL^{-1}) and day 7 (BD values of 1.780, 1.769, 1.762 and 1.758 g mL^{-1}) was selected for further investigation. These samples (indicated by arrows in Figure 3.2), were submitted for Illumina sequencing. After Mothur analysis, the final number of sequences obtained was 2,010,477 and 2,073,705 for days 3 and 7, respectively. The chimeric percentage was 1.32% and 1.93% on days 3 and 7, respectively. Among the final sequences, < 2% were unique at both time points.

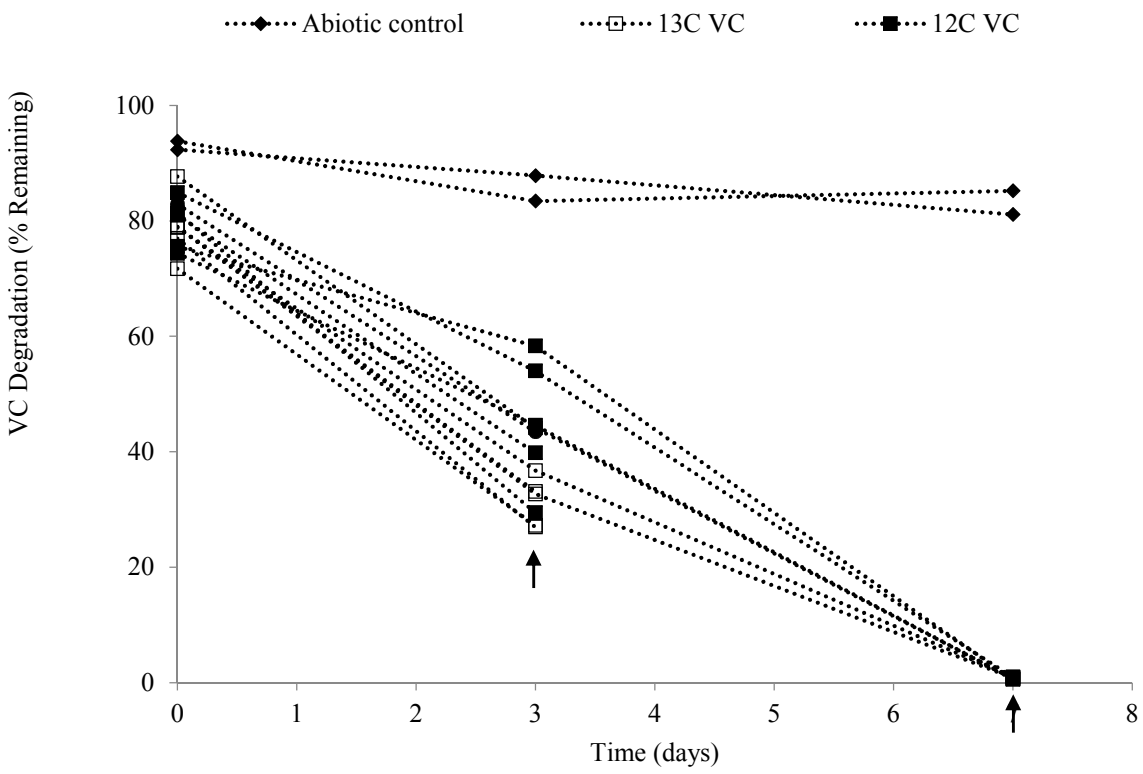

Figure 3.1. VC degradation over time in cultures amended with 13C vinyl chloride (□), 12C vinyl chloride (■) and abiotic controls (□). Arrows indicate when DNA was extracted.

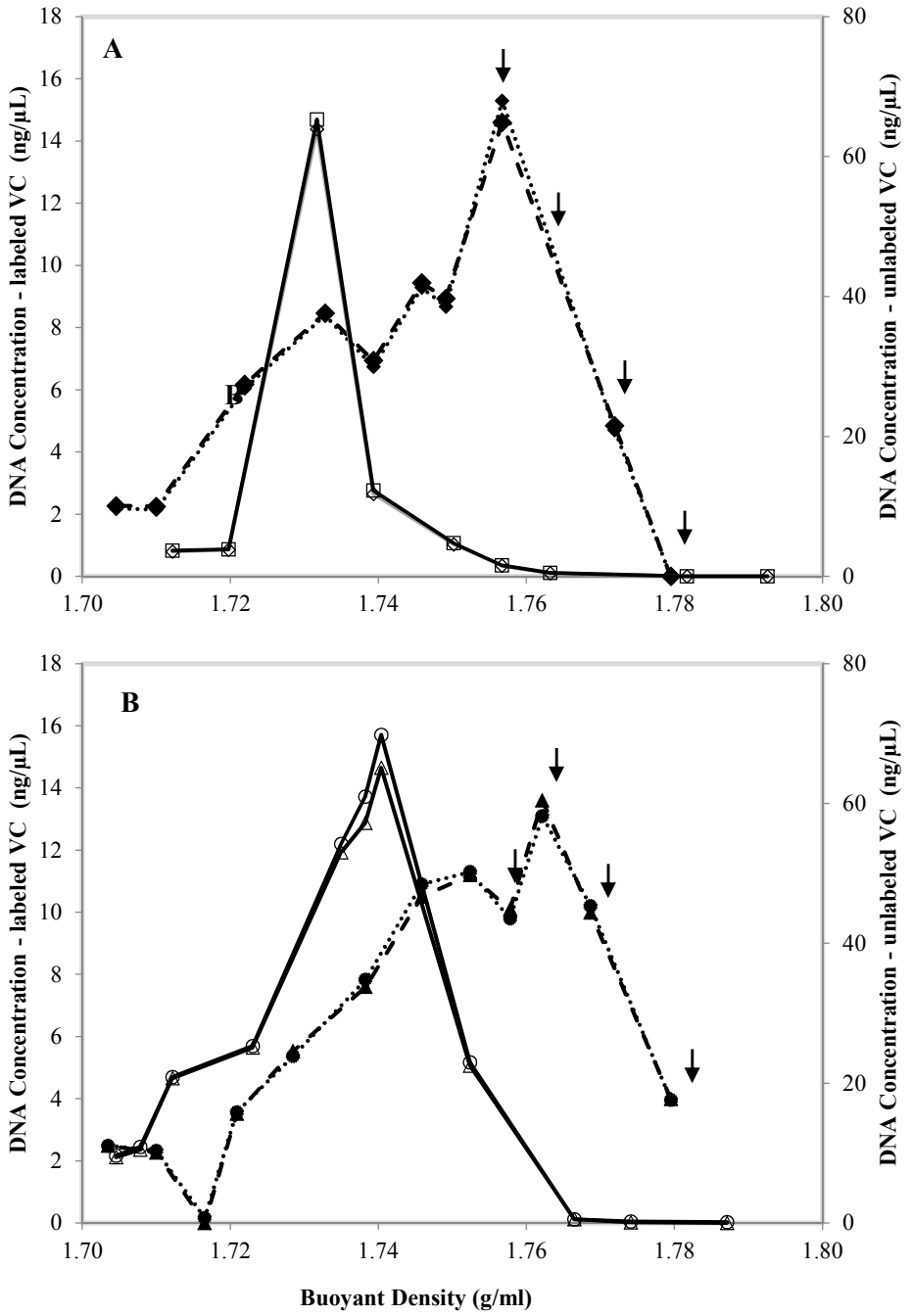

Figure 3.2. DNA concentration (ng/µL) at day 3 (A) and day 7 (B) in fractions obtained from the labeled VC and unlabeled VC amended cultures. The complete and dashed lines represent DNA concentrations from the unlabeled and labeled cultures, respectively. Replicate DNA measurements are shown. Arrows indicate samples selected for sequencing.

Identification of VC assimilators in heavy fractions

The microorganisms present in the heavy fractions were determined with high throughput sequencing. Two time points (day 3 and 7) were chosen to control for label cross feeding over time. Cross feeding may occur when a microorganism able to uptake the label produces metabolites (or dies); then the labeled element could be released and subsequently assimilated by other microorganisms. By considering label uptake over time, more information is gained on the primary assimilators.

On day 3, the most abundant phylotypes in the four heavy fractions classified within the phyla *Proteobacteria*, *Actinobacteria*, *Bacteroidetes* and *Verrucomicrobia* (Figure 3.3). The same phylotypes were abundant on day 7 except that *Stenotrophomonas* and *Sphingomonas* were present and *Burkholderia* and *Phenylobacterium* were absent (Figure 3.3). Interestingly, at both time points, four genera were dominant in the heavy fractions: *Nocardioides (Actinobacteria)* 33.4 – 49.7% on day 3 and 34.2 – 41.4% on day 7; *Sediminibacterium (Bacteroidetes)* 22.9 – 25.9% on day 3 and 22.2 – 29.4% on day 7; *Aquabacterium (Proteobacteria)* 10.3 – 22.1% on day 3 and 17.6 – 19.2% on day 7 and *Variovorax (Proteobacteria)* 3 – 4.3% on day 3 and 6.7 – 11.3% on day 7. The data indicate these are the key microorganisms assimilating the labeled carbon derived from VC in the mixed culture.

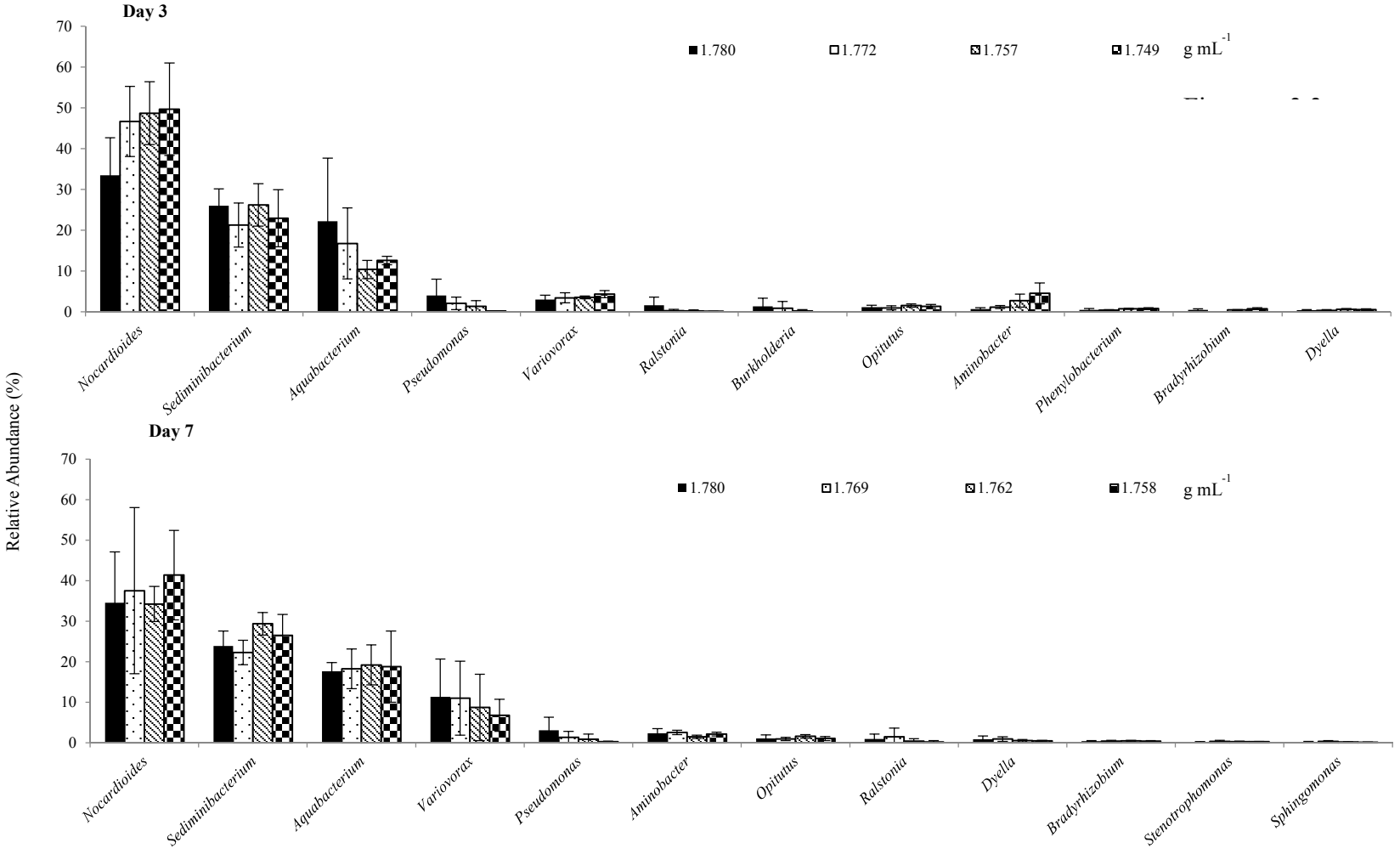

Figure 3.3. Relative abundance of phylotypes in the four heavy fractions from 13C VC amended cultures. The error bars represent standard deviations from six samples that were submitted for sequencing.

Primer design, specificity test and abundance in SIP fractions

The data generated by Illumina MiSeq sequencing was used to design specific primers to target three of the four dominant genera in the heavy fractions: *Sediminibacterium (Bacteroidetes)*, *Aquabacterium (Proteobacteria)* and *Variovorax (Proteobacteria).* *Nocardioides* was not targeted as this genus has already been linked to VC metabolism. The specificities of the designed primers were tested by amplifying DNA, creating 16S rRNA gene clone libraries, and then Sanger sequencing these clones. For this, 16 clones were sequenced for each primer set.

For *Sediminibacterium*, 14 of 16 clones (primer set *sedF* and *sedR*) were 100% identical with the *Sediminibacterium* sequence, and 2 of 16 clones aligned at a 99% identify level. For *Aquabacterium*, 13 of 16 clones (primer set *aquaF* and *aquaR*) aligned at 100%, 2 of 16 aligned at 99% and 1 of 16 aligned at 98% with the *Aquabacterium* sequence. For *Variovorax*, 8 of 13 clones (primer set *varF* and *varR*) aligned at 100% and 5 of 13 aligned at 98.8% with the *Variovorax* sequence. These data indicate the designed primers were specific to the targeted phylotypes.

Quantitative PCR assays for *Sediminibacterium* (*sedF* and *sedR*), *Aquabacterium* (*aquaF* and *aquaR*) and *Variovorax* (*varF* and *varR*) were performed on all of the fractions across the BD gradient to confirm label uptake by these phyloytpes at both time points. The average qPCR efficiencies for 16S rRNA genes amplified from primer sets *sedF-sedR*, *aquaF-aquaR* and *varF-varR* were high for all primer pairs and timepoints (greater than 96%). The average standardization slopes were -2.77 and -3.30 for *sedF-sedR,* -3.16 and -3.49 for *aquaF-aquaR* and -2.99 and -2.66 for *varF-varR* for days 3 and 7, respectively. On day 3, the R^2 values were 0.9796, 0.9905 and 0.9886 for *sedF-sedR*, *aquaF-aquaR* and *varF-varR*, respectively. For day 7,

the R^2 values were 0.9796, 0.9932, and 0.9862 for *sedF-sedR*, *aquaF-aquaR* and *varF-varR*, respectively. The detection limits were <100 copies μL^{-1} for all primer pairs. Overall, the highest unlabeled peaks were observed in the lighter BD fractions and the highest labeled peaks were observed in the heavier BD fractions.

Sediminibacterium 16S rRNA gene copies per µL over the BD ranged from $2.5x\ 10^2$ – $9.2x10^7$ for labeled and $1.3x10^2$ – $7.4x10^8$ for unlabeled microcosms on day 3 and from $2.3x10^2$ – $5.1x10^8$ for labeled and $1x10^2$ – $6x10^8$ for unlabeled microcosms on day 7. On day 3, the highest labeled microcosm peak occurred at BD 1.756 g mL^{-1} and the unlabeled microcosm peak occurred at BD 1.731 g mL^{-1}. A similar trend was observed on day 7, when the highest labeled microcosm peak was seeming at BD 1.766 g mL^{-1} and the unlabeled microcosm peak was seeming at BD 1.7425g mL^{-1} (Figure 3.4).

The range of 16S rRNA gene copies per µL for *Aquabacterium* varied from 0 – $6.1x10^5$ and 0 – $1x10^7$ for labeled and unlabeled microcosms on day 3 and $1.7x10^3$ – $7.9x10^8$ and $3.6x10^3$ – $1.6x10^9$ for labeled and unlabeled microcosms on day 7, respectively. Similarly, to *Sediminibacterium*, the highest unlabeled peak was observed at a lighter BD (1.719 g mL^{-1} on day 3 and 1.700 g mL^{-1} on day 7) and the highest labeled peak was observed at a heavier BD (1.756 g mL^{-1} on day 3 and 1.766 g mL−1 on day 7) (Figure 3.4).

The number of 16S rRNA gene copies per µL for *Variovorax* showed a noticeable increase from day 3 to day 7. On day 3, the number of copies varied from 0 – $5.3x10^4$ and 0 – $8.6x10^4$ for labeled and unlabeled microcosms and 0 – $3.2x10^9$ and 5 – $3.4x10^9$ for labeled and unlabeled microcosms on day 7. Similarly, to the other two genera, the highest unlabeled peak occurred at a lighter BD (1.712 g mL^{-1} on day 3 and 1.731 g mL^{-1} on day 7) and the labeled peak occurred at a heavier BD (1.756 g mL^{-1} on day 3 and 1.756 g mL^{-1} on day 7) (Figure 3).

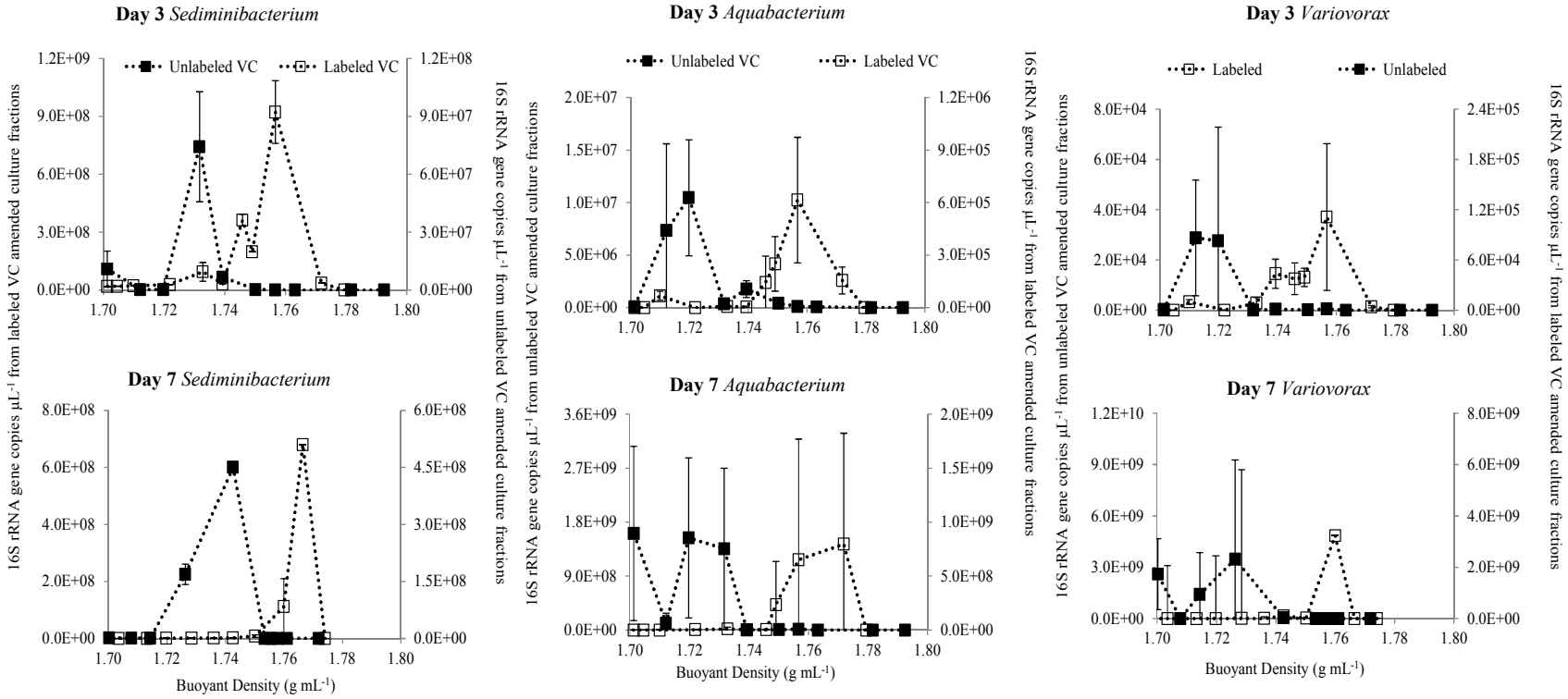

Figure 3.4. *Sediminibacterium, Aquabacterium and Variovorax* 16S rRNA gene copies over the buoyant density range in DNA extracted from labeled and unlabeled VC amended cultures at days 3 and 7. Error bars represent standard deviation from three qPCR measurements.

Isolations

Three visually distinct pure cultures were obtained after 10 rounds of purification. The DNA of these three cultures were extracted and submitted to MiSeq Illumina to determine if their identity would classify with the VC degraders (genera *Sediminibacterium, Aquabacterium* or *Variovorax*). Unfortunately, the Illumina data revealed that the sequences did not match the novel VC-degraders identified in this study. Instead, they classified as *Chryseobacterium, Rhodococcus* and *Stenotrophomonas*.

Microbial community during VC degradation

As expected, degradation of VC occurred in the live cultures but not in the abiotic control (Figure 3.5). DNA extracted over the time course of VC removal (days 2, 9, 10, 13, 14 and 16) was examined with high throughput sequencing. The data generated indicated that *Nocardioides* was dominant (18-33 % RA). Further, *Sediminibacterium, Aquabacterium* and *Pseudomonas* were present and appeared to increase with time (Figure 3.6). All four of these phylotypes were enriched in the heavy fractions, as described above (Figure 3.3), thus these results confirm their role in the uptake of carbon from VC.

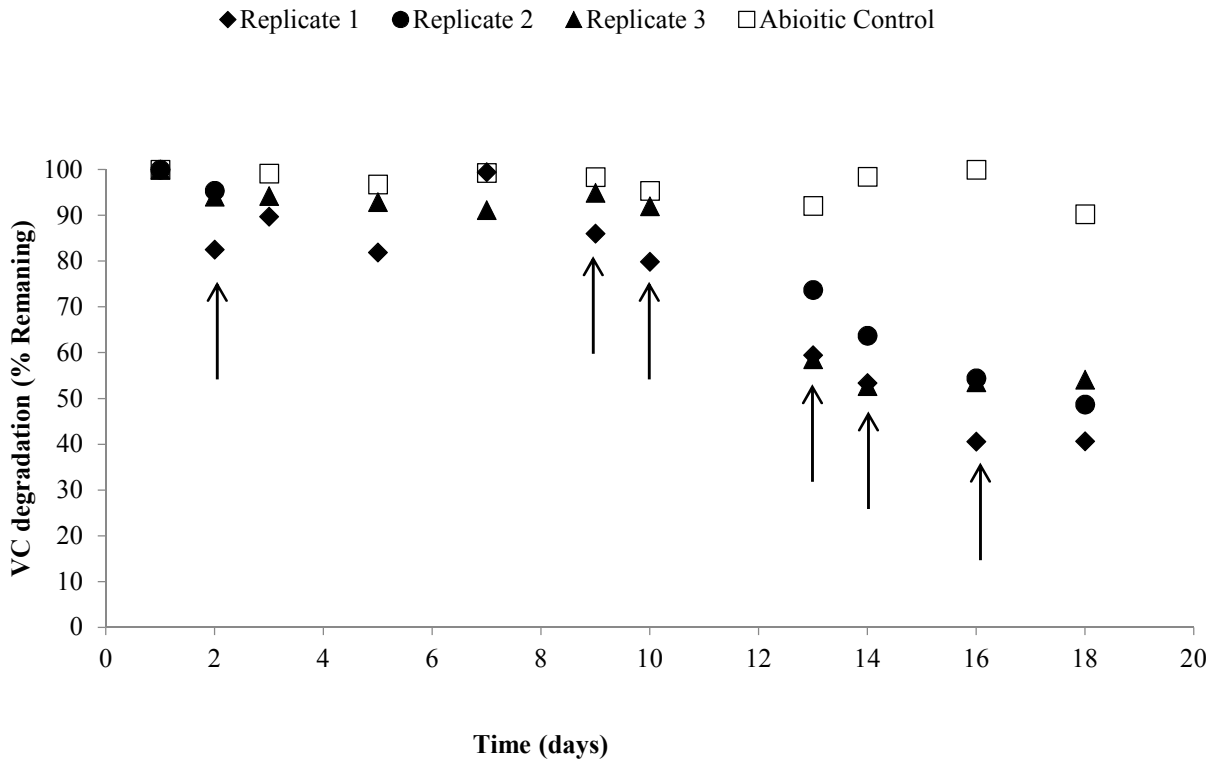

Figure 3.5. Vinyl chloride remaining over time in triplicate live culturesand an abiotic control. The arrows indicate when DNA was extracted from these samples for Illumina sequencing

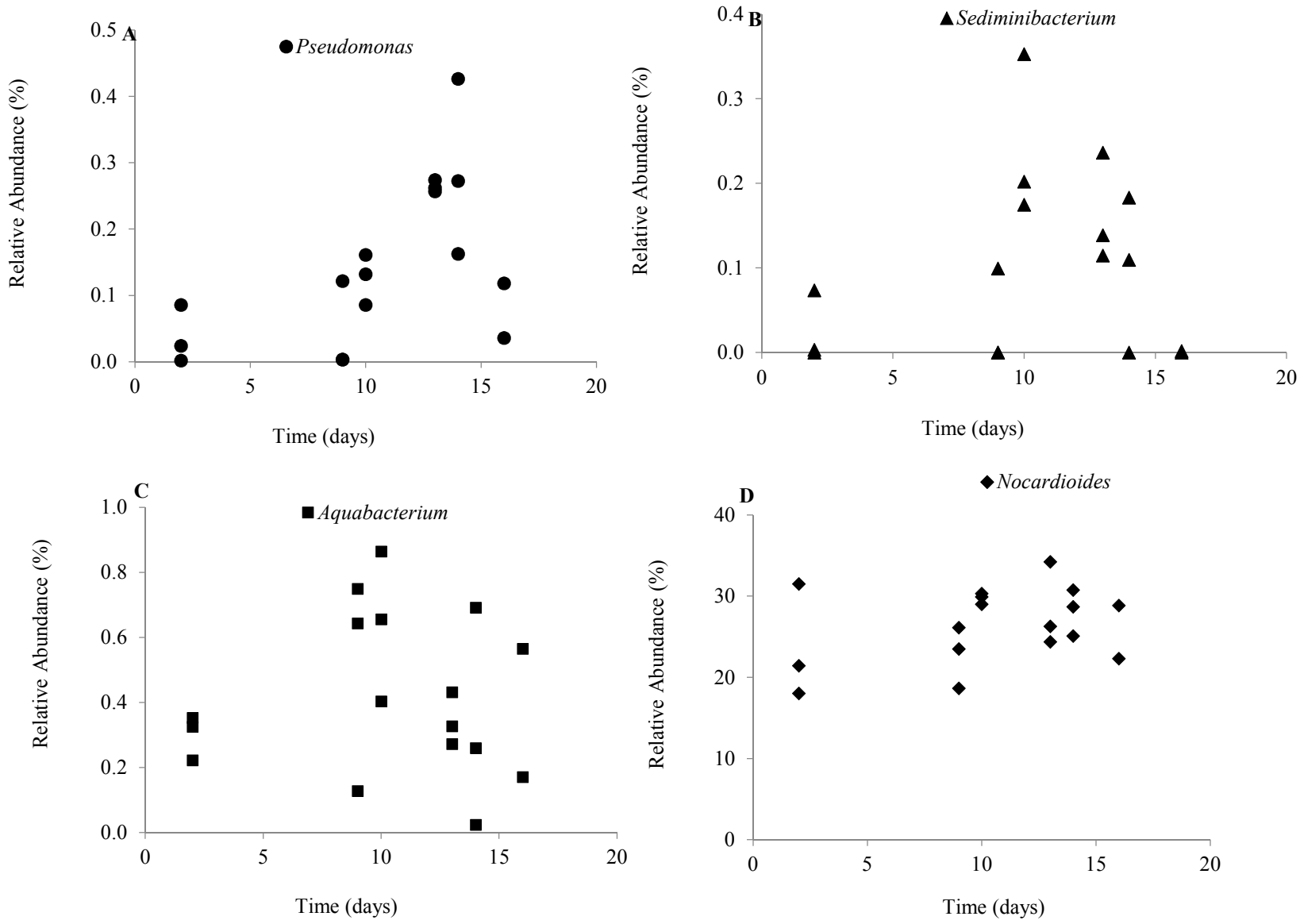

Figure 3.6. The relative abundance *Pseudomonas* (A), *Sediminibacterium* (B), *Aquabacterium* (C) and *Nocardioides* (D) in a vinyl chloride degrading culture. The y-axis has different scales. The relative abundance of *Variovorax* was <0.0017% in these cultures.

Discussion

VC was degraded by the mixed culture in only 7 days. Direct aerobic VC oxidation was first reported in groundwater samples from an aquifer [26] followed by other studies of aerobic degradation of VC that also isolated VC-degrading microorganisms [7-16]. These authors observed degradation over a wide range of time period, from as little as 2-20 days [10-13] to 55-476 days [9, 10, 15].

In the present study, active VC-assimilating microorganisms were identified from a mixed culture using SIP, high throughput sequencing and qPCR. These molecular tools were selected because the greater diversity of VC assimilators in the environment is likely not represented in pure culture. Following ultracentrifugation, the fractions obtained behaved as expected for SIP experiments (Figure 3.2), *i.e.*, is the presence of unlabeled peaks in the lighter BD fractions and labeled peaks in the heavier BD fractions confirmed the expected labeled VC uptake by the microcosms. The heavy fractions obtained from the labeled microcosms on days 3 and 7 were within the BD range previously found to contain ^{13}C labeled DNA (25, 26). In the present study, the sequencing data generated from the heavy fractions revealed four phylotypes primarily responsible for label uptake (Figure 3.3), whether directly from VC or from VC degradation products.

The most abundant phylotypes enriched in the heavy fractions were, *Nocardioides* (*Actinobacteria)*, *Sediminibacterium* (*Bacteroidetes*), *Aquabacterium* (*Proteobacteria*) and *Variovorax (Proteobacteria).* To date, known aerobic VC degrading microorganisms belong to the phyla *Actinobacteria* and *Proteobacteria*. Within these two phyla, isolated genera that have been reported include *Mycobacterium spp*. [7, 8, 10, 12, 14-16, 27], *Pseudomonas* [9, 28], *Nocardioides* [10], *Ochrobactrum* [11], and *Ralstonia* [13].

In agreement with previous research [10], the current study indicates that the genus *Nocardioides* (*Actinobacteria*) was primarily responsible for carbon uptake from VC. *Mycobacterium spp*. is the other VC-assimilating phylotype within the *Actinobacteria* [7, 8, 10, 12, 14-16], but it was not enriched in the current study. Overall, of the four enriched phylotypes, *Nocardioides* is the only genus previously linked to VC degradation [10].

The phylum *Bacteroidetes* has been associated with anaerobic, but not aerobic, degradation of VC [29], and has been found in contaminated groundwater sites [30], enrichment cultures capable of reducing TCE [31] and natural biofilms from household taps in drinking water distribution systems [32]. Additionally, the genus *Sediminibacterium* has been reported in groundwater sites contaminated with chlorinated aliphatic hydrocarbons [27].

Among the *Proteobacteria,* the genera *Aquabacterium* and *Variovorax* have not yet been associated with VC degradation, but *Aquabacterium* has been previously reported in groundwater sites contaminated with chlorinated aliphatic hydrocarbons [27]. Previously identified *Proteobacteria* VC degraders include *Pseudomonas* (*Gammaproteobacteria*) [9, 11], *Ochrobactrum* (*Alphaproteobacteria*) [11], and *Ralstonia* (*Betaproteobacteria*) [13]. In the current study, *Pseudomonas* and *Ralstonia* were present in the heavy fractions of the labeled microcosms, but their relatively lower abundance indicated that *Aquabacterium* and *Variovorax* contributed more to the VC degradation in this mixed community.

Quantitative PCR has emerged as the method of choice for enumerating targeted genes. *Dehalococcoides* 16S rRNA primers have been tested and used for site assessment and bioremediation implementation for chlorinated pollutants under anaerobic conditions [33]. In the present study, the 16S rRNA primers designed for the novel aerobic VC degraders identified by SIP (*Sediminibacterium*, *Aquabacterium* and *Variovorax)* were successfully tested for specificity

and applied to confirm label uptake from VC. The shifts observed in the 16S rRNA gene abundance peaks toward heavier fractions during the VC degradation process indicate the accumulation of ^{13}C in the 16S rRNA genes of *Sediminibacterium*, *Aquabacterium* and *Variovorax*. Similar shifts have been observed by other authors who combined SIP and qPCR for toluene-degrading cultures with the gene *bssA* [34].

The relative abundances of the phylotypes identified as assimilators of VC (*Sediminibacterium, Aquabacterium, Variovorax* and *Pseudomonas*) were low during the second VC degradation experiment. It is likely this occurred because the culture was stored for approximately one year following the first VC degradation experiment. In contrast, *Nocardioides* was present at a high RA. It is possible that the culture storage and resulting change in microbial community resulted in the longer timeframe for VC removal.

Bacteria able to degrade VC aerobically have been isolated, and they include the genera *Mycobacterium* [7, 8, 10, 12, 14-16], *Pseudomonas* [9, 11], *Nocardioides* [35], *Ochrobactrum* [11] and *Ralstonia* [13]. In the present study, we identified *Sediminibacterium*, *Aquabacterium* and *Variovorax* as novel VC degraders using SIP, however, we were unsuccessful in the attempts to isolate them [36-38].

In summary, the microorganisms responsible for assimilating ^{13}C from VC were identified by combining SIP analysis and Illumina MiSeq. Four phylotypes were primarily responsible for ^{13}C uptake: *Nocardioides* (*Actinobacteria*), *Sediminibacterium* (*Proteobacteria*), *Aquabacterium* (*Proteobacteria*) and *Variovorax* (*Proteobacteria*). The results indicate that both previously identified VC assimilators (*Nocardioides*) and novel VC assimilators (the other three phylotypes) were responsible for label uptake from VC in this mixed culture. Specific primers designed for these three novel VC assimilators were successfully validated for the culture. The

data suggest that previous studies involving isolations may not have accurately represented the real biodiversity of active VC assimilators in mixed communities. Further, these specific primers have the potential to advance our capability for monitoring VC bioremediation *in situ.*

REFERENCES

REFERENCES

[1] US Environmental Protect Agency, Basic information about vinyl chloride in drinking water, in, 2012.

[2] T.E. Mattes, A.K. Alexander, N.V. Coleman, Aerobic biodegradation of the chloroethenes: pathways, enzymes, ecology, and evolution, Fems Microbiology Reviews, 34 (2010) 445-475.

[3] P.M. Bradley, History and ecology of chloroethene biodegradation: A review, Bioremediation Journal, 7 (2003) 81-109.

[4] J. He, Kirsti M. Ritalahti, Kun-Lin Yang, Stephen S. Koenigsberg, F.E. Löffler, Detoxification of vinyl chloride to ethene coupled to growth of an anaerobic bacterium, Nature, 424 (2003) 62-65.

[5] A.M. Cupples, A.M. Spormann, P.L. McCarty, Growth of a *Dehalococcoides*-like microorganism on vinyl chloride and cis-dichloroethene as electron acceptors as determined by competitive PCR, Applied and Environmental Microbiology, 69 (2003) 953-959.

[6] F.E. Loffler, J. Yan, K.M. Ritalahti, L. Adrian, E.A. Edwards, K.T. Konstantinidis, J.A. Muller, H. Fullerton, S.H. Zinder, A.M. Spormann, *Dehalococcoides mccartyi* gen. nov., sp nov., obligately organohalide-respiring anaerobic bacteria relevant to halogen cycling and bioremediation, belong to a novel bacterial class, *Dehalococcoidia classis* nov., order *Dehalococcoidales* ord. nov and family *Dehalococcoidaceae* fam. nov., within the phylum *Chloroflexi*, International Journal of Systematic and Evolutionary Microbiology, 63 (2013) 625-635.

[7] S. Hartmans, J.A.M. Debont, J. Tramper, K. Luyben, Bacterial degradation of vinyl chloride, Biotechnol. Lett., 7 (1985) 383-388.

[8] S. Hartmans, J.A.M. Debont, Aerobic vinyl chloride metabolism in *Mycobacterium aurum* L1, Applied and Environmental Microbiology, 58 (1992) 1220-1226.

[9] M.F. Verce, R.L. Ulrich, D.L. Freedman, Characterization of an isolate that uses vinyl chloride as a growth substrate under aerobic conditions, Applied and Environmental Microbiology, 66 (2000) 3535-3542.

[10] N.V. Coleman, T.E. Mattes, J.M. Gossett, J.C. Spain, Phylogenetic and kinetic diversity of aerobic vinyl chloride-assimilating bacteria from contaminated sites, Applied and Environmental Microbiology, 68 (2002) 6162-6171.

[11] A.S. Danko, M.Z. Luo, C.E. Bagwell, R.L. Brigmon, D.L. Freedman, Involvement of linear plasmids in aerobic biodegradation of vinyl chloride, Applied and Environmental Microbiology, 70 (2004) 6092-6097.

[12] B.Z. Fathepure, V.K. Elango, H. Singh, M.A. Bruner, Bioaugmentation potential of a vinyl chloride-assimilating Mycobacterium sp., isolated from a chloroethene-contaminated aquifer, Fems Microbiology Letters, 248 (2005) 227-234.

[13] V.K. Elango, A.S. Liggenstoffer, B.Z. Fathepure, Biodegradation of vinyl chloride and *cis*-dichloroethene by a *Ralstonia* sp strain TRW-1, Applied Microbiology and Biotechnology, 72 (2006) 1270-1275.

[14] A.E. Taylor, M.E. Dolan, P.J. Bottomley, L. Semprini, Utilization of fluoroethene as a surrogate for aerobic vinyl chloride transformation, Environmental Science & Technology, 41 (2007) 6378-6383.

[15] Y.O. Jin, T.E. Mattes, Adaptation of aerobic, ethene-assimilating *Mycobacterium* strains to vinyl chloride as a growth substrate, Environmental Science & Technology, 42 (2008) 4784-4789.

[16] Y.O. Jin, S. Cheung, N.V. Coleman, T.E. Mattes, Association of missense mutations in epoxyalkane coenzyme M transferase with adaptation of *Mycobacterium* sp strain JS623 to growth on vinyl chloride, Applied and Environmental Microbiology, 76 (2010) 3413-3419.

[17] H. Fullerton, R. Rogers, D. Freedman, S. Zinder, Isolation of an aerobic vinyl chloride oxidizer from anaerobic groundwater, Biodegradation, 25 (2014) 893-901.

[18] S. Radajewski, P. Ineson, N.R. Parekh, J.C. Murrell, Stable-isotope probing as a tool in microbial ecology, Nature, 403 (2000) 646-649.

[19] A.M. Cupples, The use of nucleic acid based stable isotope probing to identify the microorganisms responsible for anaerobic benzene and toluene biodegradation, Journal of Microbiological Methods, 85 (2011) 83-91.

[20] N.V. Coleman, T.E. Mattes, J.M. Gossett, J.C. Spain, Biodegradation of *cis*-dichloroethene as the sole carbon source by a beta-proteobacterium, Applied and Environmental Microbiology, 68 (2002) 2726-2730.

[21] J.M. Gossett, Measurement of Henrys Law constants for C1 and C2 chlorinated hydrocarbons, Environmental Science & Technology, 21 (1987) 202-208.

[22] J.G. Caporaso, C.L. Lauber, W.A. Walters, D. Berg-Lyons, C.A. Lozupone, P.J. Turnbaugh, N. Fierer, R. Knight, Global patterns of 16S rRNA diversity at a depth of millions of sequences per sample, Proceedings of the National Academy of Sciences of the United States of America, 108 (2011) 4516-4522.

[23] P.D. Schloss, S.L. Westcott, T. Ryabin, J.R. Hall, M. Hartmann, E.B. Hollister, R.A. Lesniewski, B.B. Oakley, D.H. Parks, C.J. Robinson, J.W. Sahl, B. Stres, G.G. Thallinger, D.J. Van Horn, C.F. Weber, Introducing mothur: open-source, platform-independent, community-

supported software for describing and comparing microbial communities, Applied and Environmental Microbiology, 75 (2009) 7537-7541.

[24] E. Pruesse, C. Quast, K. Knittel, B.M. Fuchs, W. Ludwig, J. Peplies, F.O. Gloeckner, SILVA: a comprehensive online resource for quality checked and aligned ribosomal RNA sequence data compatible with ARB, Nucleic Acids Research, 35 (2007) 7188-7196.

[25] K.M. Ritalahti, B.K. Amos, Y. Sung, Q.Z. Wu, S.S. Koenigsberg, F.E. Loffler, Quantitative PCR targeting 16S rRNA and reductive dehalogenase genes simultaneously monitors multiple *Dehalococcoides* strains. , Appl. Environ. Microbiol, 72 (2006) 2765-2774.

[26] J. Davis, C. Carpenter, Aerobic degradation of vinyl chloride in groundwater samples, Applied and Environmental Microbiology, 56 (1990) 3878-3880.

[27] X.Y. Guan, F. Liu, Y.X. Xie, L.L. Zhu, B. Han, Microbiota associated with the migration and transformation of chlorinated aliphatic hydrocarbons in groundwater, Environ. Geochem. Health, 35 (2013) 535-549.

[28] N.V. Coleman, J.C. Spain, Distribution of the coenzyme m pathway of epoxide metabolism among ethene- and vinyl chloride-degrading Mycobactefium strains, Applied and Environmental Microbiology, 69 (2003) 6041-6046.

[29] M. Duhamel, E.A. Edwards, Microbial composition of chlorinated ethene-degrading cultures dominated by *Dehalococcoides*, Fems Microbiology Ecology, 58 (2006) 538-549.

[30] G. Imfeld, C.E. Aragones, I. Fetzer, E. Meszaros, S. Zeiger, I. Nijenhuis, M. Nikolausz, S. Delerce, H.H. Richnow, Characterization of microbial communities in the aqueous phase of a constructed model wetland treating 1,2-dichloroethene-contaminated groundwater, Fems Microbiology Ecology, 72 (2010) 74-88.

[31] A.Z. Gu, B.P. Hedlund, J.T. Staley, S.E. Strand, H.D. Stensel, Analysis and comparison of the microbial community structures of two enrichment cultures capable of reductively dechlorinating TCE and *cis*-DCE, Environmental Microbiology, 6 (2004) 45-54.

[32] W.F. Lin, Z.S. Yu, X. Chen, R.Y. Liu, H.X. Zhang, Molecular characterization of natural biofilms from household taps with different materials: PVC, stainless steel, and cast iron in drinking water distribution system, Applied Microbiology and Biotechnology, 97 (2013) 8393-8401.

[33] J.K. Hatt, F.E. Loffler, Quantitative real-time PCR (qPCR) detection chemistries affect enumeration of the *Dehalococcoides* 16S rRNA gene in groundwater, Journal of Microbiological Methods, 88 (2012) 263-270.

[34] W.M. Sun, A.M. Cupples, Diversity of five anaerobic toluene-degrading microbial communities investigated using stable isotope probing, Applied and Environmental Microbiology, 78 (2012) 972-980.

[35] N.V. Coleman, J.C. Spain, T. Duxbury, Evidence that RDX biodegradation by *Rhodococcus* strain DN22 is plasmid-borne and involves a cytochrome p-450, Journal of Applied Microbiology, 93 (2002) 463-472.

[36] J.H. Ou, H.L. Yuan, Sediminibacterium salmoneum gen. nov., sp nov., a member of the phylum Bacteroidetes isolated from sediment of a eutrophic reservoir, International Journal of Systematic and Evolutionary Microbiology, 58 (2008) 2191-2194.

[37] W.M. Chen, N.T. Cho, S.H. Yang, A.B. Arun, C.C. Young, S.Y. Sheu, Aquabacterium limnoticum sp nov., isolated from a freshwater spring, International Journal of Systematic and Evolutionary Microbiology, 62 (2012) 698-704.

[38] J.L. Gao, M. Yuan, X.M. Wang, T.L. Qiu, J.W. Li, H.C. Liu, X.A. Li, J. Chen, J.G. Sun, Variovorax guangxiensis sp nov., an aerobic, 1-aminocyclopropane-1-carboxylate deaminase producing bacterium isolated from banana rhizosphere, Antonie Van Leeuwenhoek International Journal of General and Molecular Microbiology, 107 (2015) 65-72.

CHAPTER 4

MICROBIAL COMMUNITY CHARACTERIZATION AND FUNCTIONAL GENE QUANTIFICATION IN RDX DEGRADING COMMUNITIES DERIVED FROM TWO NAVAL SITES

Abstract

The explosive hexahydro-1,3,5-trinitro-1,3,5-triazine (RDX) is the most widely used military explosive. RDX has become an environmental pollutant over the last few decades owing to its production, storage and use. RDX contamination is a cause for concern because this chemical is classified as a possible human carcinogen by the EPA. Efforts to remediate RDX-contaminated soils and groundwater have been ongoing for decades. In recent years, much interest has focused on using bioremediation to clean up these sites. A number of bacteria capable of degrading RDX in pure culture have been described; however, little is known about the mixed microbial communities responsible for *in situ* degradation. Also, a limited number of studies have investigated the occurrence of RDX degrading functional genes in different environments. The current study investigated the microorganisms and functional genes (*xenA, xenB* and *xplA*) linked to RDX biodegradation in microcosms composed of sediments or groundwater from two RDX-contaminated Navy sites. Sediment samples from five depths (5 ft to 30 ft) at two wells were studied from one Navy site. Also, groundwater upstream and downstream of an emulsified biobarrier were studied from another Navy site. The study found that phylotypes from *Firmicutes, Actinobacteria, Proteobacteria, Acidobacteria* and *Bacteroidetes* benefited from RDX degradation. A notable trend was the increase in *xplA* and *xenB* gene copies in the majority

of sediment microcosms derived from one Navy site compared to the controls. Gene copies of *xenA* increased in a smaller number of the treatments. Interestingly, *Pseudomonas* (previously associated with *xenA* and *xenB*) and *Rhodococcus (*associated with *xplA)* also illustrated a high level of enrichment in many of these RDX amended microcosms. The data provide insight into the microorganisms potentially responsible RDX degradation at these contaminated sites. Further, the functional gene primers designed in this study could be used to facilitate the prediction of RDX biodegradation rates at contaminated sites.

Introduction

Hexahydro-1,3,5-trinitro-1,3,5-triazine (RDX) is the most widely used military explosive [1]. The continued global demand for munitions suggests that RDX manufacture and use will occur for the foreseeable future. RDX has long been recognized as a problematic pollutant and efforts to remediate RDX-contaminated soil and groundwater have been ongoing for decades. Contamination is particularly problematic on military training ranges where energetic materials are detonated on a regular basis. Pollution can originate from unexploded ordinance or from diffuse sources. In either case, RDX tends to be recalcitrant and can remain in the soil and also move to groundwater. Groundwater contamination is a cause for concern because RDX is classified as a possible human carcinogen by the EPA. In recent years, much interest has focused on using bioremediation to clean up these sites; however the microorganisms responsible for *in situ* degradation are generally unknown [2].

To determine which microorganisms are linked to RDX degradation at contaminated sites, methods such as stable isotope probing (SIP) and high throughput sequencing have been utilized. For example, using SIP 5 phylotypes similar to known RDX degraders and 10

phylotypes not previously linked to RDX degradation were associated with RDX degradation in samples from Picatinny Arsenal (NJ) [3]. Another set of SIP experiments showed the importance of *Pseudomonas* phylotypes in label uptake [4]. In contrast, *Rhodococcus* was identified by SIP as the primary degrader in soils from the Eglin Air Force Base bombing range (Eglin, FL) [5]. Recently, also through the use of SIP, *Pseudomonadaceae* and *Comamonas* were identified as RDX-degraders in soil from a Navy Installation in Virginia [6]. The growing literature on phylotypes identified as RDX degraders at contaminated sites has the potential to improve current bioremediation approaches. However, to date, the distribution of RDX degraders throughout the soil profile at such sites has not been investigated. This information is important because of the risk of RDX movement from soils to groundwater.

Bioremediation efforts have been significantly enhanced in the past decade using functional gene data. For example, the dehalogenase reductive genes responsible for vinyl chloride degradation, *bvcA* and *vcrA*, are routinely quantified in groundwater from chlorinated-solvent contaminated sites to determine the dechlorination potential of *in situ* dechlorinators [7]. With respect to RDX degradation, several functional genes have been identified, including two that encode for flavin mononucleotide-containing oxidoreductases (called xenobiotic reductases) from *Pseudomonas putida* II-B (*xenA*) and *P. fluorescens I-C* (*xenB*) [8]. For these, the primary RDX degradation path is through methylenedinitramine (MEDINA) and then to formaldehyde. RDX transformation was faster under anaerobic compared to aerobic conditions. Under anaerobic conditions, *P. fluorescens I-C* (*xenB*) degraded RDX more rapidly than *P. putida* II-B (*xenA*). Both genes have been cloned, sequenced and characterized [9], providing an excellent opportunity to examine gene abundance at contaminated sites.

The enzyme diaphorase from the anaerobic bacterium *Clostridium kluyveri* has also been linked to RDX degradation [10]. The biotransformation pathway mediated by diophorase involves two important domains, a flavin-reductase and a rubredoxin-like domain and catalyzes RDX degradation via denitration prior to ring cleavage [11]. MEDINA was detected as the transient intermediate, along with the formation of nitrite, formaldehyde, ammonium, and nitrous oxide. The gene sequence (*diaA*) encoding diaphorase from *C. kluyveri* has also been determined [12]. Another functional gene related to RDX degradation is *hydA* from *C. acetobutylicum* [13]. Also, an oxygen-insensitive (type I) NADPH nitroreductases (*nsfI*) enzyme able to degrade RDX has been detected in enteric bacteria *Enterobacter cloacae* and *Morganella morganii*, and cloned from *E. cloacae* [14].

Among all functional genes associated with RDX degradation, *xplA* has perhaps been the most studied. This gene has been associated with both aerobic and anaerobic pathways and it was initially isolated from *Rhodococcus rhodochrous* 11Y [15]. It has been identified in isolates of the genera *Rhodococcus, Gordonia, Williamsia* (all three are in the suborder *Corynebacterineae*, phylum *Actinobacteria*) and *Microbacterium* (suborder *Micrococcineae*, phylum *Actinobacteria*) [1, 15-22]. Both *xplA* and its partnering *xplB* gene (encodes a flavin reductase) are carried by a plasmid, and research suggests that they are likely part of a class I transposable element [20].

A limited number of studies have investigated the occurrence of RDX functional genes in different environments. One project examined RDX-contaminated groundwater from two sites (Pueblo Chemical Depot and Picatinny Arsenal) where bioremediation was ongoing [2]. Using conventional PCR the authors were not able to detect any of the five RDX functional genes investigated (*xplA, hydA, onr, xenA, xenB)*[2]. A recent metagenomic study on ovine rumen microbiota capable of RDX degradation found sequence homologues to five RDX-degrading

genes (*diaA, xenA, xenB, xplA* and *xplB*) [23]. Among these, *diaA* was the most abundant, followed by *xenA* and *xenB*. In contrast, *xplA* and *xplB* were barely detectable and homologues of *nsfI* were not detected [24].

In the current study, the abundance of three functional genes (*xplA, xenA* and *xenB*) associated with RDX degradation was investigated in RDX-degrading microcosms derived from two Naval sites. It was deemed important to include *xplA*, given the large and growing interest in this gene. The genes *xenA* and *xenB* were included because previous research indicated *Pseudomonadaceae* were important for RDX degradation in environmental samples or *in situ* [2, 3, 6]. In addition, the microbial community linked to RDX degradation was examined using high throughput sequencing. This research investigated 1) RDX degradation, 2) the abundance of three RDX functional genes, and 3) microbial community changes in microcosms derived from sediment at three to five different depths from two wells at one Navy site. The same objectives were investigated using microcosms consisting of groundwater obtained from both upstream and downstream of a buffered emulsified oil biobarrier from a second Navy site. The biobarrier had been installed to facilitate bioremediation of RDX, octahydro-1,3,5,7-tetranitro-1,3,5,7-tetrazocine (HMX, another explosive) and perchlorate.

Methods

Chemicals

RDX dissolved in acetonitrile was purchased from Cambridge Isotope Laboratories, Inc. (Tewksbury, MA). HPLC grade acetonitrile (≥99.8 % purity) was purchased from EMD Chemicals Inc. (New Jersey, USA). Other reagents were purchased from Sigma-Aldrich (St. Louis, MO, USA), Fisher BioReagent (New Jersey, USA), or Invitrogen (Carlsbad, CA, USA)

unless otherwise stated.

Experimental design

Sediment samples from different depths (5, 10, 20, 25 and 30 ft deep) were collected from two wells (MW 61 and MW 58), both located on an RDX-contaminated U.S. Navy site (Bangor Trident Base, WA, hereafter, called site 1). Groundwater samples from a second U.S. Navy site (Dahlgren, VA, site 2) were collected from both upstream and downstream of an installed buffered emulsified oil biobarrier.

From each sample, triplicates of live and killed abiotic controls (autoclaved) microcosms were prepared. The microcosms were established as previously described, with modifications [18, 25]. Briefly, each microcosm consisted of a 60 mL serum bottle containing 4 mL of a minimal salts media (MSM) (28, 34), 10 mg L^{-1} RDX dissolved in acetonitrile (as the sole nitrogen source), and the sample: either 2 g sediment (wet weight) or 1 mL groundwater. Live microcosms with an equal volume of acetonitrile, but not containing RDX, were also prepared as described above in triplicate for all sediment and groundwater samples. Finally, because an additional carbon source is commonly used to accelerate RDX biodegradation at contaminated sites, live and killed abiotic control microcosms were prepared for the groundwater samples with the addition of 201.6 mg L^{-1} glucose. All microcosms were sealed with rubber stoppers and aluminum seals and were covered with aluminum foil to prevent photodegradation. The sediment microcosms were incubated between 6 to 19 weeks. while the groundwater microcosms were incubated between 9 to 15 weeks. All microcosms were stored at room temperature (~20 °C) without shaking.

Analytical methods

RDX concentrations were determined using high performance liquid chromatography (HPLC) as previously described [18] with modifications. For each microcosm, a 0.2mL aliquot was extracted with a 1 mL BD syringe (with a 21-gauge needle) and combined with an equal volume of acetonitrile in a 1.7 mL sterile microcentrifuge tube. Tubes were shaken for 30 min at room temperature to extract RDX from microcosm aliquot. The samples were then centrifuged for 5 minutes at 10,000 x g and the supernatant was filtered using acetonitrile-wetted filters (PVDF, 0.22 μm, Whatman) into HPLC amber vials (Sigma-Aldrich, St. Louis, MO, USA). External standards for the calibration curve were prepared with a dilution factor of 2 to account for the sample dilution at the liquid-liquid extraction step. The HPLC parameters were as follows: column: injector volume, 20 μL for samples and standards; isocratic conditions (40% acetonitrile and 60% 0.1% $H_3PO_4^-$ acidified water, 1 mL min^{-1}); Supelco C18 (25 cm X 4.6 mm, 5 μm); Perkin Elmers Series 200 autosampler; PE binary LC Pump 250; Waters UV detector; wavelength 255 nm (detection limit was 500 μg/L).

DNA extraction

DNA was extracted from all live microcosms inoculated with sediment or groundwater (RDX-amended and live controls). For this, DNA was extracted from analiquot of 0.5 mL removed from each live microcosm using 1 mL BD syringes (21-gauge needle). For the sediment microcosms, (site 1), DNA extraction occurred for aliquots removed at 2 time points for all depths (MW 61 at days 45 and 90; MW 58 at days 90 and 130). For the groundwater microcosms (site 2), DNA was extracted at day 67 and 100 for the downstream and upstream groundwater samples, respectively. In addition, the total genomic DNA was extracted in

triplicate from all original sediment and water samples collected at the two U.S. navy sites to establish the baseline microbial community (called No RDX, Time 0). The Power Sediment DNA extraction kit (MO BIO Laboratories, Inc., Carlsbad, CA) was used to all DNA extractions following the manufacturer's recommended procedure.

Quantitative PCR (qPCR)

Gene copy numbers for three functional genes associated with RDX degradation were investigated using qPCR. Quantification was performed in triplicate using DNA extracted from a subset of the RDX degrading microcosms, live controls (no RDX) and initial samples (groundwater or sediment). Primers were designed to target *xplA, xenA* and *xenB* using Primer-BLAST (http://www.ncbi.nlm.nih.gov/tools/primer-blast/) (Table S4.1) and the primers were supplied by Integrated DNA Technologies (IDT, Coralville, IA). Although primers have been published for several of these genes (for example [2]), new primers were designed to be current with the new sequence data available in GenBank.

Amplification and qPCR measurements were conducted in a Chromo 4 real-time PCR cycler (Bio-Rad, Philadelphia, PA) using a QuantiTect SYBR Green PCR Kit (Qiagen Inc.) and the primer sets for *xplA, xenA* and *xenB*. Each 25-µL qPCR reaction contained 12.5 µL QuantiTect SYBR Green PCR Master Mix solution, 1.25 µL each 10 uM primer, 8 µL DNA-free water and 2 µL DNA template. The thermal protocol consisted of an initial denaturation (95°C, 15 min), 40 cycles of amplification (95°C, 15 s; 58°C, 20 s; 72°C 20 s), and a terminal extension step (72°C, 2 min). Melting curves were constructed from 55°C to 95°C and read every 0.6°C for 2 s.

Standard curves were developed in triplicate using plasmid DNA (partial *xplA xenA* and

xenB sequences, Table S4.1). The number of gene copies was calculated using as described previously [26] (plasmid size was 2710 bp, in addition to inserts of 382 bp for *xplA*, 324 bpfor *xenA* and 351 bp for *xenB*). For all standard curves, the range of target gene copies was 10^3-10^{10} and the overall qPCR efficiency was 100.22% (Table S4.2).

MiSeq Illumina sequencing and data analysis

Total genomic DNA extracted from all live microcosms (both sediment and groundwater microcosms) was submitted for high throughput sequencing (MiSeq Illumina Sequencing) at the Research Technology Support Facility (RTSF) at Michigan State University (MSU, East Lansing, MI).

PCR and Illumina sequencing were performed at RTSF using a previously described protocol [27], which involves the amplification of the V4 region of the 16S rRNA gene using a set of multiplex indexed primers. Following amplification, individual reactions were quantified (Picogreen assay), a pool of equimolar amounts of each was made, and these were purified using Ampure XP beads. A final gel purification step was included to ensure non-specific products were eliminated. The combined library was loaded onto the Illumina MiSeq Platform using a standard MiSeq paired end (2x250 bp) flow cell and reagent cartridge.

The amplicon sequencing data generated by the Illumina MiSeq Platform (*.fastq files) were analyzed using the Mothur software [28] following the MiSeq standard operating procedure (SOP) developed by Schloss (http://www.mothur.org/wiki/MiSeq_SOP). This involved the construction of contigs, error and chimera removal followed by sequence alignment for OTU assignment based on the SILVA database [29]. Final data matrices were exported to Excel 2013 SR-1 (Microsoft Corporation, Redmond, WA).

To identify which OTUs were responsible for the label uptake in each fraction at each time point, the relative abundance (RA, %) of each OTU was calculated. The RA of the most abundant phylotypes in the microcosms showing RDX degradation (relative abundance greater than 1%) were compared to the OTU RA values from the microcosms not amended with RDX and the initial samples (sediment or groundwater) to determine which of the most abundant phylotypes were linked to RDX uptake. All Illumina sequencing data generated in this study were deposited in the NCBI Sequence Read Archive under Bioproject Number PRJ302752.

Results

RDX degradation and quantitative PCR (qPCR)

RDX degradation occurred in both sediment (MW 58 and 61) and groundwater (GW) microcosms amended with RDX but not in the abiotic controls, confirming biological removal (Figures 4.1, 4.2, 4.3). RDX degradation appeared to occur faster in microcosms derived from MW 61 compared to MW 58. For both experiments, no clear trends between sediment depth and RDX removal rates were observed. In general, RDX removal was greater at day 67 in the microcosms inoculated with groundwater from downstream of the biobarrier (Figure 4.4A & B) compared to derived from groundwater upstream of the biobarrier (Figure 4.4C & D). Total genomic DNA extracted from all of the original samples (time 0) and from the live microcosms inoculated with sediment or groundwater (RDX-amended and No-RDX controls) were subject to qPCR to enumerate RDX functional genes and Illumina sequencing to identify the dominant phylotypes.

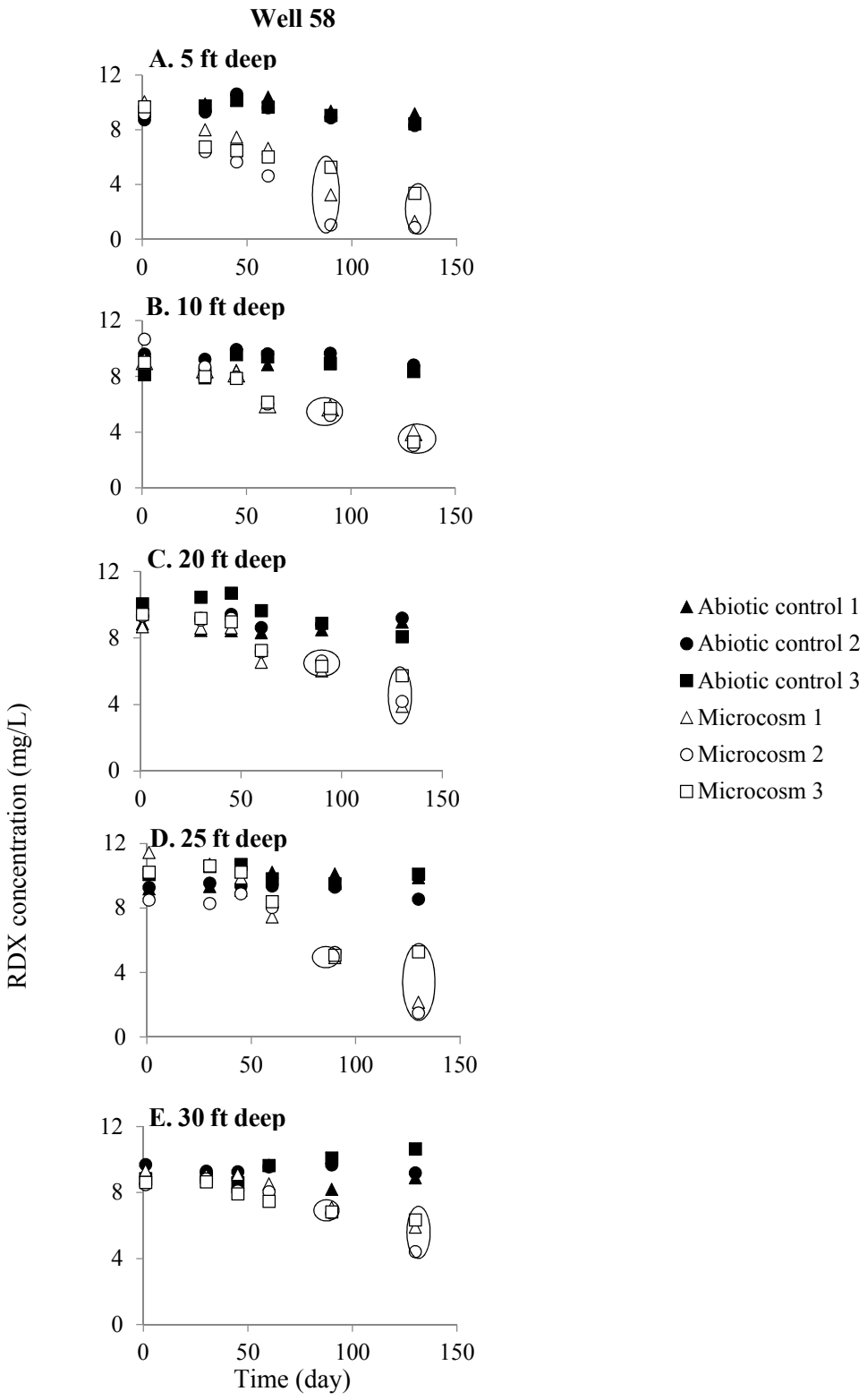

Figure 4.1. RDX concentrations (mg/L) in RDX-amended microcosms and abiotic controls containing sediment from well 58 at 5 ft (A), 10 ft (B), 20 ft (C), 25 ft (D) and 30 ft depth (E). The samples subjected to DNA extraction and community analysis are circled (days 90 and 130).

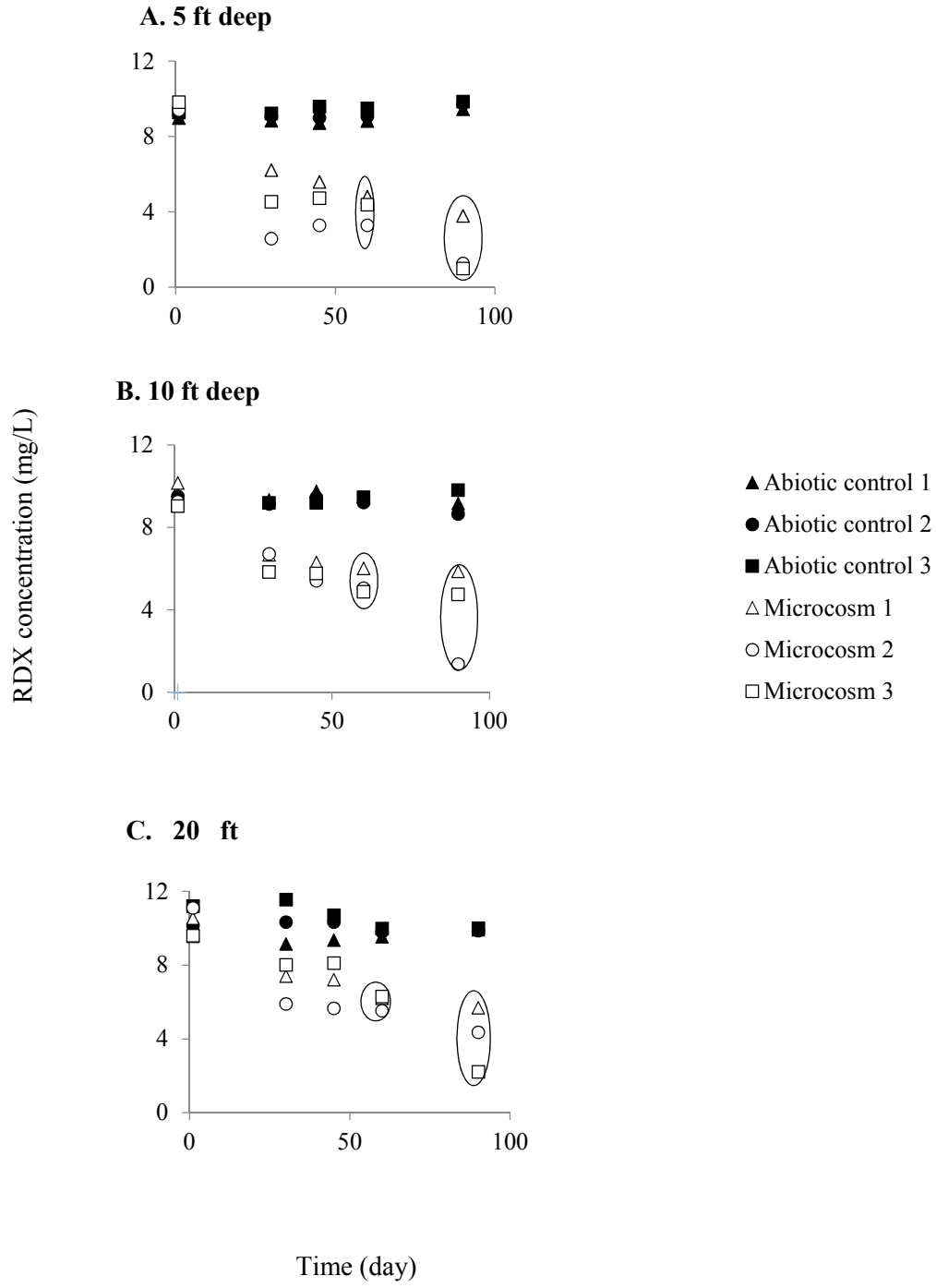

Figure 4.2. RDX concentrations (mg/L) in RDX amended microcosms and abiotic controls containing sediment from well 61 at 5 ft deep (A), 10 ft deep (B) and 20 ft depth (C). The samples subject to DNA extraction and community analysis are circled (days 45 and 90).

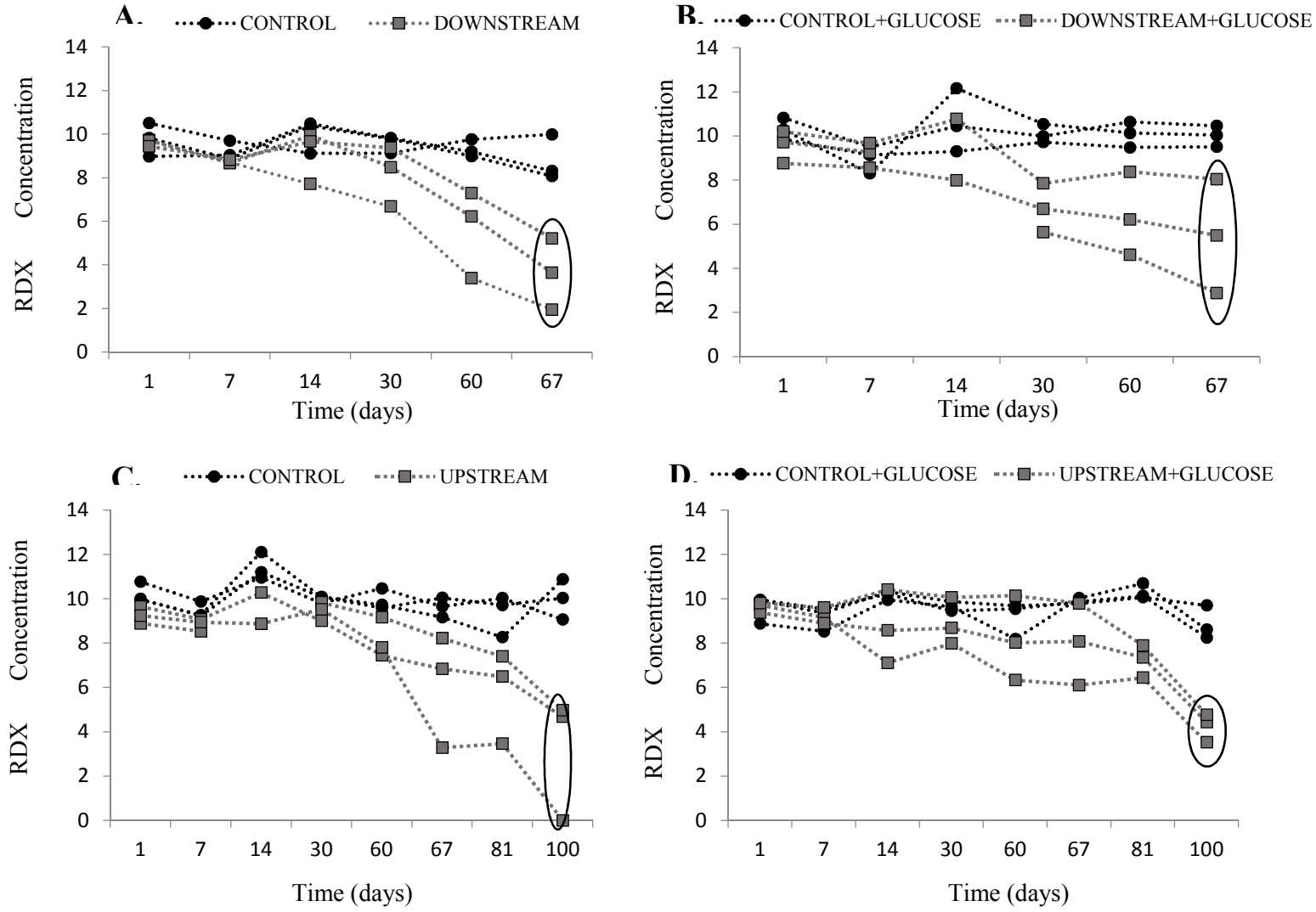

Figure 4.3. RDX concentrations (mg/L) in RDX-amended microcosms and abiotic controls containing groundwater from downstream (A, B) and upstream (C, D) of a buffered emulsified oil biobarrier. The samples subjected to DNA extraction and community analysis are circled (days 67 and 100 for downstream and upstream respectively).

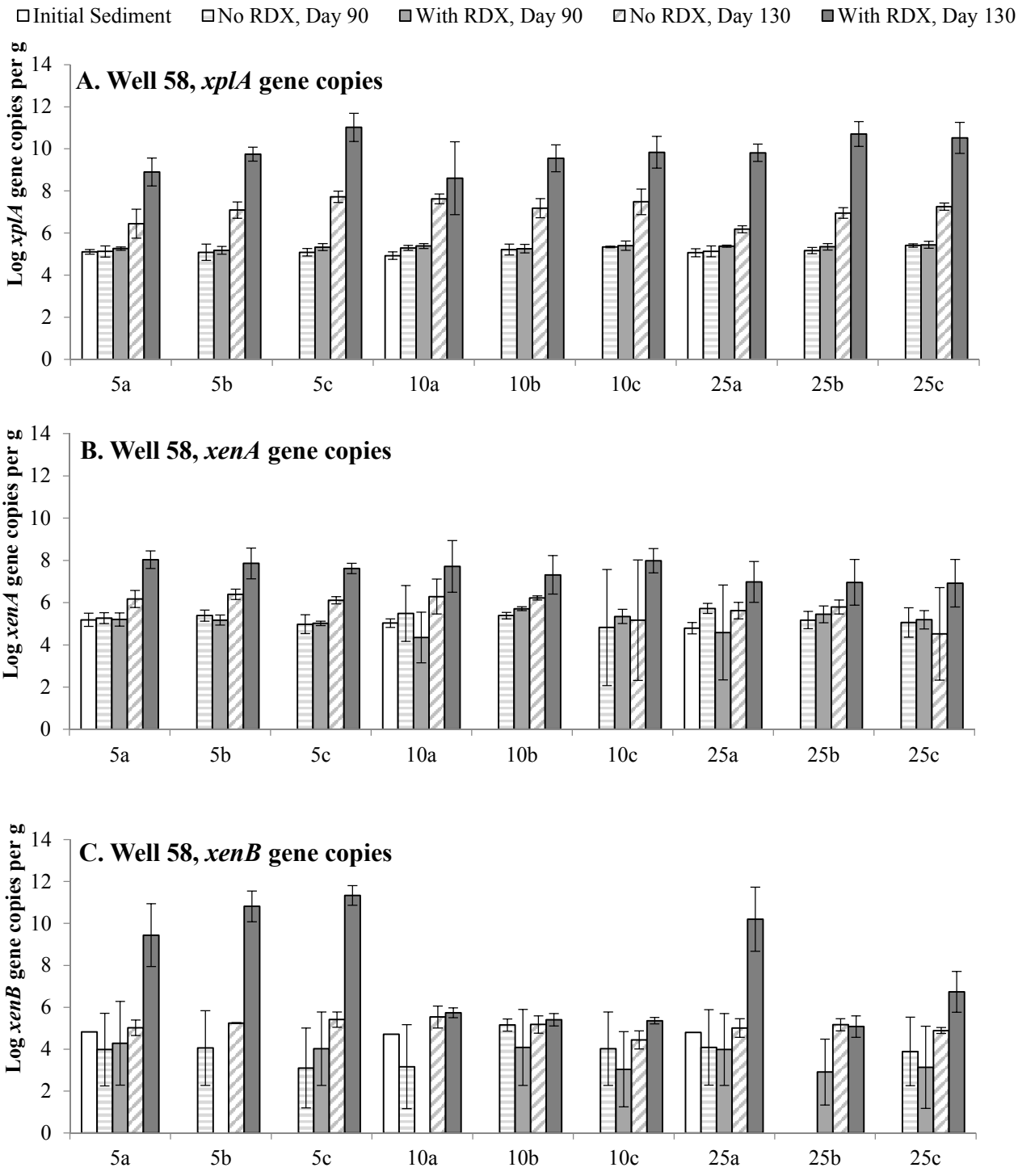

Figure 4.4. Average (±SD, and n= 3) gene copies of *xplA* (A)*, xenA* (B) and *xenB* (C) in the initial samples, RDX- and No-RDX- amended microcosms containing sediment from well 58 at 5 ft, 10 ft and 25 ft depth on day 90 and 130 (a, b and c indicate the three replicates of each treatment).

Three functional genes (*xplA, xenA* and *xenB*) were quantified in both the initial MW 58 sediment samples and in microcosms inoculated with sediment from three depths (MW 58) at two time points (days 90 and 130) during RDX degradation (Figure 4.4). Similarly, both the initial sediment samples and microcosms inoculated from sediment from three depths at two time points (days 45 and 90) were investigated from MW 61 (Figure 4.5). Finally, the three functional genes were also quantified in groundwater (upstream and downstream of the biobarrier) and in groundwater inoculated microcosms (Figure 4.6).

In MW 58 microcosms, the number of gene copies of *xplA, xenA* and *xenB* increased over time in all RDX-amended microcosms, in all tested depths (Figure 4.4). Also, the number of gene copies of *xplA, xenA* and *xenB* in the No-RDX microcosms and in the initial samples were lower than the RDX-amended microcosms, indicating a positive relationship between RDX degradation and functional gene copy numbers for all tested depths from MW 58. The difference in gene copy numbers between the RDX amended samples and No-RDX controls from MW 58 were statistically significant ($p < 0.05$) for all three functional genes at both time points (Table 4.1).

In MW 61, for RDX-amended microcosms from all depths, the difference between the log value of *xplA* gene copies per gram of day 45 and 90 were not as great as the difference between RDX-amended microcosms of day 90 and 130 from MW 58 (Figure 4.5A). Still, RDX-amended microcosms contained higher numbers of gene copies of *xplA* compared to the No-RDX microcosms and initial sample at all depths. Again, the differences between the RDX amended microcosms and the No-RDX controls were statistically different ($p < 0.05$) at both time points for MW 61 (Table 4.1).

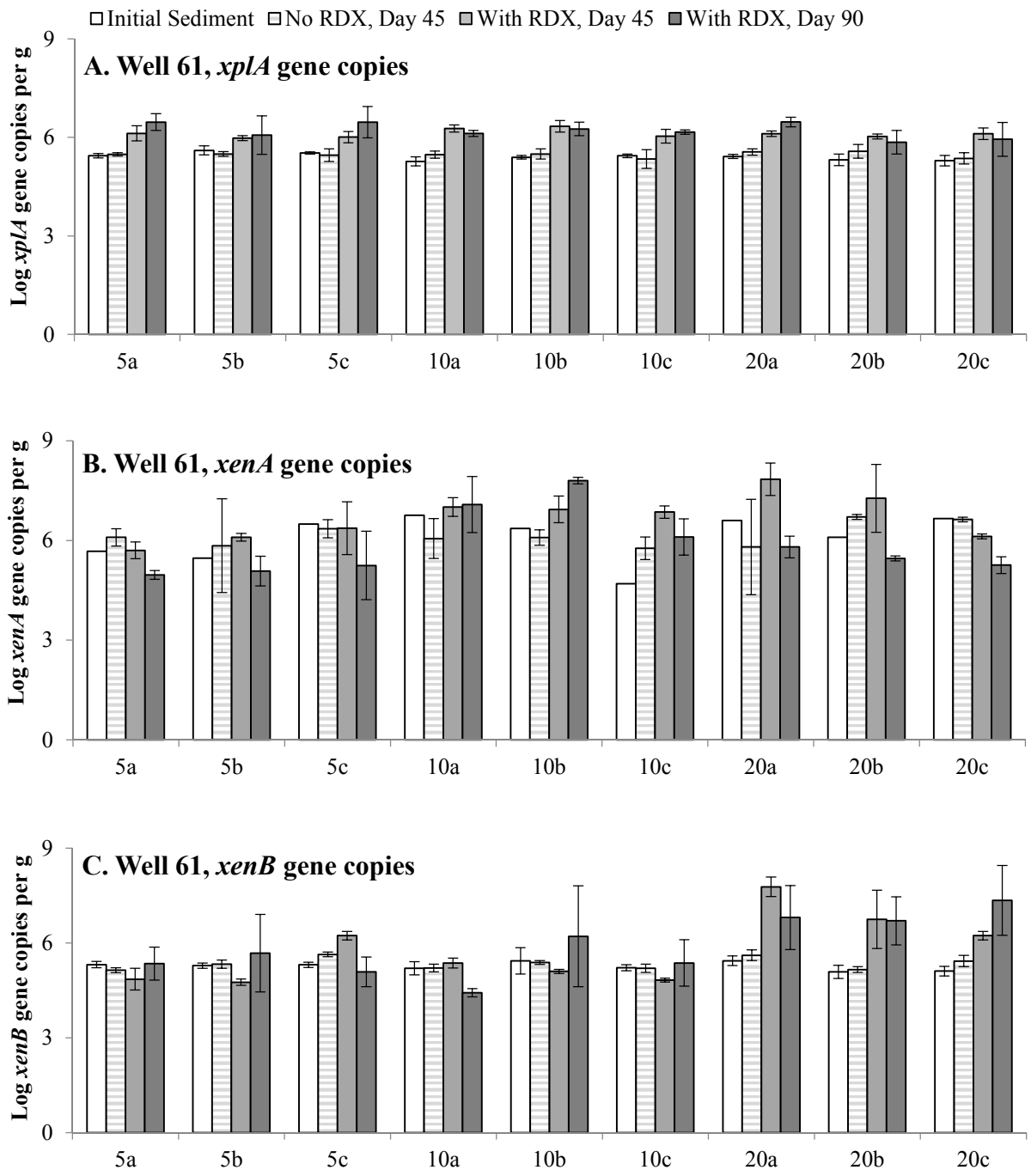

Figure 4.5. Average (±SD, and n= 3) gene copies of *xplA* (A), *xenA* (B) and *xenB* (C) in the initial samples, RDX- and No-RDX- amended microcosms containing sediment from well 61 at 5 ft, 10 ft and 20 ft depth on day 45 and 90 (a, b and c indicate the three replicates of each treatment).

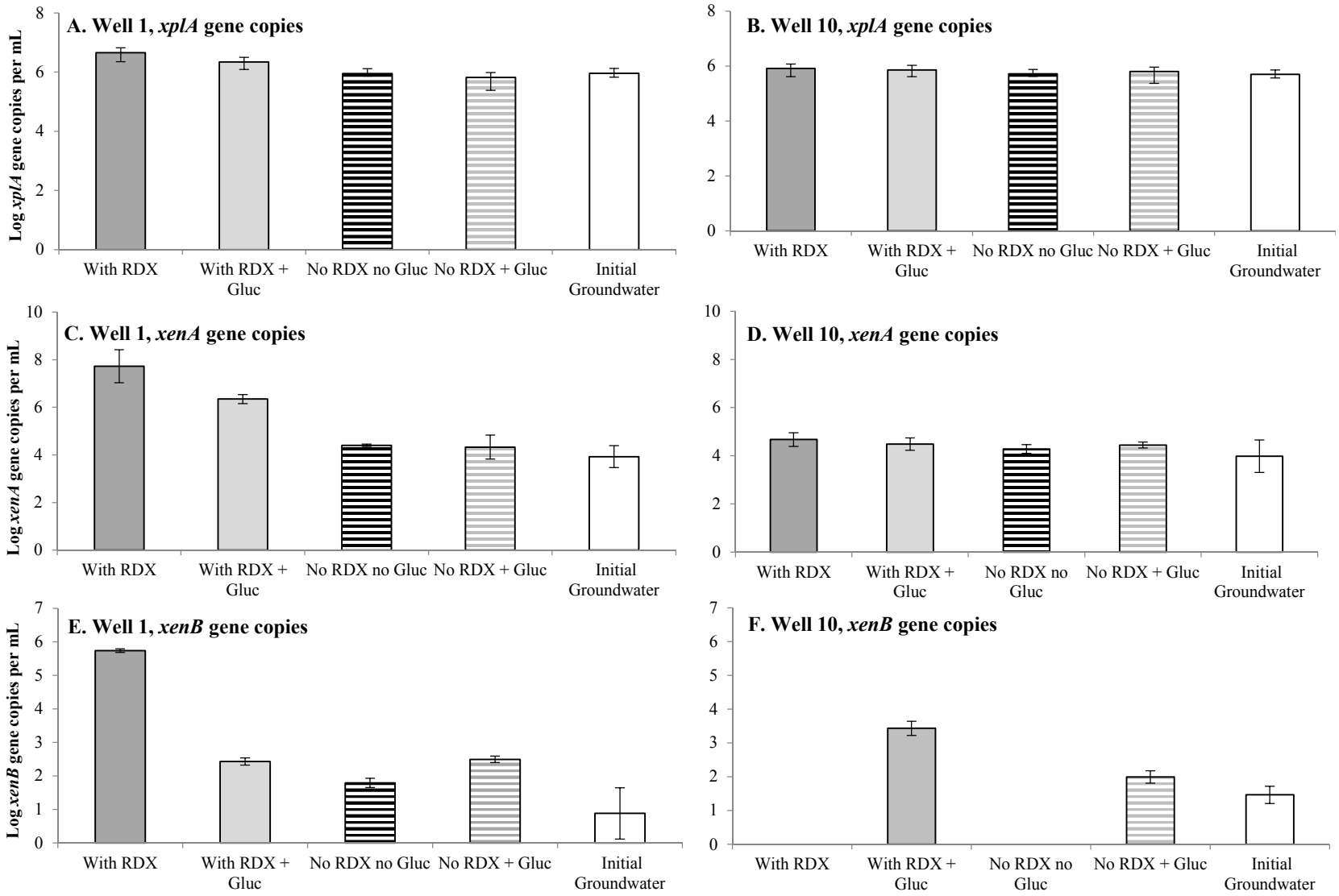

Figure 4.6. Average (±SD, and n= 3) gene copies of *xplA* (A, B), *xenA* (C, D) and *xenB* (E, F) in the initial samples, RDX- and No-RDX- amended microcosms with and without glucose) containing groundwater from downstream (day 67) and upstream (day 100) of an installed buffered emulsified oil biobarrier (a, b and c indicate the three replicates of each treatment).

Table 4.1. T-test results (*p* values) comparing *xenA, xenB* and *xplA* gene copies between RDX amended samples and the No-RDX controls from sediment and groundwater inoculated microcosms.

	Sediment Microcosms				Groundwater Microcosms	
Gene	**Well 58 Day 90**	**Well 58 Day 130**	**Well 61 Day 45**	**Well 61 Day 90**	**Well 10 (upstream)**	**Well 1 (downstream)**
xplA	0.0128	0.0416	0.0000	0.0003	NS	0.0274
xenA	0.0395	0.0003	NS	NS	NS	NS
xenB	0.0010	0.0480	NS	0.0497	NS	0.0387

NS=not significant

Regarding *xenA* measurements for MW 61 microcosms, those containing sediments from the 5ft-depth did not show clear differences between RDX-amended and No-RDX microcosms. In some cases, the RDX-amended microcosms containing sediments from 10- and 20- ft depths yielded more *xenA* copies compared to live controls and the initial samples (Figure 4.5B). However, there was no statistically significant difference between the RDX amended samples and No-RDX controls for *xenA* from MW 61 (Table 4.1).

The *xenB* abundance in MW 61 RDX-amended microcosms on day 45 and 90 was higher than *xenB* abundance in No-RDX microcosms and initial samples from sediment depths of 20 ft (Figure 4.5C). For microcosms containing sediments from 5 and 10 ft deep, no clear difference was observed between RDX-amended and No RDX microcosms (Figure 4.5C). For MW 61, there was no statistically significant difference in *xenB* copy numbers between the RDX amended microcosms and the No-RDX controls for day 45, however there was a difference ($p < 0.05$) for day 90 (Table 4.1).

The groundwater microcosms showed an overall trend of higher functional gene copy numbers in downstream microcosms than in upstream microcosms (Figure 4.6). For the downstream microcosms (Figure 4.6A), there was a statistically significant difference ($p < 0.05$) in *xplA* gene copies in the RDX amended microcosms compared to the No-RDX microcosms (Table 4.1). However, no significant difference was noted for *xplA* in the upstream microcosms (Figure 4.6B).

In the downstream microcosms, *xenA* gene abundance appeared to increase in RDX-amended microcosms (with and without glucose) compared to the No-RDX controls (Figure 4.6C), however, this difference was not statistically significant. Similarly, there was no difference in the upstream microcosms compared to the No-RDX controls for *xenA* (Figure

4.6D).

RDX-amended microcosms from the downstream groundwater samples illustrated a higher abundance of *xenB* compared to initial sample and the No RDX-amended microcosms (Figure 4.6E). For the downstream groundwater, RDX-amended microcosms without glucose showed a greater difference between the experiment and live control. On the other hand, glucose addition increased *xenB* abundance in the upstream treatment (Figure 4.6F). The difference between the RDX amended samples and No-RDX controls for *xenB* was statistically significant ($p<0.05$) only for the downstream microcosms (Table 4.1). For the upstream experiments, it is unclear why the *xenB* gene abundance values were lower in RDX-amended and No-RDX microcosms without glucose compared to the initial sample (Figure 4.6F).

MiSeq Illumina sequencing and data analysis

The relative abundance (RA, %) of phylotypes were calculated using high throughput sequencing analysis (MiSeq Illumina/Mothur) of the DNA extracted from initial samples (time 0), microcosms following RDX degradation, and live controls (No- RDX controls) of MW 58 (Figure 4.7), MW 61 (Figure 4.8) and GW down- and upstream experiments (Figure 4.9). A comparison of RA values illustrated that for each experiment, several phylotypes increased in abundance in microcosms amended with RDX compared to the controls (time 0 and No-RDX microcosms).

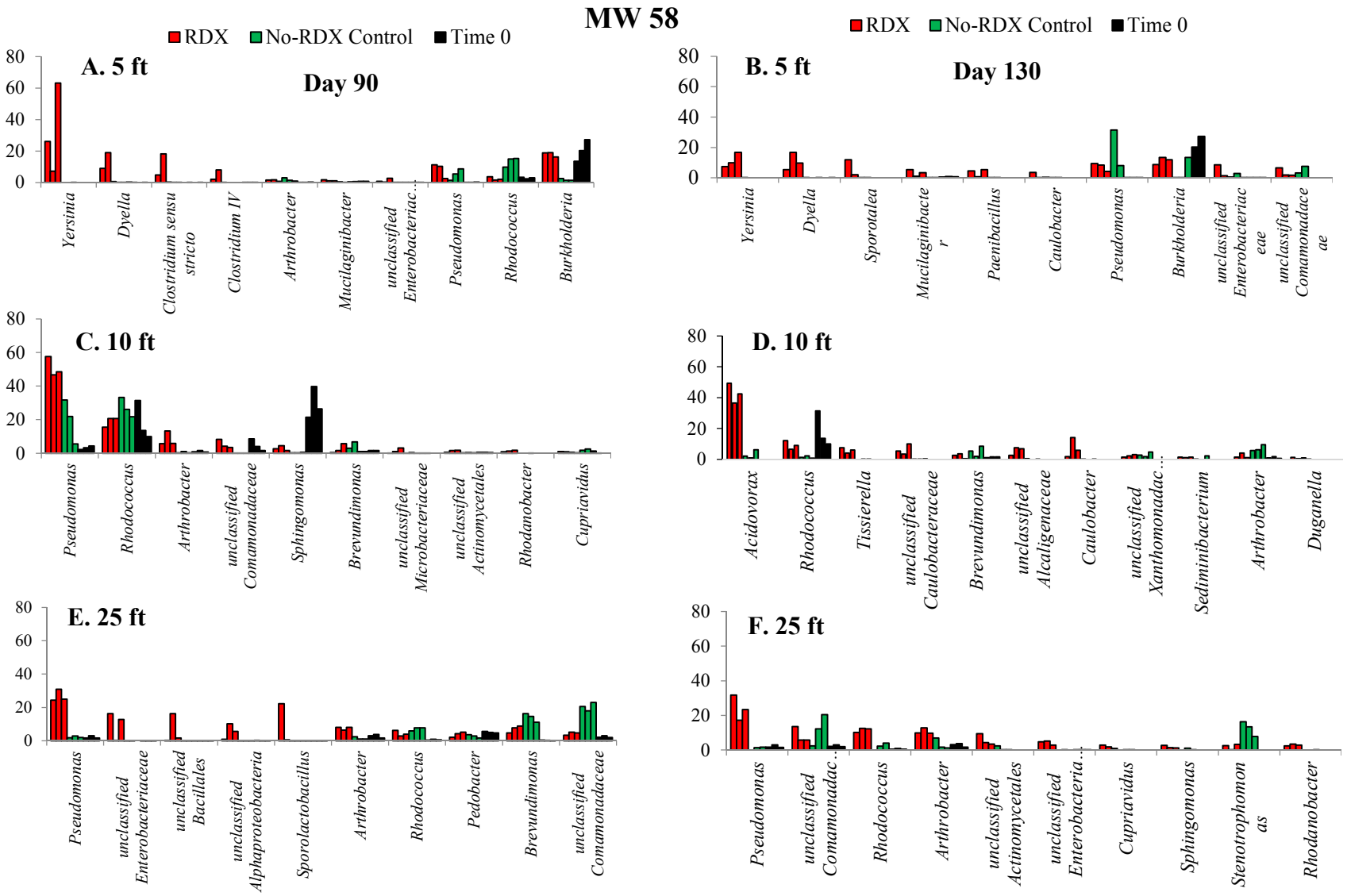

Figure 4.7. Relative abundance (RA, %) of phylotypes in DNA extracted from initial samples, RDX- and No-RDX- amended microcosms containing sediments from MW 58 at depths 5 (A, B), 10 (C, D) and 25 ft (E, F) at day 90 and 130 in triplicates.

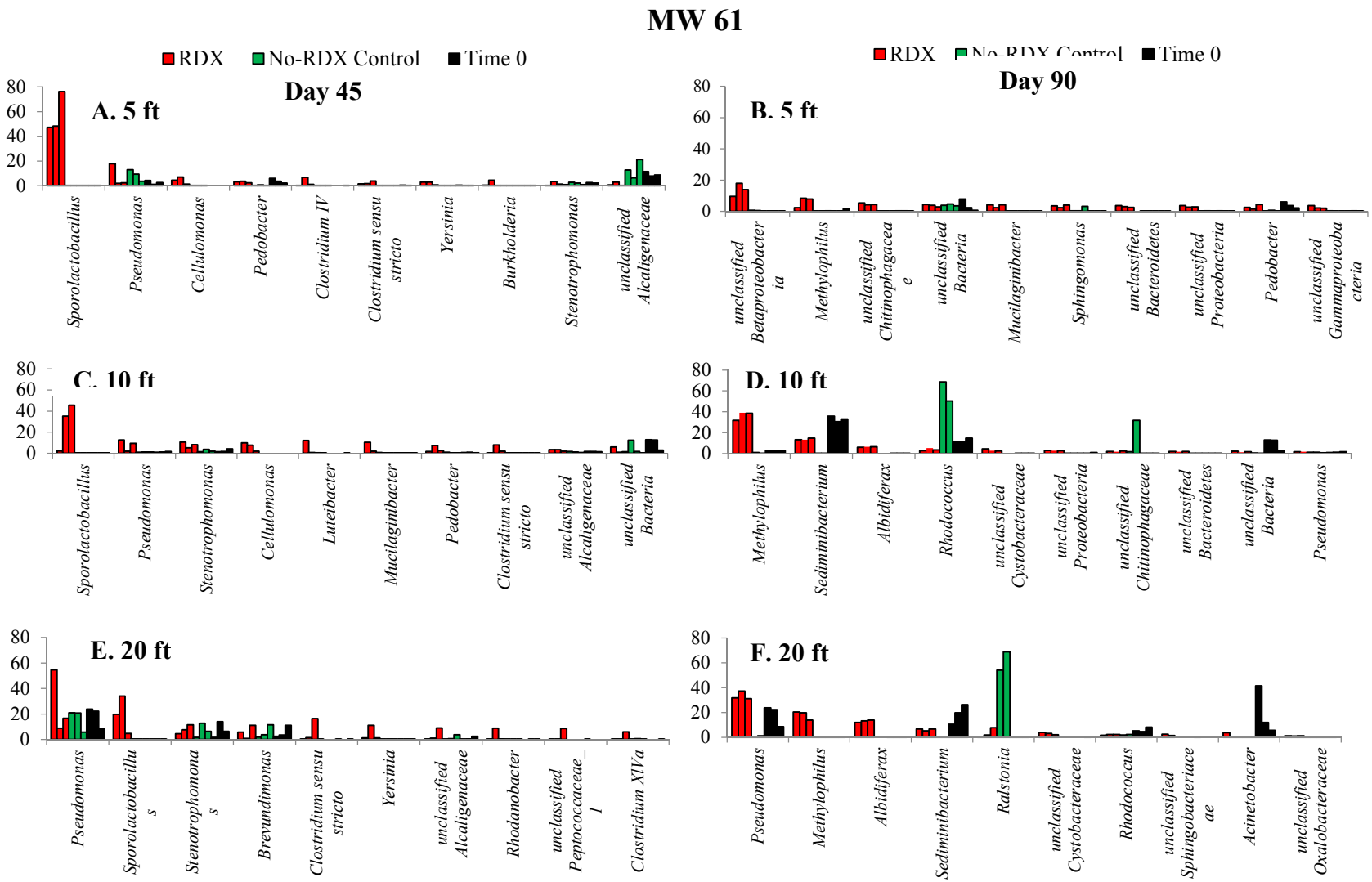

Figure 4.8. Relative abundance (RA, %) of phylotypes in DNA extracted from initial samples, RDX- and No-RDX- amended microcosms containing sediments from MW 61 at depths 5 (A, B), 10 (C, D) and 20 ft (E, F) at day 45 and 90 in triplicates.

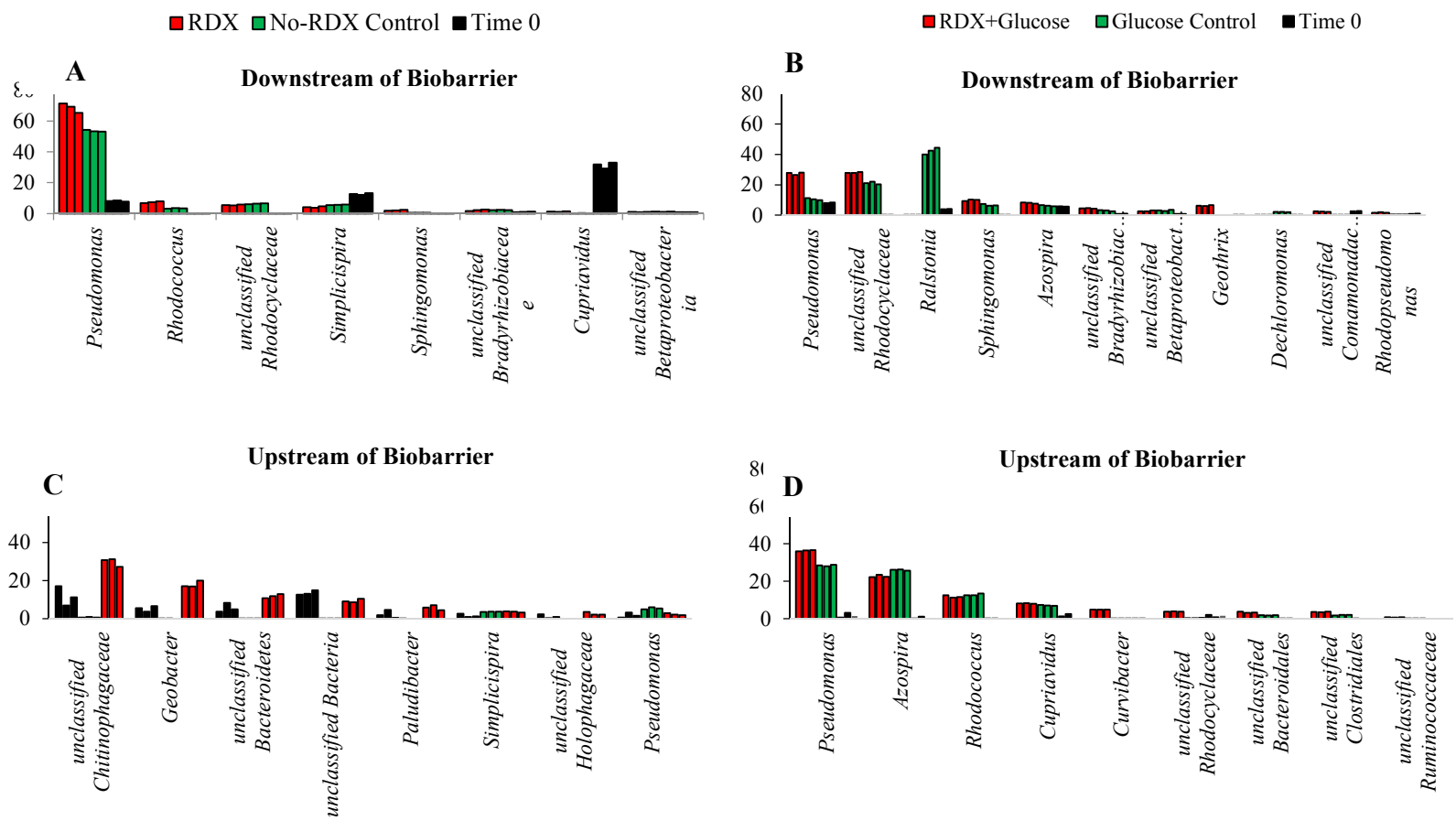

Figure 4.9. Relative abundance (RA, %) of phylotypes in DNA extracted from initial samples, RDX- and No-RDX- amended microcosms (both with and without glucose) containing groundwater from downstream (A and B, day 67) and upstream (C and D, day 100) of an installed buffered emulsified oil biobarrier in triplicates.

For MW 58, the most abundant phylotypes in the RDX-amended microcosms from the 5 ft depth on day 90 were *Yersinia, Dyella, Clostridium (stricto senso and IV), Burkholderia* and *Pseudomonas* (Figure 4.7A). Still, *Burkholderia* and *Pseudomonas* also presented high RA in time 0 and live controls, respectively. On day 130, at 5 ft depth, while *Yersinia* and *Dyella,* were still among the most dominant phylotypes in the RDX-amended samples, *Sporotalea, Mucilaginibacter* and *Paenibacillus* also increased in abundance during RDX degradation compared to the controls. Similar to day 90, *Pseudomonas* and *Burkholderia* presented high RA not only in the RDX-amended microcosms, but also in time 0 and live controls (Figure 4.7B).

For depths 10 ft (Figure 4.7C) and 25 ft (Figure 4.7E), the genus *Pseudomonas* presented the highest RA in all RDX-amended microcosms from day 90. Although a high RA of *Pseudomonas* was also observed in the No-RDX microcosms at depth 10 ft on day 90, this genus' RA was higher in the RDX-amended microcosms (Figure 4.7C). On day 130, *Pseudomonas* still showed the highest RA in the RDX-amended microcosms at 25 ft (Figure 4.7F), but for the 10 ft RDX-amended microcosms, *Acidovorax* illustrates the highest RA (Figure 4.7D). Other genera presenting higher RA in RDX-amended microcosms compared to time 0 and live controls at 10 ft depth were *Arthrobacter* on day 90 (Figure 4.7C) and *Tissierella, unclassified Caulobacteraceae, Caulobacter* and *unclassified Alcaligenaceae* on day 130 (Figure 4.7D). At depth 25 ft, *Pseudomonas*, *unclassified Enterobacteriaceae, unclassified Bacillales, unclassified Alphaproteobacteria, Sporolactobacillus* and *Arthrobacter* illustrated high RA in RDX-amended microcosms compared to time 0 and live controls at day 90 (Figure 4.7E) while *Rhodococcus, Arthrobacter, unclassified Actinomycetales* and *unclassified Enterobacteriaceae* showed high RA in RDX-amended microcosms compared to time 0 and live controls on day 130 (Figure 4.7F).

For MW 61, on day 45, the phylogenetic analyses from the sediment microcosms illustrated that *Pseudomonas* and *Sporolactobacillus* increased in abundance in the RDX-amended microcosms compared to the controls, thus indicating these phylotypes are important for RDX removal (Figure 4.8A, C, E).

On day 90, a change in the most dominant phylotypes occurred in most depths. At depth 5 ft, *unclassified Betaproteobacteria, Methylophilus* and *unclassified Chitinophagaceae* showed higher RA in the RDX-amended microcosms compared to time 0 and live controls (Figure 4.8B). At depth 10 ft, *Methylophilus, Sediminibacterium,* and *Albidiferax* showed the highest RA in RDX-amended microcosms, but *Sediminibacterium* also showed high RA at time 0 (Figure 4.8D). At depth 20 ft, *Pseudomonas*, *Methylophilus* and *Albidiferax* showed the highest RA in RDX-amended microcosms, but *Pseudomonas* also showed high RA at time 0 (Figure 4.8F).

Overall, for MW 58, the genera that were more dominant in the RDX-amended microcosms throughout the tested depths and time points included *Arthrobacter, Pseudomonas, Rhodococcus, unclassified Comamonadaceae* and *unclassified Enterobacteriaceae* (Table 4.2). For MW 61, *Pseudomonas* was the most dominant genus thus being related to RDX removal throughout the tested depths and time points. Other dominant genera in the RDX-amended microcosms included *Clostridium sensu stricto, Methylophilus, Pedobacter, Sporolactobacillus, Stenotrophomonas, unclassified Alcaligenaceae* and *unclassified Bacteria* (Table 4.3). Interestingly, several dominant phylotypes were common to both MW 58 and MW 61 in most depths. Specifically, both *Pseudomonas* and spore forming bacteria (for example, *Clostridium stricto senso, Clostridium IV, Sporolactobacillus*) were related to RDX degradation as they increased in abundance in the RDX-amended microcosms compared to the controls.

Table 4.2. Most dominant phylotypes in DNA extracted from RDX- amended microcosms containing sediments from MW 58 at depths 5, 10 and 25 ft depth at day 90 and 130 and analyzed by MiSeq Illumina.

Genus	Well 58 - Day 90			Well 58 - Day 130			Total
	5 ft	10 ft	20 ft	5 ft	10 ft	20 ft	
Arthrobacter	**X**	**X**	**X**		**X**	**X**	**5**
Pseudomonas	**X**	**X**	**X**	**X**		**X**	**5**
Rhodococcus	**X**	**X**	**X**		**X**	**X**	**5**
unclassified Comamonadaceae		**X**	**X**	**X**		**X**	**4**
unclassified Enterobacteriaceae	**X**		**X**	**X**		**X**	**4**
Brevundimonas		X	X		X		3
Caulobacter				X	X		3
Burkholderia	X			X			2
Cupriavidus		X				X	2
Dyella	X			X			2
Mucilaginibacter	X			X			2
Rhodanobacter		X				*X*	2
Sphingomonas		X				X	2
unclassified Actinomycetales		X				X	2
Yersinia	X			X			2
Acidovorax					X		1
Clostridium IV	X						1
Clostridium sensu stricto	X						1
Paenibacillus				X			1
Pedobacter			X				1
Sediminibacterium					X		1
Sporolactobacillus			X				1
Sporotalea				X			1
Stenotrophomonas						X	1
Tissierella					X		1
unclassified Alcaligenaceae					X		1
unclassified Alphaproteobacteria			X				1
unclassified Bacillales			X				1
unclassified Caulobacteraceae					X		1
unclassified Microbacteriaceae		X					1

Table 4.3. Most dominant phylotypes in DNA extracted from RDX- amended microcosms containing sediments from MW 61 at depths 5, 10 and 20 ft depth at day 45 and 90 and analyzed by MiSeq Illumina.

Genus	Well 61 - Day 45			Well 61 - Day 90			Total
	5 ft	10 ft	20 ft	5 ft	10 ft	20 ft	
Pseudomonas	**X**	**X**	**X**		**X**	**X**	**5**
Clostridium sensu stricto	**X**	**X**	**X**				**3**
Methylophilus				**X**	**X**	**X**	**3**
Pedobacter	**X**	**X**		**X**			**3**
Sporolactobacillus	**X**	**X**	**X**				**3**
Stenotrophomonas	**X**	**X**	**X**				**3**
unclassified Alcaligenaceae	**X**	**X**	**X**				**3**
unclassified Bacteria		**X**		**X**	**X**		**3**
Albidiferax					X	X	2
Cellulomonas	X	X					2
Mucilaginibacter		X		X			2
Rhodococcus					X	X	2
Sediminibacterium					X	X	2
unclassified Bacteroidetes				X	X		2
unclassified Chitinophagaceae				X	X		2
unclassified Cystobacteraceae					X	X	2
unclassified Proteobacteria				X	X		2
Yersinia	X		X				2
Acinetobacter						X	1
Brevundimonas			X				1
Burkholderia	X						1
Clostridium IV	X						1
Clostridium XlVa			X				1
Luteibacter		X					1
Ralstonia						X	1
Rhodanobacter			X				1
Sphingomonas				X			1
unclassified Betaproteobacteria				X			1
unclassified Gammaproteobacteria				X			1
unclassified Oxalobacteraceae						X	1
unclassified Peptococcaceae_1			X				1
unclassified Sphingobacteriaceae						X	1

For the downstream groundwater microcosms, *Pseudomonas* illustrated the greatest RA in the RDX-amended microcosms, with or without glucose (Figure 4.9A, B). This genus also increased in the No-RDX amended microcosms, but showed lower RA compared to RDX-amended microcosms. The RA of *Pseudomonas* in downstream time zero microcosms, with or without glucose, was lower than the No- and RDX-amended microcosms (Figure 4.9A, B). Following *Pseudomonas*, other genera presenting higher RA included *Rhodococcus, unclassified Rhodocyclaceae* and *Sphingomonas* for the RDX-amended microcosms not containing glucose (Figure 4.9A) and *unclassified Rhodocyclaceae*, *Sphingomonas, Azospira* and *Geotrix* for RDX-amended microcosms containing glucose (Figure 4.9B).

Pseudomonas was also detected in the upstream groundwater study as a putative RDX degrader when glucose was present (Figure 4.9D), but did not present a high RA in the RDX-amended microcosms not containing glucose (Figure 4.9C). In these microcosms, *unclassified Chitinophagaceae, Geobacter, unclassified Bacteroidetes, Paludibacter* and *unclassified Bacteria* presented the highest RA (Figure 4.9C). Overall, *Pseudomonas* and *unclassified Rhodocyclaceae* were the most dominant genera in the RDX-amended microcosms (with or without glucose) in both the down- and upstream microcosms (Table 4.4). These data indicate, that, similar to MW 58 and 61, *Pseudomonas* also played an important role in RDX removal in the groundwater microcosms.

Table 4.4. Most dominant phylotypes in DNA extracted from RDX- amended microcosms (both with and without glucose) containing groundwater from downstream and upstream of an installed buffered emulsified oil biobarrier and analyzed by MiSeq Illumina.

	Downstream		**Upstream**		
Genus	**RDX**	**RDX+Glucose**	**RDX**	**RDX+Glucose**	**Total**
Pseudomonas	**X**	**X**	**X**	**X**	**4**
unclassified Rhodocyclaceae	**X**	**X**	**X**		**3**
Rhodococcus	X		X		2
Simplicispira	X			X	2
Sphingomonas	X	X			2
unclassified Bradyrhizobiaceae	X	X			2
Cupriavidus	X		X		2
unclassified Betaproteobacteria	X	X			2
Azospira		X	X		2
Ralstonia		X			1
Geothrix		X			1
Curvibacter			X		1
unclassified Bacteroidales			X		1
unclassified Clostridiales			X		1
unclassified Chitinophagaceae				X	1
Geobacter				X	1
unclassified Bacteroidetes				X	1
unclassified Bacteria				X	1
Paludibacter				X	1
unclassified Holophagaceae				X	1

Discussion

The biological removal of RDX has been widely reported, however a large number of these studies were based on culture based methods of microbial isolation. Because of this, the potential for any site to naturally biodegrade RDX becomes difficult to predict. The use of molecular tools to study RDX-degraders aims to overcome this limitation. To date, a range of molecular methods have been used to study microbial communities at RDX contaminated sites, including terminal restriction fragment length polymorphism (TRFLP), lipid biomarker analysis [30], denaturing gradient gel electrophoresis [31-33], amplified 16S rRNA restriction analysis (ARDRA) [34], cloning and Sanger sequencing [31, 33-35]. There also have been studies applying SIP to examine RDX degradation [5, 25, 36-38] and, recently, high throughput sequencing has been applied to examine RDX degrading microbial communities [39, 40].

This study contributes to an improved understanding of RDX degradation by using two approaches. Firstly, the most dominant microorganisms in RDX degrading microcosms containing sediment from different depths or groundwater from down- and upstream of an emulsified biobarrier following RDX degradation were identified using high throughput sequencing. While it cannot be stated that these microorganisms were growing using RDX as a carbon, nitrogen or energy source specifically, the study illustrates the phylotypes illustrating an increase in RA following RDX degradation benefited from this process. Secondly, the functional genes *xenA, xenB* and *xplA* were quantified in these microcosms (containing sediment or groundwater under different conditions) following RDX degradation. To our knowledge, the distribution of RDX degraders or their functional genes throughout the soil profile for a

contaminated site has not previously been reported. Additionally, the literature does not contain such information for groundwater samples surrounding a biobarrier.

The known RDX degrading bacterial isolates classify within the phyla *Firmicutes, Actinobacteria, Proteobacteria* and *Fusobacteria*. *Bacteroidetes, Chlorobi* and *Fibrobactere* have also been listed in RDX-degradation studies, although RDX degrading isolates have not been reported from these phyla [41]. The current study found that phylotypes from *Firmicutes, Actinobacteria, Proteobacteria, Acidobacteria* and *Bacteroidetes* benefited from RDX degradation.

The phylum *Firmicutes* contains RDX degrading bacteria within the *Clostridia* or *Bacilli* [40, 42-50]. In fact, the first anaerobic RDX-degrader isolated was *Clostridium bifermentans* [44]. In the current study, *Clostridium sensu stricto, Clostridium IV, Tissierella* and unclassified *Clostridiales*, as well as several *Bacilli (Paenibacillus, Sporolactobacillius,* and unclassified *Bacillales*) were among the most dominant phylotypes following RDX degradation in the microcosms inoculated with sediment from MW 61. *Sporotalea*, belonging to the class *Negativucutes* (*Firmicutes)* was enriched in MW 61 at 5 ft depth and has not been previously related to RDX degradation. *Sporolactobacillus* exhibited the highest RA at the first time point at 5 ft and 10 ft depth from MW 61. A study on RDX degradation in groundwater samples from two navy sites (Pueblo Chemical Depot, CO and Picatinny Arsenal, NJ) has also detected *Clostridium* and *Sporolactobacillus* among the dominant 16S rRNA gene sequences [2]. *Sporotalea* has been previously found in the intestinal tract of soil-feeding termite [51] and detected in a propane biostimulation study in biologically activated carbon [52].

Actinobacteria is also an important phylum related to RDX degradation. The known RDX degrading isolates include the genera *Rhodococcus* [15, 16, 19, 21, 53-56] , *Williamsia* [18] and *Gordonia* [18, 57]. From the *Actinobacteria*, the current work indicates that *Rhodococcus* and *Arthrobacter* increased in abundance following RDX degradation. For the groundwater microcosms, *Rhodococcus* was present in microcosms from both downstream (without glucose) and upstream (with glucose) of the biobarrier. A previous SIP study of contaminated sediments from the same Navy site (Dahlgren, VA) reported the presence of 16S rRNA genes of *Azohydromonas* and *Rhodococcus* when RDX degradation occurred without the presence of glucose [40]. The presence of *Rhodococcus* in the sediment microcosms studied here was observed at most depths and time points from both MW 58 and 61 (Bangor, WA). *Rhodococcus* was present in the RDX-amended microcosms, and in the No-RDX amended microcosms as well as the initial samples. The presence of *Rhodococcus* throughout all treatments may be explained by the previous selection of RDX degraders at these contaminated sites. *Arthrobacter* was present in MW 58 throughout the depths except for 5 ft depth on day 130, but similar to *Rhodococcus*, *Arthrobacter* did not present a clear correlation with RDX degradation.

RDX degrading isolates in the phylum *Proteobacteria* are found within the *Alpha-, Gamma-* and *Deltaproteobacteria*. In the current study, *Alpha-, Gamma-* and *Betaproteobacteria* were recovered from the RDX-amended microcosms from all sites.

Alphaproteobacteria phylotypes enriched following RDX degradation in the current study included unclassified *Caulobacter* and unclassified *Alphaproteobacteria*. For the *Betaproteobacteria*, the phylotypes *Methylophilus, Albidiferax, Acidovorax* and unclassified

Rhodocyclaceae were enriched following RDX degradation. *Acidovorax* was the most abundant phylotype on MW 58 10 ft depth at day 130 in the RDX-amended microcosms and the phylotype seemed to benefit from RDX degradation in those microcosms. The unclassified *Rhodocyclaceae* partial 16S rRNA gene sequence was found to be 100 % similar to *Propionivibrio militaris* (NCBI reference sequence: NR_125528.1), a perchlorate-reducing bacteria [36]. In MW 61, at 10 ft depth at day 130, *Methylophilus* was the most dominant phylotype in the RDX-amended microcosms but was not enriched in the No-RDX control and initial sample. No pure cultures of *Betaproteobacteria* have been shown to be capable of RDX degradation [40].

The *Gammaproteobacteria* phylotypes detected as most abundant (high RA) in RDX-amended microcosms in this study were *Pseudomonas*, *Yersinia, Stenotrophomonas* and *unclassified Enterobacteriaceae*. Among these, *Pseudomonas* was the most enriched phylotype in many of the RDX-amended microcosms of MW 58, MW 61 and groundwater. In some cases, the No-RDX controls did not present a high RA for this phylotypes (i.e., Figure 4.7E, F, MW 58 25 ft depth) and in other cases, *Pseudomonas* increased also in the No-RDX controls (i.e., Figure 4.8A, D, groundwater). Similar to *Rhodococcus*, this may be explained by the fact that the samples originated from two contaminated sites, where the selection of RDX degraders may have already occurred. Confirming the data from the current study, the participation of *Pseudomonas* in RDX degradation has been previously reported [50, 58]. *Yersinia* was also abundant in some MW 58 RDX amended microcosms but not in the No-RDX controls and the initial sample. These results are consistent with previous research, as many *Gammaproteobacteria* isolates have been linked to RDX degradation [14, 40, 50, 58-62].

RDX degradation also appeared to benefit phylotypes belonging to the phylum *Acidobacteria (Dyella,* MW 58 5ft depth), as well as the phylum *Bacteroidetes (Mucilaginibacter, Pedobacter* and unclassified *Chitinophagaceae,* MW 58 5 ft depth and MW 61 5 and 10 ft depth). Although *Acidobacteria* are widespread and abundant in soils, little is known about these organisms [63]. *Acidobacteria Gp1* and *Gp 3* [25] as well as an uncultured *Acidobacteria* bacterium clone [64] have been associated with RDX degradation (in mixed cultures), but the genus *Dyella* has not yet been linked to RDX biodegradation. The genus *Dyella* has been isolated with an ability to biodegrade biphenyl, polychlorinated biphenyls, benzoate and naphthalene [65-67].

For the phylum *Bacteroidetes*, uncultured bacterium clones belonging to *Sphingobacteria* [64], unclassified *Sphingobacteriales* [25] and unclassified *Chitinophagaceae* [38] have been previously reported in RDX-biodegradation related studies. The genera *Pedobacter* and *Mucilaginibacter* were enriched in the current study and both belong to the family *Sphingobacteriaceae*. Unclassified *Chitinophagaceae* (class *Sphingobacteria*) was also among the most abundant phylotypes in the RDX-amended microcosms. The unclassified *Chitinophagaceae* partial 16S rRNA gene sequence recovered in the current study was 98 % similar to *Sediminibacterium salmoneum* (NCBI reference sequences: NR_114255.1 and NR_044197.1), a cultivable bacteria isolated from sediments of an eutrophic reservoir in China [68].

The nitro groups are often involved in RDX transformation, by reduction or by denitration [41], followed by ring cleavage that leads to MEDINA or 4-nitro-2,4-diazabutanal (NDAB). The functional genes *xenA* and *xenB,* from *Pseudomonas* strains, have been associated

with these degradation products [8]. In the current study, *xenA* and *xenB* were widely detected in the sediment and groundwater microcosms. Here, the gene copies of *xenA* were significantly different ($p < 0.05$) between the RDX-amended samples and the No-RDX controls in the microcosms from MW 58. Gene copies of *xenB* were also significantly different ($p < 0.05$) between the RDX amended samples and No-RDX controls from these microcosms. *Pseudomonas* illustrated a high level of enrichment in many of these RDX amended samples too.

A metagenomic study on ovine rumen microbiota found sequence homologues to five RDX-degrading genes including *xenA* and *xenB* [23]. Other studies (on environmental samples) have tested for *xplA, hydA, onr, xenA* or *xenB* in groundwater DNA [2] from Navy sites or *xplA* on DNA extracted from sediment microcosms [64]. Using conventional PCR, no RDX functional genes were detected. Thus, from the results in the current research, the use of a more sensitive method, such as qPCR, would be recommended for the future detection of these RDX functional genes.

RDX denitration has been catalyzed by a cytochrome P450 enzyme encoded by the *xplA* gene and this has been demonstrated in *Rhodococcus* strains DN22 [54], YH1 [17] and 11Y [19]. The mechanism is thought to involve initial denitration followed by spontaneous ring cleavage and mineralization [15]. Here, *xplA* was more abundant in the majority (except Well 10) of the RDX amended microcosms compared to the No RDX controls.

Rhodococcus was also found in many of the microcosms in this study, but a direct relationship between the increase in *xplA* gene copy numbers and an increase in *Rhodococcus* RA phylotypes in each microcosm over time (for sediments) was not observed. While the regulation of *xplA* has not yet been elucidated, resting-cell incubations of *R. rhodochrous* 11Y

have shown that although the activity towards RDX is present in the absence of RDX, activity significantly increased when cells were grown with RDX supplied as the sole nitrogen source [51].

An RDX degradation study detected *xplA* in 11 of the 16 soils tested [5] but, in some of the detected samples, no apparent correlation existed between the presence of the *xplA* gene or *xplA* gene copy number and RDX degradation under the conditions tested. Another study evaluated a bioaugmentation strategy at a Navy site, by detecting *xplA* from the bioaugmentation cultures *Rhodococcus* and *Gordonia* using qPCR [69].

The capacity to monitor the presence of specific microorganisms and/or genes coding enzymes involved in RDX degradation in environmental samples is critical for remediation strategies that rely on *in situ* bioaugmentation, biostimulation or monitored natural attenuation. Towards this goal, *xenA, xenB* and *xplA* were enumerated in microcosms where RDX degradation was observed. Also, Illumina sequencing data indicated several phylotypes increased in abundance following RDX degradation compared to the initial soil and No-RDX controls. These trends suggest a growth benefit caused by the degradation of RDX as the microorganisms were directly benefiting from RDX or from RDX metabolites. Primers designed towards these phylotypes would be advantageous for investigating the feasibility of bioremediation across RDX contaminated sites. Combined with functional genes, these biomarkers can be used to estimate the genetic catabolic potential for degradation thus providing a strong argument supporting remediation through biological pathways.

APPENDIX

Table S4.1. Sequence, target and amplicon length of the primers designed to amplify the three RDX-degrading functional genes**.**

Target Gene	Forward or Reverse	Sequence (5´ to 3´)	Tm (°C)	Gene Target Match (Accession #)	Target Match Position	Target Size (bp)
xplA	Forward	AGGCTATCGCCACGATTCTG	59.97	*Rhodococcus rhodochrous* strain 11Y cytochrome P450-like protein XplA (AF449421)	1139 to 1158	382
xplA	Reverse	ATCTGTCCCGCACAGGAATG	60.11	As above	1520 to 1501	382
xenA	Forward	CACCATTCCCGAGACCAACA	59.96	*Pseudomonas putida* xenobiotic reductase A (AF154061)	909 to 928	324
xenA	Reverse	TTTAGATTCGGGGGCTGCTG	60.11	As above	1232 to 1213	324
xenB	Forward	ACCTTCACCTATGTTGCTCGC	60.68	*Pseudomonas fluorescens* xenobiotic reductase B (AF154062)	931 to 951	351
xenB	Reverse	CGTTTCTAGCGTTTCATGCGGT	62.05	As above	1281 to 1260	351

Table S4.2. Characteristics of the standard curves used to enumerate *xplA, xenA* and *xenB* in sediment (MW 58 and 61) and groundwater (GW) microcosms.

Gene	Linear Range (target gene copies per reaction)	Slope (average ± standard deviation)	R^2 (average ± standard deviation)	Amplification Efficiency (%) (average ± standard deviation)
xplA MW 58	10^3-10^{10}	-3.18±0.09	0.97±0.01	106.25±4.19
xenA MW 58	10^3-10^9	-3.51±0.05	0.97±0.02	92.75±1.69
xenB MW 58	10^3-10^{10}	-3.59±0.02	0.99±0.002	90.10±0.56
xplA MW 61	10^3-10^{10}	-3.18±0.08	0.96±0.01	106.29±3.54
xenA MW 61	10^3-10^9	-3.34±0.46	0.96±0.02	101.69±20.85
xenB MW61	10^3-10^{10}	-3.99±0.39	0.99±0.01	78.74±10.63
xplA GW	10^3-10^{10}	-3.51±0.33	0.95±0.02	93.95±12.87
xenA GW	10^3-10^{10}	-3.18±0.02	0.98±0.02	106.33±0.93
xenB GW	10^3-10^{10}	-2.83±0.19	0.97±0.01	125.87±12.88

REFERENCES

REFERENCES

[1] E.L. Rylott, R.G. Jackson, F. Sabbadin, H.M.B. Seth-Smith, J. Edwards, C.S. Chong, S.E. Strand, G. Grogan, N.C. Bruce, The explosive-degrading cytochrome P450 XplA: Biochemistry, structural features and prospects for bioremediation, Bba-Proteins Proteom, 1814 (2011) 230-236.

[2] M.E. Fuller, K. McClay, M. Higham, P.B. Hatzinger, R.J. Steffan, Hexahydro-1,3,5-trinitro-1,3,5-triazine (RDX) Bioremediation in Groundwater: Are Known RDX-Degrading Bacteria the Dominant Players?, Bioremediation Journal, 14 (2010) 121-134.

[3] H. Roh, C.P. Yu, M.E. Fuller, K.H. Chu, Identification of hexahydro-1,3,5-trinitro-1,3,5-triazine-degrading microorganisms via ^{15}N stable isotope probing, Environ Sci Technol, 43 (2009) 2505-2511.

[4] K.C. Cho, D.G. Lee, H. Roh, M.E. Fuller, P.B. Hatzinger, K.H. Chu, Application of ^{13}C stable isotope probing to identify RDX-degrading microorganisms in groundwater, Environ Pollut, 178 (2013) 350-360.

[5] P. Andeer, D.A. Stahl, L. Lillis, S.E. Strand, Identification of microbial populations assimilating nitrogen from RDX in munitions contaminated military training range soils by high sensitivity stable isotope probing, Environmental Science & Technology, 47 (2013) 10356-10363.

[6] I. Jayamani, A.M. Cupples, Stable isotope probing reveals the importance of *Comamonas* and *Pseudomonadaceae* in RDX degradation in samples from a Navy detonation site, Environ Sci Pollut R, 22 (2015) 10340-10350.

[7] J.K. Hatt, K.M. Ritalahti, D.M. Ogles, C.A. Lebron, F.E. Loffler, Design and application of an internal amplification control to improve *Dehalococcoides mccartyi* 165 rRNA gene enumeration by qPCR, Environ Sci Technol, 47 (2013) 11131-11138.

[8] M.E. Fuller, K. McClay, J. Hawari, L. Paquet, T.E. Malone, B.G. Fox, R.J. Steffan, Transformation of RDX and other energetic compounds by xenobiotic reductases *XenA* and *XenB*, Applied Microbiology and Biotechnology, 84 (2009) 535-544.

[9] D.S. Blehert, B.G. Fox, G.H. Chambliss, Cloning and sequence analysis of two *Pseudomonas* flavoprotein xenobiotic reductases, J Bacteriol, 181 (1999) 6254-6263.

[10] B. Bhushan, A. Halasz, J.C. Spain, J. Hawari, Diaphorase catalyzed biotransformation of RDX via N-denitration mechanism, Biochem Bioph Res Co, 296 (2002) 779-784.

[11] R.W. Li, J.G. Giarrizzo, S. Wu, W. Li, J.M. Duringer, A.M. Craig, Metagenomic Insights into the RDX-Degrading Potential of the Ovine Rumen Microbiome, Plos One, 9 (2014).

[12] S. Chakraborty, M. Sakka, T. Kimura, K. Sakka, Cloning and expression of a *Clostridium kluyveri* gene responsible for diaphorase activity, Biosci Biotech Bioch, 72 (2008) 735-741.

[13] W.M. M., C. S., K. R., H. S., R.F. B., H.J. B., B.G. N., 2,4,6-trinitrotoluene reduction by an Fe-only hydrogenase in Clostridium acetobutylicum, applied and environmental microbiology, 69 (2003) 1542-1547.

[14] C.L. Kitts, C.E. Green, R.A. Otley, M.A. Alvarez, P.J. Unkefer, Type I nitroreductases in soil enterobacteria reduce TNT (2,4,6-trinitrotoluene) and RDX (hexahydro-1,3,5-trinitro-1,3,5-triazine), Can J Micro, 46 (2000) 278-282.

[15] H.M.B. Seth-Smith, S.J. Rosser, A. Basran, E.R. Travis, E.R. Dabbs, S. Nicklin, N.C. Bruce, Cloning, sequencing, and characterization of the hexahydro-1,3,5-trinitro-1,3,5-triazine degradation gene cluster from *Rhodococcus rhodochrous*, Applied and Environmental Microbiology, 68 (2002) 4764-4771.

[16] N.V. Coleman, D.R. Nelson, T. Duxbury, Aerobic biodegradation of hexahydro-1,3,5-trinitro-1,3,5-triazine (RDX) as a nitrogen source by a *Rhodococcus* sp., strain DN22, Soil Biology & Biochemistry, 30 (1998) 1159-1167.

[17] A. Nejidat, L. Kafka, Y. Tekoah, Z. Ronen, Effect of organic and inorganic nitrogenous compounds on RDX degradation and cytochrome P-450 expression in *Rhodococcus* strain YH1, Biodegradation, 19 (2008) 313-320.

[18] K.T. Thompson, F.H. Crocker, H.L. Fredrickson, Mineralization of the cyclic nitramine explosive hexahydro-1,3,5-trinitro-1,3,5-triazine by *Gordonia* and *Williamsia* spp., Applied and Environmental Microbiology, 71 (2005) 8265-8272.

[19] H.M.B. Seth-Smith, J. Edwards, S.J. Rosser, D.A. Rathbone, N.C. Bruce, The explosive-degrading cytochrome P450 system is highly conserved among strains of *Rhodococcus* spp., Applied and Environmental Microbiology, 74 (2008) 4550-4552.

[20] P.F. Andeer, D.A. Stahl, N.C. Bruce, S.E. Strand, Lateral transfer of genes for hexahydro-1,3,5-trinitro-1,3,5-triazine (RDX) degradation, Applied and Environmental Microbiology, 75 (2009) 3258-3262.

[21] A. Bernstein, E. Adar, A. Nejidat, Z. Ronen, Isolation and characterization of RDX-degrading *Rhodococcus* species from a contaminated aquifer, Biodegradation, 22 (2011) 997-1005.

[22] K.J. Indest, F.H. Crocker, R. Athow, A TaqMan polymerase chain reaction method for monitoring RDX-degrading bacteria based on the xp1A functional gene, Journal of Microbiological Methods, 68 (2007) 267-274.

[23] R.W. Li, J.G. Giarrizzo, S.T. Wu, W.Z. Li, J.M. Duringer, A.M. Craig, Metagenomic insights into the RDX-degrading potential of the ovine rumen microbiome, Plos One, 9 (2014).

[24] C.S. Chong, D.K. Sabir, A. Lorenz, C. Bontemps, P. Andeer, D.A. Stahl, S.E. Strand, E.L. Rylott, N.C. Bruce, Analysis of the xplAB-Containing Gene Cluster Involved in the Bacterial Degradation of the Explosive Hexahydro-1,3,5-Trinitro-1,3,5-Triazine, Applied and Environmental Microbiology, 80 (2014) 6601-6610.

[25] I. Jayamani, M.P. Manzella, A.M. Cupples, RDX degradation potential in soils previously unexposed to RDX and the identification of RDX-degrading species in one agricultural soil using stable isotope probing, Water Air Soil Pollution, 224 (2013) 1745-1760.

[26] K.M. Ritalahti, Amos, B.K., Sung, Y., Wu, Q.Z., Koenigsberg, S.S. and Loffler, F.E., Quantitative PCR targeting 16S rRNA and reductive dehalogenase genes simultaneously monitors multiple Dehalococcoides strains., Appl. Environ. Microbiol., 72 (2006) 2765-2774.

[27] J.G. Caporaso, C.L. Lauber, W.A. Walters, D. Berg-Lyons, C.A. Lozupone, P.J. Turnbaugh, N. Fierer, R. Knight, Global patterns of 16S rRNA diversity at a depth of millions of sequences per sample, Proceedings of the National Academy of Sciences of the United States of America, 108 (2011) 4516-4522.

[28] P.D. Schloss, A high-throughput DNA sequence aligner for microbial ecology studies, PLOS, 4 (2009).

[29] E. Pruesse, C. Quast, K. Knittel, B.M. Fuchs, W. Ludwig, J. Peplies, F.O. Gloeckner, SILVA: a comprehensive online resource for quality checked and aligned ribosomal RNA sequence data compatible with ARB, Nucleic Acids Research, 35 (2007) 7188-7196.

[30] D. Ringelberg, M. Richmond, K. Foley, C. Reynolds, Utility of lipid biomarkers in support of bioremediation efforts at army sites, J Micro Meth, 74 (2008) 17-25.

[31] Z. Ronen, Y. Yanovich, R. Goldin, E. Adar, Metabolism of the explosive hexahydro-1,3,5-trinitro-1,3,5-triazine (RDX) in a contaminated vadose zone, Chemosphere, 73 (2008) 1492-1498.

[32] S.S.B. Moshe, Z. Ronen, O. Dahan, N. Weisbrod, L. Groisman, E. Adar, R. Nativ, Sequential biodegradation of TNT, RDX and HMX in a mixture, Environmental Pollution, 157 (2009) 2231-2238.

[33] M.E. Fuller, K. McClay, M. Higham, P.B. Hatzinger, R.J. Steffan, Hexahydro-1,3,5-trinitro-1,3,5-triazine (RDX) bioremediation in groundwater: are known RDX-degrading bacteria the dominant players?, Bioremed J, 14 (2010) 121-134.

[34] M.J. Kwon, K.T. Finneran, Electron shuttle-stimulated RDX mineralization and biological production of 4-nitro-2,4-diazabutanal (NDAB) in RDX-contaminated aquifer material, Biodegradation, 21 (2010) 923-937.

[35] M.J. Kwon, E.J. O'Loughlin, D.A. Antonopoulos, K.T. Finneran, Geochemical and microbiological processes contributing to the transformation of hexahydro-1,3,5-trinitro-1,3,5-triazine (RDX) in contaminated aquifer material, Chemosphere, 84 (2011) 1223-1230.

[36] K.C. Cho, D.G. Lee, H. Roh, M.E. Fuller, P.B. Hatzinger, K.-H. Chu, Application of ^{13}C-stable isotope probing to identify RDX-degrading microorganisms in groundwater, Environmental Pollution, 178 (2013) 350-360.

[37] H. Roh, C.P. Yu, M.E. Fuller, K.H. Chu, Identification of hexahydro-1,3,5-trinitro-1,3,5-triazine-degrading microorganisms via ^{15}N-stable isotope probing, Environmental Science & Technology, 43 (2009) 2505-2511.

[38] I. Jayamani, A.M. Cupples, A comparative study of microbial communities in four soil slurries capable of RDX degradation using Illumina sequencing, Biodegradation, 26 (2015) 247-257.

[39] J. Livermore, Y. Oh Jin, M. LePuil, R. Arnseth, T.E. Mattes, Microbial community dynamics during acetate biostimulation of RDX-contaminated groundwater, Environmental Science & Technology, 47 (2013) 7672-7678.

[40] I. Jayamani, A.M. Cupples, Stable isotope probing reveals the importance of *Comamonas* and *Pseudomonadaceae* in RDX degradation in samples from a Navy Detonation Site, Environmental Science and Pollution Research, 22 (2015) 10340-10350.

[41] A.M. Cupples, RDX degrading microbial communities and the prediction of microorganisms responsible for RDX bioremediation, Int Biodeter Biodegr, 85 (2013) 260-270.

[42] J.S. Zhao, L. Paquet, A. Halasz, J. Hawari, Metabolism of hexahydro-1,3,5-trinitro-1,3,5-triazine through initial reduction to hexahydro-1-nitroso-3,5-dinitro-1,3,5-triazine followed by denitration in *Clostridium bifermentans* HAW-1, Appl Micro Biotec, 63 (2003) 187-193.

[43] N.R. Adrian, C.M. Arnett, Anaerobic biodegradation of hexahydro-1,3,5-trinitro-1,3,5-triazine (RDX) by *Acetobacterium malicum* strain HAAP-1 isolated from a methanogenic mixed culture, Current Micro, 48 (2004) 332-340.

[44] K.M. Regan, R.L. Crawford, Characterization of *Clostridium bifermentans* and its biotransformation of 2,4,6-trinitrotoluene (TNT) and 1,3,5-triaza-1,3,5-trinitrocyclohexane (RDX), Biotec Lett, 16 (1994) 1081-1086.

[45] B. Bhushan, A. Halasz, S. Thiboutot, G. Ampleman, J. Hawari, Chemotaxis-mediated biodegradation of cyclic nitramine explosives RDX, HMX, and CL-20 by *Clostridium* sp. EDB2, Biochem Biophys Res Commun, 316 (2004) 816-821.

[46] C.L. Zhang, J.B. Hughes, Biodegradation pathways of hexahydro-1,3,5-trinitro-1,3,5-triazine (RDX) by *Clostridium acetobutylicum* cell-free extract, Chemos, 50 (2003) 665-671.

[47] J.S. Zhao, J. Spain, M. Hawari, Phylogenetic and metabolic diversity of hexahydro-1,3,5-trinitro-1,3,5-triazine (RDX)-transforming bacteria in strictly anaerobic mixed cultures enriched on RDX as nitrogen source, FEMS Micro Ecol, 46 (2003) 189-196.

[48] L.A. Sherburne, J.D. Shrout, P.J.J. Alvarez, Hexahydro-1,3,5-trinitro-1,3,5-triazine (RDX) degradation by *Acetobacterium paludosum*, Biodegradation, 16 (2005) 539-547.

[49] M.J. Kwon, K.T. Finneran, Hexahydro-1,3,5-trinitro-1,3,5-triazine (RDX) and octahydro-1,3,5,7-tetranitro-1,3,5,7-tetrazocine (HMX) biodegradation kinetics amongst several Fe(III)-reducing genera, Soil Sed Contam, 17 (2008) 189-203.

[50] R. Singh, P. Soni, P. Kumar, S. Purohit, A. Singh, Biodegradation of high explosive production effluent containing RDX and HMX by denitrifying bacteria, World J Micro Biotech 25 (2009) 269-275.

[51] H.I. Boga, R. Ji, W. Ludwig, A. Brune, Sporotalea propionica gen. nov sp nov., a hydrogen-oxidizing, oxygen-reducing, propionigenic firmicute from the intestinal tract of a soil-feeding termite, Archives of Microbiology, 187 (2007) 15-27.

[52] K.M. Mikkelson, C.L. Homme, D. Li, J.O. Sharp, Propane biostimulation in biologically activated carbon (BAC) selects for bacterial clades adept at degrading persistent water pollutants, Environmental Science-Processes & Impacts, 17 (2015) 1405-1414.

[53] B. Bhushan, S. Trott, J.C. Spain, A. Halasz, L. Paquet, M. Hawari, Biotransformation of hexahydro-1,3,5-trinitro-1,3,5-triazine (RDX) by a rabbit liver cytochrome p450: insight into the mechanism of RDX biodegradation by *Rhodococcus* sp strain DN22, Applied and Environmental Microbiology, 69 (2003) 1347-1351.

[54] N.V. Coleman, J.C. Spain, T. Duxbury, Evidence that RDX biodegradation by *Rhodococcus* strain DN22 is plasmid-borne and involves a cytochrome p-450, Journal of Applied Microbiology, 93 (2002) 463-472.

[55] D. Fournier, A. Halasz, J. Spain, P. Fiurasek, J. Hawari, Determination of key metabolites during biodegradation of hexahydro-1,3,5-trinitro-1,3,5-triazine with *Rhodococcus* sp strain DN22, Applied and Environmental Microbiology, 68 (2002) 166-172.

[56] M.E. Fuller, N. Perreault, J. Hawari, Microaerophilic degradation of hexahydro-1,3,5-trinitro-1,3,5-triazine (RDX) by three *Rhodococcus* strains, Letters in Applied Microbiology, 51 (2010) 313-318.

[57] K.J. Indest, C.M. Jung, H.P. Chen, D. Hancock, C. Florizone, L.D. Eltis, F.H. Crocker, Functional characterization of pGKT2, a 182-kilobase plasmid containing the xplAB genes, which are involved in the degradation of hexahydro-1,3,5-trinitro-1,3,5-triazine by *Gordonia* sp. strain KTR9, Applied and Environmental Microbiology, 76 (2010) 6329-6337.

[58] Y.S. Cho, B.U. Lee, K.H. Oh, Simultaneous degradation of nitroaromatic compounds TNT, RDX, atrazine, and simazine by *Pseudomonas putida* HK-6 in bench-scale bioreactors, Journal of Chemical Technology and Biotechnology, 83 (2008) 1211-1217.

[59] D.M. Young, P.J. Unkefer, K.L. Ogden, Biotransformation of hexahydro-1,3,5-trinitro-1,3,5-triazine (RDX) by a prospective consortium and its most effective isolate *Serratia marcescens*, Biotec Bioeng, 53 (1997) 515-522.

[60] J.S. Zhao, A. Halasz, L. Paquet, C. Beaulieu, J. Hawari, Biodegradation of hexahydro-1,3,5-trinitro-1,3,5-triazine and its mononitroso derivative hexahydro-1-nitroso-3,5-dinitro-1,3,5-triazine by *Klebsiella pneumoniae* strain SCZ-1 isolated from an anaerobic sludge, Applied and Environmental Microbiology, 68 (2002) 5336-5341.

[61] C.L. Kitts, D.P. Cunningham, P.J. Unkefer, Isolation of three hexahydro-1,3,5-trinitro-1,3,5-triazine-degrading species of the family *Enterobacteriaceae* from nitramine explosive-contaminated soil, Appl Env Micro, 60 (1994) 4608-4611.

[62] I.B. Pudge, A.J. Daugulis, C. Dubois, The use of *Enterobacter cloacae* ATCC 43560 in the development of a two-phase partitioning bioreactor for the destruction of hexahydro-1,3,5-trinitro-1,3,5-s-triazine (RDX), J Biotec, 100 (2003) 65-75.

[63] L. Zhang, Z.H. Xu, Assessing bacterial diversity in soil, Journal of Soils and Sediments, 8 (2008) 379-388.

[64] A.M. Cupples, Final Report: Development of Biomarkers for Assessing in Situ RDX Biodegradation Potential, in, Strategic Environmental Research and Development Program (SERDP) 2010.

[65] J.X. Hu, M.R. Qian, Q. Zhang, J.L. Cui, C.N. Yu, X.M. Su, C.F. Shen, M.Z. Hashmi, J.Y. Shi, Sphingobium fuliginis HC3: A Novel and Robust Isolated Biphenyl- and Polychlorinated Biphenyls-Degrading Bacterium without Dead-End Intermediates Accumulation, Plos One, 10 (2015).

[66] Y.Y. Qu, C.L. Kong, H. Zhou, E. Shen, J.W. Wang, W.L. Shen, X.W. Zhang, Z.J. Zhang, Q. Ma, J.T. Zhou, Catalytic properties of 2,3-dihydroxybiphenyl 1,2-dioxygenase from Dyella Ginsengisoli LA-4 immobilized on mesoporous silica SBA-15, Journal of Molecular Catalysis B-Enzymatic, 99 (2014) 136-142.

[67] O. Uhlik, J. Wald, M. Strejcek, L. Musilova, J. Ridl, M. Hroudova, C. Vlcek, E. Cardenas, M. Mackova, T. Macek, Identification of Bacteria Utilizing Biphenyl, Benzoate, and Naphthalene in Long-Term Contaminated Soil, Plos One, 7 (2012).

[68] J.H. Ou, H.L. Yuan, Sediminibacterium salmoneum gen. nov., sp nov., a member of the phylum Bacteroidetes isolated from sediment of a eutrophic reservoir, International Journal of Systematic and Evolutionary Microbiology, 58 (2008) 2191-2194.

[69] F.H. Crocker, K.J. Indest, C.M. Jung, D.E. Hancock, M.E. Fuller, P.B. Hatzinger, S. Vainberg, J.D. Istok, E. Wilson, M.M. Michalsen, Evaluation of microbial transport during aerobic bioaugmentation of an RDX-contaminated aquifer, Biodegradation, 26 (2015) 443-451.

CHAPTER 5

CONCLUSIONS

The present work identified the key microorganisms responsible for the degradation of VC as well as the microorganisms benefiting from the degradation of RDX in samples derived from a number of contaminated sites (Chapters 2, 3 and 4).

Regarding VC, the putative VC-degraders identified in this research include the genera *Nocardioides, Pseudomonas* and *Ralstonia* as well as the novel genera *Brevundimonas, Tissierella, Rhodoferax Sediminibacterium, Aquabacterium* and *Variovorax* (Chapters 2 and 3).

For RDX, the most dominant phylotypes in microcosms containing sediment from different depths or groundwater from down- and upstream of an emulsified biobarrier following RDX degradation classified within the phyla *Firmicutes, Actinobacteria, Proteobacteria, Acidobacteria* and *Bacteroidetes*. In sediment microcosms, several dominant phylotypes were common to most depths in both studied wells. Specifically, *Pseudomonas* and spore forming bacteria (such as *Clostridium* and *Bacilli*) were associated with RDX degradation as their abundance increased in the RDX-amended microcosms compared to the controls. For the groundwater microcosms, *Pseudomonas* and unclassified *Rhodocyclaceae* were the most dominant genera in the RDX-amended microcosms (with or without glucose) in both of the down- and upstream groundwater inoculated microcosms. While it cannot be stated that these microorganisms were growing using RDX as a carbon, nitrogen or energy source specifically, the research detected the phylotypes illustrating a growth benefit caused by the degradation of RDX. SIP studies on these contaminated samples could clarify the relationship between these dominant phylotypes and RDX degradation. Overall, Chapter 4 provides novel information on

the distribution of potential RDX degraders throughout two soil profiles for a contaminated site as well as for groundwater samples surrounding a biobarrier.

Despite the diversity of the newly discovered VC-assimilators, the functional gene *etnE* (associated with VC assimilation) was relatively conserved in the mixed culture, as the *etnE* sequences detected were similar to those found in *Nocardioides* (Chapter 2). Specific 16S rRNA primers were designed to quantify the novel phylotypes involved in VC degradation. These primers were tested for specificity and successfully confirmed label uptake from VC by showing the accumulation of ^{13}C in the 16S rRNA genes of *Sediminibacterium, Aquabacterium* and *Variovorax*. The primers designed in Chapter 3 could be used to quantify these phylotypes at contaminated sites.

Specific primers towards the functional genes *xenA, xenB* and *xplA*, associated with RDX degradation, were designed and were used to quantify these genes in contaminated samples and experimental microcosms (containing sediment or groundwater under different conditions) following RDX degradation (Chapter 4). Limited data exists on the presence and abundance of these genes at contaminated sites, therefore these primers and this approach should be valuable for others interested in RDX bioremediation.

Overall, the capacity to monitor the presence of specific microorganisms and/or genes coding enzymes involved in either VC or RDX degradation in environmental samples is critical for remediation strategies that rely on in situ bioaugmentation, biostimulation or monitored natural attenuation. Towards this goal, 16S rRNA biomarkers were developed for the novel phylotypes involved in VC degradation. The combination of functional genes and 16S rRNA

biomarkers can be used to estimate the genetic catabolic potential for degradation, thus providing a strong argument supporting remediation through biological pathways.

Future work

To continue to improve our understanding of the biodegradation of VC and RDX at contaminated sites, the follow is suggested:

- For the VC project:
    - Improvement on the isolation approaches, such as the use of a desiccator with ethene for incubation, to better select for VC-degraders (*Brevundimonas, Tissierella, Rhodoferax Sediminibacterium, Aquabacterium* and *Variovorax*).

    - qPCR of the functional genes (i.e. *etnE* for Chapter 3 and *etnC* for Chapters 2 and 3) related to aerobic VC degradation in the SIP heavy fractions could further contribute to the estimation of the genetic potential for degradation by the mixed cultures.

- For the RDX project:
    - SIP experiments on the sediments and groundwater samples could indicate which phylotypes are involved carbon or nitrogen uptake from RDX. 16S rRNA biomarkers could be developed for the RDX- degraders revealed by SIP studies.

- Because *Clostridium* and unclassified *Enterobacteriacea* were among the most dominant phylotypes, qPCR measurements of other RDX functional genes such as *diaA, hydA* and *nsfI* could further contribute to this research.

- Future RDX biodegradation studies of functional pathways should involve the measurement of the RDX degradation products, such as MEDINA, NDAB, HMX, etc.